Regulation of constitutive heterochromatin during fission yeast meiosis

Inauguraldissertation

zur

Erlangung der Würde eines Doktors der Philosophie

vorgelegt der

Philosophisch-Naturwissenschaftlichen Fakultät

der Universität Basel

von

Tahsin Kuzdere

2022

Genehmigt von der Philosophisch-Naturwissenschaftlichen Fakultät

auf Antrag von

Prof. Dr. Marc Bühler

Prof. Dr. Helge Grosshans

Prof. Dr. Viesturs Simanis

Basel, den 22.02.2022

Prof. Dr. Marcel Mayor

Dekan

SUMMARY

The genetic information of eukaryotes is stored in the form of DNA inside the nucleus of the cell. There, the DNA molecules do not exist as naked nucleic acids but are rather wound around histone proteins, forming a higher-level structure called chromatin. Over the years chromatin was categorized into two distinct classes, euchromatin and heterochromatin, using broadly speaking “key features” such as histone modifications or transcriptional activity. Whereas euchromatin is regarded as loose and active, heterochromatin is classically viewed as an inert and silent chromatin state marked by mono-, di-, and tri-methylation of lysine 9 of histone H3 (H3K9me/me2/me3). H3K9 methylation, the hallmark of heterochromatin, plays crucial roles in chromatin-dependent gene silencing and maintenance of genome stability by repressing repetitive DNA elements or recruiting downstream factors essential for faithful chromosome segregation. Many of the fundamental principles and mechanisms of these processes have been elucidated using the fission yeast *Schizosaccharomyces pombe* (*S. pombe)* as a model system. Importantly, most of our knowledge about the heterochromatic landscape in organisms, as well as its regulation, results from studies performed in mitotically growing cells. Indeed, spatial and temporal regulation of H3K9 methylation during sexual differentiation has remained understudied even though it is such an important aspect of the cell cycle where precise orchestration of chromatin-related events is needed to prevent aberrant chromosome segregation resulting otherwise in diseases associated with aneuploidy.

The fact that the H3K9 methylation landscape during sexual differentiation of *S. pombe* was still uncharted area marked the beginning of my PhD project. I set out to map H3K9me2 and H3K9me3 during fission yeast meiosis and I was curious to see

whether these modifications change throughout meiotic progression. If so, I wanted to figure out how these changes would be regulated.

I was successful in mapping the two heterochromatic histone marks genome-wide during meiosis and showed that constitutive heterochromatin, especially centromeres, loses H3K9me2 temporarily and becomes H3K9me3 when cells initiate sexual differentiation. This is of particular importance since cells lacking the ability to tri-methylate H3K9 exhibit severe meiotic (but not mitotic) chromosome segregation defects. Trying to understand how such a switch in methylation preference can be achieved, I discovered that the histone lysine methyltransferase (HKMT) responsible for methylating H3K9 in *S. pombe*, Clr4, is differentially phosphorylated during mitosis and early meiosis and that its phosphorylation state anticorrelates with H3K9me3 activity. Lastly, I identified the cyclin-dependent kinase (CDK) Cdc2 as an enzyme required for Clr4 phosphorylation whose inhibition is a prerequisite for meiotic commitment, coinciding well with the timing of Clr4 dephosphorylation.

In summary, my PhD work revealed the dynamics of constitutive heterochromatin during sexual differentiation and demonstrated that different methylation states of H3K9 are of physiological relevance. What I find fascinating is the fact that Cdc2, a highly conserved master regulator of the cell cycle, is involved in the regulation of the specificity of a HKMT. In general, the high degree of conservation of the proteins involved in my PhD work suggest broad conservation of the mechanism described here. If faithful segregation of chromosomes during meiosis in humans is controlled similarly, this could have key implications for understanding genetic disorders, such as Down syndrome or certain forms of cancer.

TABLE OF CONTENTS

SUMMARY I

TABLE OF CONTENTS III

LIST OF FIGURES V

ABBREVIATIONS VII

INTRODUCTION 1

1. THE RISING OF *SCHIZOSACCHAROMYCES POMBE* AS A MODEL SYSTEM 1

2. LIFE CYCLE OF THE FISSION YEAST *S. POMBE* 2

2.1. The mitotic cell cycle of S. pombe 3

2.1.1. Cyclin-dependent kinases 5

2.1.2. Cdc2 during cell cycle regulation 6

2.2. The meiotic program of S. pombe 7

2.2.1. Mitotic exit and meiotic commitment 8

2.2.2. First and second meiotic divisions 10

2.2.3. Studying fission yeast meiosis 12

3. HETEROCHROMATIN 15

3.1. Histones and chromatin structure 15

3.2. Histone tail modifications 17

3.3. H3K9 methylation 19

3.4. The family of SET-domain containing methyltransferases 20

3.5. Clr4, the S. pombe H3K9 methyltransferase 21

3.5.1. The autoregulatory loop of Clr4 23

3.6. The heterochromatin protein 1 homolog Swi6 24

3.7. Constitutive Heterochromatin in S. pombe 26

3.8. Facultative heterochromatin in S. pombe 28

3.9. RNA interference and the different forms of gene silencing 29

3.9.1. Formation of constitutive heterochromatin at centromeres 30

3.10. The role of H3K9 methylation in genome stability and disease 33

TABLE OF CONTENTS

4. AIM OF THIS THESIS 34

RESULTS 36

1. CDC2-DEPENDENT PHOSPHORYLATION OF CLR4 CONTROLS A H3 METHYLATION SWITCH THAT IS ESSENTIAL FOR GAMETOGENESIS 36

SUMMARY 36

CONTRIBUTIONS 38

2. ADDITIONAL DATA 38

2.1. Facultative heterochromatin islands in S. pombe 38

2.2. Site-directed mutagenesis of Clr4 ARL 40

DISCUSSION 42

H3K9 METHYLATION DYNAMICS AT CONSTITUTIVE HETEROCHROMATIN DURING MEIOSIS 42

FACULTATIVE HETEROCHROMATIN IN DIFFERENT WILD-TYPE *S. POMBE* STRAINS 45

THE ROLE OF PERICENTROMERIC H3K9ME3 IN CHROMOSOME SEGREGATION 48

TEMPORAL H3K9 METHYLATION SWITCH AS A RECRUITING MECHANISM 53

ROLE OF CLR4 PHOSPHORYLATION IN CONTROLLING THE H3K9 METHYLATION SWITCH 56

PHOSPHOREGULATION OF THE SUV FAMILY OF H3K9 METHYLTRANSFERASES 63

CONCLUSION 68

ACKNOWLEDGMENTS 71

REFERENCES 74

APPENDIX 97

MANUSCRIPT: CDK1-DEPENDENT PHOSPHORYLATION OF CLR4^{Suv39H} CONTROLS A HISTONE H3 METHYLATION SWITCH THAT IS ESSENTIAL FOR GAMETOGENESIS 97

LIST OF FIGURES

FIGURE 1. DIFFERENT PATHS OF THE *S. POMBE* LIFE CYCLE. 3

FIGURE 2. SCHEMATIC ILLUSTRATION OF THE MITOTIC CELL CYCLE PHASES IN *S. POMBE*. 4

FIGURE 3. THE MEIOTIC PROGRAM OF *S. POMBE*. 8

FIGURE 4. THE MEI3-PAT1-MEI2 PATHWAY DICTATES ENTRY INTO MEIOSIS IN *S. POMBE*. 10

FIGURE 5. OVERVIEW OF MITOTIC AND MEIOTIC CHROMOSOME SEGREGATION IN *S. POMBE*. 11

FIGURE 6. SYNCHRONIZING FISSION YEAST MEIOSIS USING THE PAT1-AS SYSTEM. 14

FIGURE 7. SCHEMATIC ILLUSTRATION OF THE NUCLEOSOME COMPOSITION IN *S. POMBE*. 16

FIGURE 8. SCHEMATIC (DE-)METHYLATION REACTION OF A HISTONE LYSINE RESIDUE BY A HKDM OR A HKMT. 21

FIGURE 9. DOMAIN ORGANIZATION OF THE *S. POMBE* HKMT CLR4. 22

FIGURE 10. CLOSE-UP CRYSTAL STRUCTURE VIEW OF CLR4'S ACTIVE SITE IN THE AUTOINHIBITED AND AUTOMETHYLATED STATE. 24

FIGURE 11. DISTRIBUTION OF CONSTITUTIVE HETEROCHROMATIN ACROSS THE THREE *S. POMBE* CHROMOSOMES. 26

FIGURE 12. SCHEMATIC ILLUSTRATION OF A CLOSE-UP VIEW OF *S. POMBE* CENTROMERE ORGANIZATION. 27

FIGURE 13. FACULTATIVE HETEROCHROMATIN ISLANDS IN WILD-TYPE *S. POMBE*. 29

FIGURE 14. SELF-REINFORCING FEEDBACK LOOP ENSURES RNAI-MEDIATED HETEROCHROMATIN FORMATION IN *S. POMBE*. 32

FIGURE 15. H3K9ME2 LEVELS AT FACULTATIVE HETEROCHROMATIN ISLANDS IN DIFFERENT WILD-TYPE *S. POMBE* STRAINS. 40

FIGURE 16. H3K9 METHYLATION LEVELS IN PHOSPHO-MIMETIC AND NON-PHOSPHORYLATABLE CLR4^{S458} MUTANTS. 41

FIGURE 17. MST2 AND EPE1 COUNTERACT THE FORMATION OF ECTOPIC H3K9ME2 SITES IN THE *S. POMBE* GENOME. 48

FIGURE 18. MITOTIC AND MEIOTIC COHESIN RECRUITMENT TO CENTROMERES DEPENDENT ON H3K9 METHYLATION LEVELS. 52

LIST OF FIGURES

FIGURE 19. THE DEGREE OF H3K9 METHYLATION DICTATES THE MECHANISM OF TRANSCRIPTIONAL GENE SILENCING.....55

FIGURE 20. CRYSTAL STRUCTURE OF AUTOINHIBITED CLR4 AND DETECTED AMINO ACID INTERACTIONS WITH THE ARL. 61

FIGURE 21. SCHEMATIC ILLUSTRATION OF POTENTIAL PHOSPHORYLATION SITES ON HUMAN SUV39H1.....64

FIGURE 22. HYPOTHETICAL MODEL OF PIN1-MEDIATED PROTEASOMAL DEGRADATION OF CLR4. 66

FIGURE 23. INHIBITION OF THE PROTEASOME STABILIZES UBIQUITINATED CLR4. 67

ABBREVIATIONS

A-loop	Activation loop
A. thaliana	*Arabidopsis thaliana*
Ago	Argonaute
Ala, A	Alanine
APC	Anaphase promoting complex
Arg, R	Arginine
ARL	Autoregulatory loop
as	Analogue-sensitive
Asp, D	Aspartate
ATP	Adenosine triphosphate
bp	base pair
C. elegans	*Caenorhabditis elegans*
CD	Chromodomain
cdc	Cell division cycle
CDK	Cyclin-dependent kinase
ChIP	Chromatin immunoprecipitation
ChIP-qPCR	ChIP-quantitative PCR
ChIP-seq	ChIP-sequencing
CKI	Cyclin-dependent kinase inhibitor
Clr4	Cryptic loci regulator 4
CLRC	Clr4 methyltransferase complex
cnt	Central core
CRL	Cullin-RING ubiquitin ligases complex
CTGS	Co-transcriptional gene silencing
D. melanogaster	*Drosophila melanogaster*
DNA	Deoxyribonucleic acid
DSR	Determinant of selective removal
EGFR	Epidermal growth factor receptor
FMI	Friedrich Miescher Institute for Biomedical Research
G_1-phase	Gap 1 phase
G_2-phase	Gap 2 phase

ABBREVIATIONS

gDNA	Genomic DNA
H. sapiens	*Homo sapiens*
H3K9me	Methylation of lysine 9 of histone H3
HKDM	Histone lysine demethylase
HKMT	Histone lysine methyltransferase
HOODs	Heterochromatin domains
HP1	Heterochromatin protein 1
IF	Immunofluorescence
imr	Innermost repeat
IP-MS	Immunoprecipitation and Mass Spectrometry
LISCB	Leicester Institute of Structural and Chemical Biology
M-phase	Mitotic phase
MBT	Malignant Brain Tumor
MEF	Mouse embryonic fibroblast
mESC	Mouse embryonic stem cells
MS	Mass spectrometry
MSA	Multiple sequence alignment
N. crassa	*Neurospora crassa*
nt	Nucleotide
omr	Outermost repeat
PCR	Polymerase chain reaction
PHD	Plant homeodomain
Phe, F	Phenylalanine
PTGS	Post-transcriptional gene silencing
PTM	Post-translational modification
RDRC	RdRP complex
RdRP	RNA-dependent RNA polymerase
RITS	RNA-induced transcriptional silencing
RNA Pol II	RNA polymerase II
RPM	Reads per million
S-phase	Synthesis phase
S. pombe	*Schizosaccharomyces pombe*
s.d.	Standard deviation

SAM	S-adenosyl-L-methionine
Ser, S	Serine
Sgo1	Shugoshin
SHREC	Snf2/histone deacetylase repressor complex
siRNA	Small interfering RNA
SNP	Single nucleotide polymorphism
TBZ	Tiabendazole
TF	Transcription factor
TGS	Transcriptional gene silencing
ts	Temperature-sensitive
Tyr, Y	Tyrosine

INTRODUCTION

This work will describe how (and why) the specificity of an enzyme involved in establishing and maintaining constitutive heterochromatin is regulated by a master regulator of the cell cycle during mitotic exit and early meiosis. I made these observations using the fission yeast *Schizosaccharomyces pombe* (*S. pombe*) as a model system, for reasons elucidated in section 1. Therefore, the focus of my thesis introduction will be on mechanisms and characteristics described in *S. pombe*, just briefly touching on conserved features. In detail comparison with homologues pathways and organisms will follow in the discussion of this thesis.

1. The rising of *Schizosaccharomyces pombe* as a model system

The fission yeast *S. pombe* has become one of the best-studied eukaryotic model organisms for molecular and cellular biology, playing a crucial role in elucidating basic mechanisms involved in transcription, translation, cell cycle control, chromatin remodeling, and centromere function. The susceptibility of the fission yeast to classical and molecular genetics as well as the increasing amount of applicable techniques helped the popularity of *S. pombe* as a model organism immensely, to a point where nowadays more than 300 laboratories worldwide are conducting research with this organism (Fantes & Hoffman, 2016; Hayles & Nurse, 2018).

This was not always the case and its beginning can be traced back to the late 1940s and early 1950s with Urs Leupold's pioneering work on isolating the first strains and performing genetic studies, and Murdoch Mitchison's contribution on investigating its cell cycle. The breakthrough for *S. pombe* as a model organism came with the seminal work of Paul Nurse and colleagues in the 1970s discovering how the cell cycle is regulated, for which he was awarded the Nobel prize in 2001 (Fantes & Hoffman,

2016; Hayles & Nurse, 2018). Ultimately, sequencing and annotation of the fission yeast genome in 2002 completed our understanding of its conserved chromosome organization, introduced *S. pombe* into the post-genomic era, and rationalized studying chromatin-related processes genome-wide in this organism (Wood et al., 2002).

2. Life cycle of the fission yeast *S. pombe*

S. pombe is a unicellular, predominantly haploid, and rod-shaped eukaryote. Heterothallic fission yeast cells express one of the two mating-type genes *mat1-P* or *mat1-M* and are classified as either P-cell (h^{+}) or M-cell (h^{-}), respectively. In contrast, homothallic strains (h^{90}) can switch readily between both mating types. Therefore, a population of h^{90} cells is a mixture of both h^{+} and h^{-} cells (Kelly et al., 1988).

Depending on environmental cues *S. pombe* switches between vegetative growth (mitotic cell cycle) and sexual phase (meiosis). Under nutrient-rich conditions the fission yeast grows by tip elongation and eventually divides by septation and medial fission (Mitchison & Nurse, 1985). When nutrients become limiting, cells exit vegetative growth and either arrest and enter a stationary phase or conjugate in the presence of a mating partner and enter the sexual phase (Costello et al., 1986; Egel, 1971). The resulting ascospores are able to germinate and re-enter the mitotic cell cycle if the necessary nutrients are provided again (Figure 1).

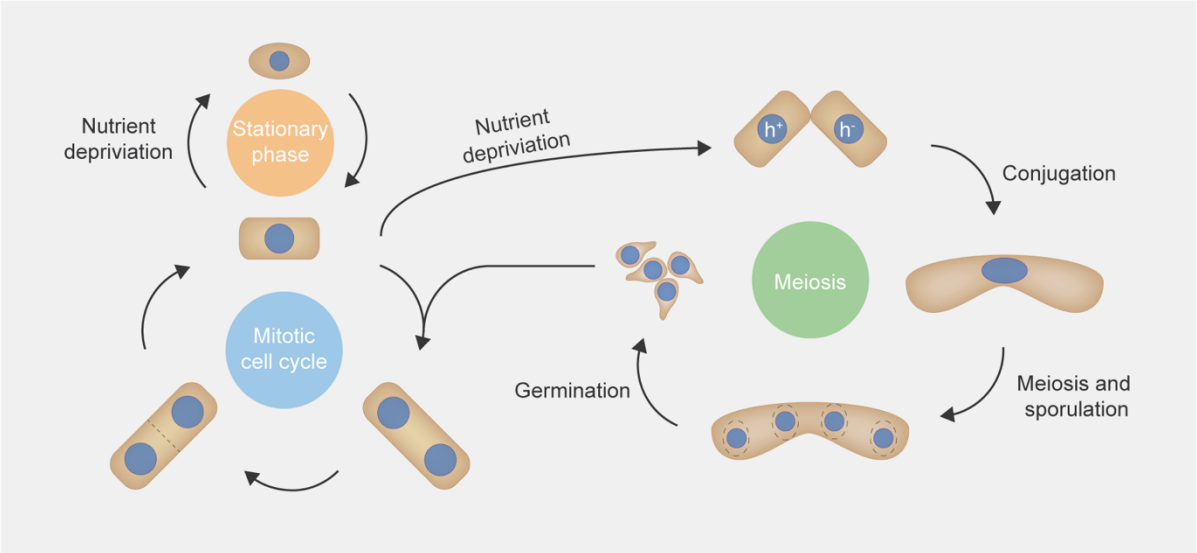

Figure 1. Different paths of the *S. pombe* life cycle.
In nutrient-rich conditions, *S. pombe* grows and divides mitotically. In response to nutrient deprivation, the fission yeast can enter either a stationary phase or conjugate in the presence of a suitable mating partner to initiate meiosis. After meiosis and sporulation, the resulting ascospores germinate and re-enter the mitotic cell cycle, if the missing nutrients are replenished again.

2.1. The mitotic cell cycle of *S. pombe*

The mitotic cell cycle consists of an extremely specialized sequence of steps to ensure correct cell growth, DNA duplication, and subsequent segregation of cellular components to daughter cells. Similar to higher eukaryotes, the cell cycle of *S. pombe* can be split into four phases, where the two key phases of DNA replication (S-phase) and mitosis (M-phase) are separated by distinct gap phases (G_1- and G_2-phase) differing in duration and function (Forsburg & Nurse, 1991) (Figure 2). The function of the G_1-, S-, and G_2-phase is to synthesize proteins needed for progression of the cell cycle, to replicate the genome, and to grow in size respectively. During M-phase the chromosomes condense and are pulled to both ends of the mitotic spindle in an equational manner. The end of M-phase is marked by cytokinesis, where the cellular content is divided equally and the two daughter cells are physically separated (Roberts et al., 2002).

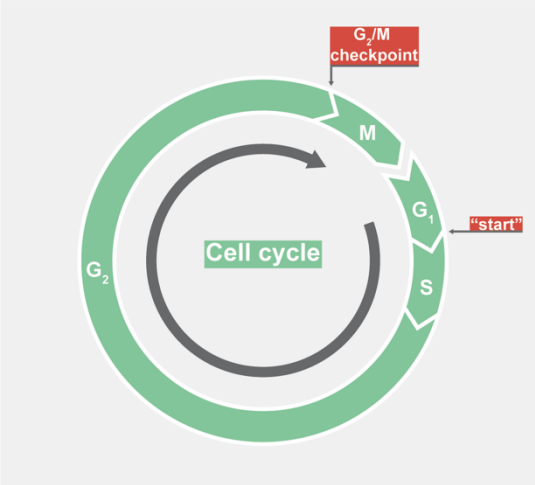

Figure 2. Schematic illustration of the mitotic cell cycle phases in *S. pombe*.
Similar to higher eukaryotes, the mitotic cell cycle of *S. pombe* can be split into four phases, namely G_1-, S-, G_2- and M-phase. Whereas each of the first three phases just occupies 10% of the cell cycle, S. pombe spends most of its time in G_2-phase. The occurrence of the two major cell size checkpoints are indicated by the grey arrows and the red boxes.

The fission yeast cell cycle has two major control points monitoring information about cell size and nutrition before allowing progression to S- or M-phase. The first checkpoint acts at the G_1/S boundary and marks the commitment to the cell cycle. Until this point, also called “start” in yeast, cells can decide to undergo different cell fates such as entering stationary phase or meiosis (Costello et al., 1986; Hartwell et al., 1974; Nurse & Bissett, 1981). This checkpoint is a cryptic one since, under conventional conditions, cells have already passed the size threshold needed to initiate DNA replication before even finishing cytokinesis of the proceeding cell cycle. Therefore, the G_1/S checkpoint only really comes into effect when cells are very small due to nutrient deprivation or mutations (Nurse et al., 1976; Nurse & Thuriaux, 1977). On the other hand, the second control point at the G_2/M boundary was identified as the rate-limiting step of the mitotic cell cycle under standard laboratory growth conditions and represents the major size check point for entry into mitosis (Mitchison & Nurse, 1985; Nurse, 1975, 1985).

Interestingly, it turned out that the same gene is crucially involved in regulating both of the above-mentioned control points (Nurse & Bissett, 1981). Nowadays we know that the product of said gene is the conserved cyclin-dependent kinase (CDK) Cdc2, also known as Cdk1 or p34 (Simanis & Nurse, 1986). The following subsections will introduce the protein family of CDKs, touch briefly on the history of their discovery, and explain the general principle of Cdc2 in cell cycle progression.

2.1.1. Cyclin-dependent kinases

As stated before, control of the mitotic cell cycle underlies a tight regulation in which CDKs play a vital role. This is not just true for yeast but rather universal for all eukaryotic cells (M. G. Lee & Nurse, 1987; Norbury & Nurse, 1989). CDKs are serine/threonine protein kinases that are phosphoproteins themselves (Simanis & Nurse, 1986). Their activity can be influenced by changes in their phosphorylation state and association with regulatory subunits called cyclins, a group of proteins which levels oscillate during the cell cycle (Murray, 2004). A change in CDK activity ultimately leads to differential phosphorylation of their target substrates which in turn impacts their mode of action.

The seminal discovery of CDKs goes back to the 1970s when Lee Hartwell and Paul Nurse used genetic screens to identify genes that are essential for progression through the cell cycle in the budding and fission yeasts, respectively (Hartwell et al., 1973; Nurse et al., 1976). These screens revealed temperature-sensitive mutant alleles that were blocked at different stages of the cell division cycle (cdc) when grown under restrictive conditions. Genetic studies eventually elucidated the importance of the *cdc2*$^+$ gene in G_2/M transition and timing of mitosis and follow-up experiments demonstrated that the *cdc2*$^+$ gene product is indeed a phosphoprotein with kinase

activity as hypothesized (Moreno et al., 1989; Nurse & Thuriaux, 1980; Simanis & Nurse, 1986).

2.1.2. Cdc2 during cell cycle regulation

CDK activity and thereby the cell cycle is controlled by complex networks and feedback loops rather than a linear pathway. Explaining each aspect of CDK regulation would go beyond the scope of this introduction and is not the main focus of this study. An in-depth description of the known mechanisms can be found in Moser & Russell (2000). However, I would like to highlight general mechanisms that become relevant later in this thesis.

In contrast to higher eukaryotes where multiple CDKs interact with their cell-cycle specific cyclins, Cdc2 is the only CDK that regulates the cell cycle in *S. pombe*. Depending on the cell cycle phase, it associates mainly with the S-phase specific cyclin Cig2 or the M-phase specific cyclin Cdc13 to achieve specificity (Mondesert et al., 1996; Moreno et al., 1989). However, Cdc13 is the only essential cyclin in the fission yeast and is sufficient to drive the cell cycle in the absence of other cyclins (Coudreuse & Nurse, 2010; Fisher & Nurse, 1996; Martin-Castellanos et al., 1996). Binding of Cdc2 to the corresponding cyclin stimulates its catalytic activity, helps translocation to the nucleus, and might influence substrate specificity (Murray, 2004). Further, phosphorylation of specific threonine and tyrosine residues in Cdc2 can act both activating as well as inhibiting. One of the main CDK inhibitors (CKI) in the fission yeast is Rum1 which periodic protein levels help to repress Cdc2 activity from late M-phase until the end of G_1-phase and hence safeguards proper partitioning of the cell cycle phases (Benito et al., 1998).

A simplistic view of the interplay of the above-mentioned mechanisms to drive the cell cycle, looks as follows: During the G_1-phase Cdc2 activity is kept at a minimum due to inhibition by Rum1. Phosphorylation and thus degradation of Rum1 at the onset of S-phase paves the way for Cdc2-Cig2 to get activated to moderate levels and allows thereby the G_1/S transition (Benito et al., 1998; Martin-Castellanos et al., 1996; Mondesert et al., 1996). An even higher activity of Cdc2 is needed to drive entry into M-phase (Fisher & Nurse, 1996). Therefore, in addition to binding the M-phase cyclin Cdc13, the inhibitory phosphorylation on Tyr15 of Cdc2, originally deposited by the Wee1 and Mik1 kinase, is removed by the protein phosphatase Cdc25 (Lundgren et al., 1991; Moreno et al., 1989; Russell & Nurse, 1987). The transition from M/G_1 is consequently associated with inactivation of Cdc2-Cdc13. To achieve that, Cdc13 is degraded in an ubiquitin-dependent manner at the end of M-phase. Moreover, Rum1 is stabilized again and can fulfil its role as the Cdc2 inhibitor until the end of G_1-phase.

2.2. The meiotic program of *S. pombe*

The meiotic program is a specialized cellular event that is accompanied by immense changes in transcription, expression of non-coding RNAs, protein synthesis, and post-translational regulation to produce haploid gametes from diploid parental cells (Andric & Rougemaille, 2021; Krapp et al., 2019; Mata et al., 2002; Sato et al., 2021; Yamashita et al., 2017a; Yamashita, 2019). In addition to creating germ cells with the correct amount of chromosomes, meiosis increases genetic variation and is the reason that genetic information can be passed on to next generations.

The different steps of fission yeast meiosis are highly comparable to those found in higher eukaryotes, differing just slightly at some stages. The meiotic program of *S. pombe* can be divided into distinct phases happening in consecutive order. First

of all, cells exit vegetative growth, commit to the meiotic program, and fuse with a mating partner (G_1 arrest and conjugation). Secondly, the DNA is replicated (premeiotic S-phase) and segregated in two consecutive M-phases (meiosis I or meiosis II), resulting in bi- and tetranucleate states each. Lastly, the four haploid nuclei form spore walls, turning into ascospores that can eventually enter the mitotic cell cycle given the nutritional conditions (sporulation and germination) (Figure 3).

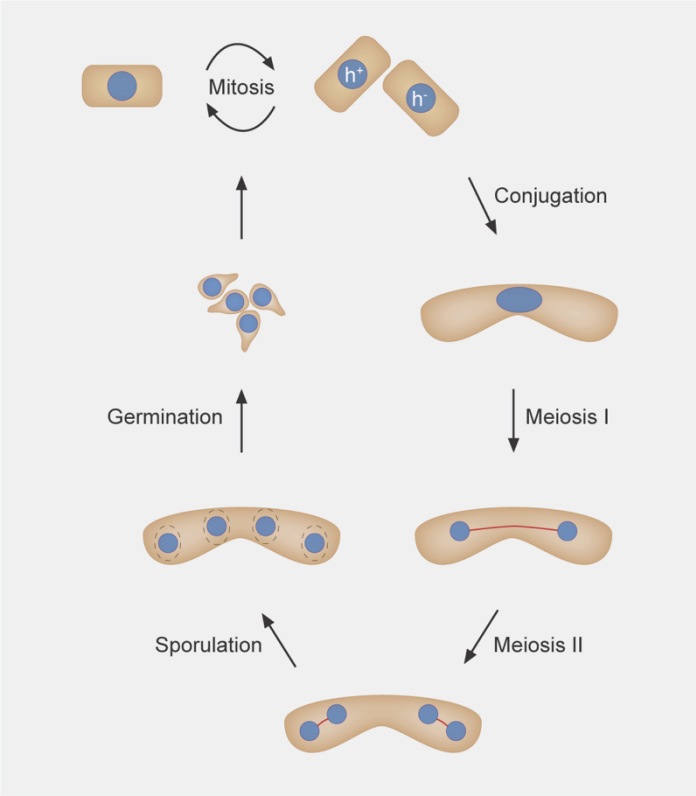

Figure 3. The meiotic program of *S. pombe*.
In nutrient-rich conditions, *S. pombe* grows and divides mitotically. In response to starvation, the fission yeast conjugates with a cell of opposite mating-type to initiate the meiotic program. After premeiotic S-phase and two consecutive rounds of meiotic division, meiosis I and meiosis II, a tetranucleate ascus is formed. Sporulation and germination creates ascospores which can re-enter the mitotic life cycle if nutrient-rich conditions are restored again.

2.2.1. Mitotic exit and meiotic commitment

Two major prerequisites need to take place for the fission yeast to exit the mitotic cell cycle and to initiate the meiotic program. One is nutrient depletion, especially that of nitrogen, which triggers multiple downstream responses in the cell.

The second requirement for starting the meiotic program is the presence of cells with opposite mating-types, h^+ and h^-.

As mentioned earlier (section 2.1), there is only a brief window of opportunity for *S. pombe* to exit vegetative growth which is before crossing "start" during the G_1-phase of the mitotic cell cycle. The CKI Rum1 has a major implication in extending the G_1-phase under nutrient-deprived conditions and allowing initiation of the meiotic program. The normally very unstable *rum1*$^+$ transcripts are stabilized in the absence of nitrogen which leads to an accumulation of Rum1 protein levels (Daga et al., 2003; Stern & Nurse, 1998). Consequently, Cdc2 activity is repressed and the onset of S-phase is delayed. Further, nutritional deprivation regulates different signal transduction pathways, such as cAMP-PKA and MAPK signaling, to ensure proper premeiotic G_1 arrest and expression of a key transcription factor (TF) for sexual development, *ste11*$^+$ (Kato et al., 1996; Maeda et al., 1990; Sugimoto et al., 1991). Ste11 activates transcription of multiple genes encoding for pheromone communication, the mating process, and the early meiotic program (Mata & Bahler, 2006). Once cells of opposite mating-types have conjugated to form a diploid cell, the last step to ultimately initiate the meiotic program is to inhibit the main inhibitory kinase of meiosis, Pat1 (formerly known as Ran1) (Iino & Yamamoto, 1985; McLeod & Beach, 1986; Nurse, 1985). The combined mating-type pheromones encoded by *mat1-P* and *mat1-M* are needed to do so by facilitating transcription of *mei3* which gene product inhibits Pat1 kinase activity by mimicking a pseudosubstrate (Li & McLeod, 1996; McLeod & Beach, 1988). This is also the reason why heterozygosity at the mating-type locus is a requirement for *S. pombe* to undergo meiosis since inhibition of Pat1 would not be possible otherwise. During vegetative growth Pat1 is constantly phosphorylating and thereby inhibiting its target, Mei2, an essential RNA binding

protein needed for the onset of premeiotic S-phase and meiosis I (Watanabe & Yamamoto, 1994). Upon induction of Mei3, Pat1 gets inactivated and levels of dephosphorylated Mei2 increase rapidly (Figure 4).

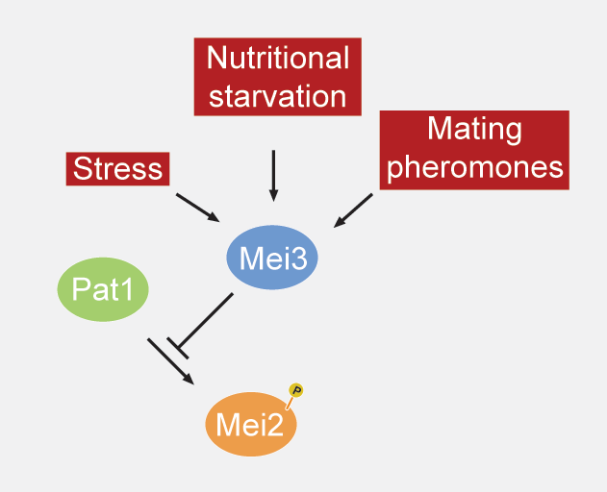

Figure 4. The Mei3-Pat1-Mei2 pathway dictates entry into meiosis in *S. pombe*.
The main inhibitory kinase of meiosis, Pat1, constantly targets and thus inhibits the RNA binding protein Mei2 in vegetative cells. Accumulation of Mei2 is essential for initiation of premeiotic S-phase and meiosis I. Upon exogenous cues, such as stress and nutritional starvation, and expression of mating-type pheromones, the Pat1 inhibitor Mei3 is expressed which consequently leads to stabilization of the *mei2*$^{+}$ gene product and thereby triggers the onset of meiosis.

2.2.2. First and second meiotic divisions

To ensure that gametes have the correct ploidy at the end of meiosis, homologous chromosomes (instead of sister chromatids) have to segregate first in a reductional manner during meiosis I. Only then sister chromatids will be separated equationally, reminiscent of chromosome segregation during mitosis (Page & Hawley, 2003). The co-segregation of homologous chromosomes during meiosis I is achieved by protection of sister chromatid cohesion, which is abolished during meiotic progression thus allowing equational segregation during the second meiotic division (Figure 5).

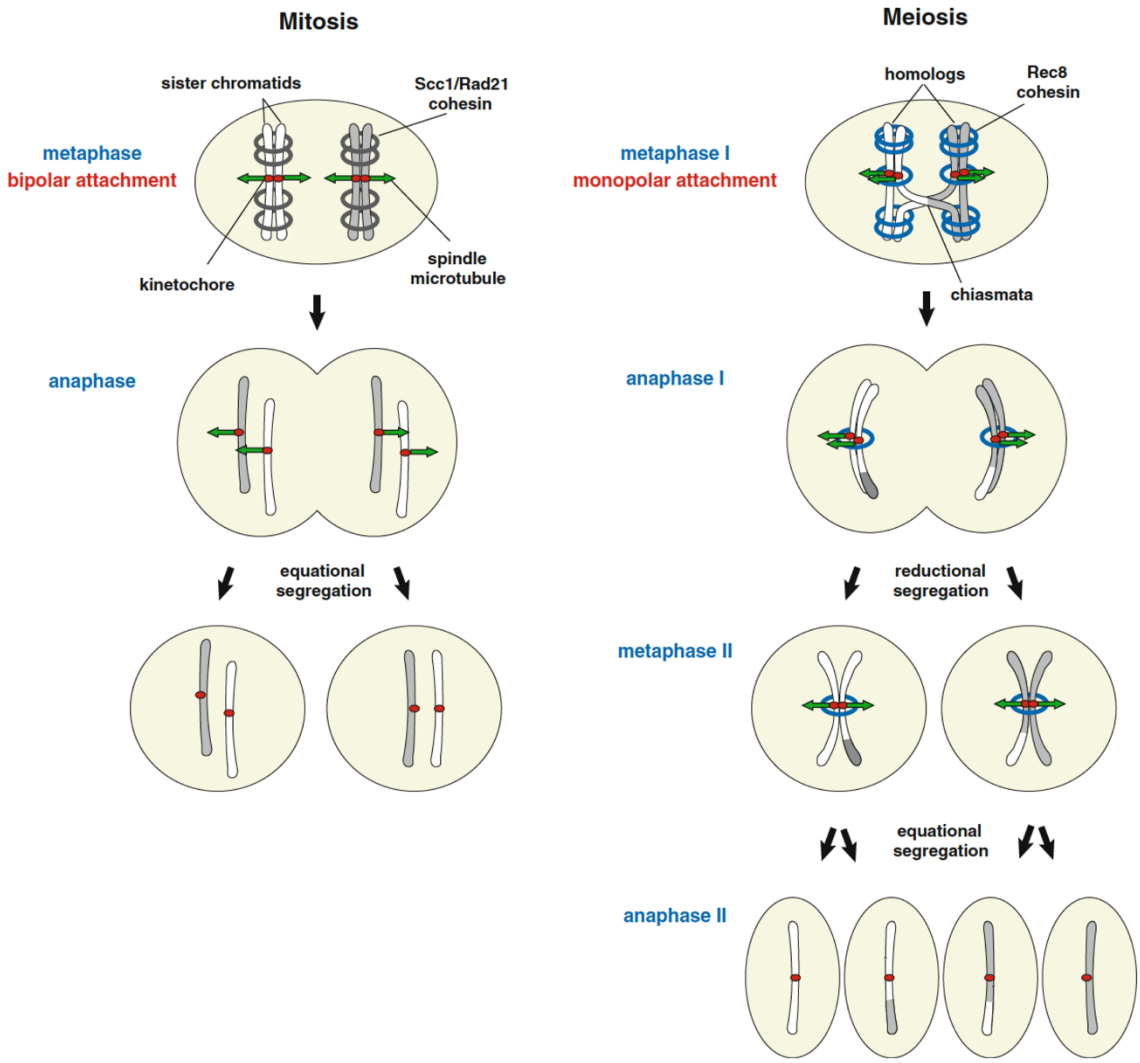

Figure 5. Overview of mitotic and meiotic chromosome segregation in *S. pombe*.
During mitosis, sister chromatids are kept together by the mitotic cohesin complex Scc1/Rad21. Rad21 causes bipolar attachment of sister kinetochores to microtubules emanating from opposite spindle poles, which results in equational segregation of sister chromatids (left). During meiosis, Rad21 is replaced with Rec8 to form the meiosis-specific cohesin complex. After meiotic recombination, both sister kinetochores attach to microtubules emerging from the same spindle pole (monopolar attachment). Thus homologs and not sister chromatids are separated during meiosis I in a reductional manner. During meiosis II, sister chromatids undergo equational segregation as in mitosis (right). Figure adapted from Sakuno & Watanabe, 2009.

Before the physical segregation of chromosomes during the first meiotic division, homologous chromosomes are attached covalently at the centromeres as well as chromosome arms by the meiosis-specific cohesin complex consisting of Rec8. This allows for the formation of chiasmata which are necessary for meiotic

recombination to take place (Yokobayashi et al., 2003). The physical connection of the chromosome arms is disrupted by separase-mediated cleavage of Rec8 which is protected by the “guardian” protein shugoshin (Sgo1) at centromeres (Ishiguro et al., 2010; Kitajima et al., 2004). The fission yeast heterochromatin protein 1 (HP1) homolog Swi6 recruits, besides the mitotic and meiotic cohesin complexes itself, also Sgo1 to pericentromeric repeats in a H3K9 methylation-dependent manner (Kitajima et al., 2003; Nonaka et al., 2002; Yamagishi et al., 2008). Therefore, cells that are devoid of H3K9 methylation or *sgo1*Δ strains struggle to properly segregate chromosomes during meiotic divisions (section 3.10). Both sister kinetochores of each chromosome pair are captured by microtubules emanating from the same spindle pole resulting in a monopolar attachment which is a prerequisite for reductional division. Once the homologous chromosome pairs have been segregated, Sgo1 is degraded in a proteasome-dependent manner due to attachment of ubiquitin chains by the anaphase promoting complex (APC). This, at last, exposes centromeric Rec8 for degradation (Kitajima et al., 2004). Therefore, cohesion of sister chromatids during meiosis II is lost and bipolar attachment of microtubules from both spindle poles leads to equational segregation of the sisters, giving rise to a tetranucleate cell with haploid DNA content each.

2.2.3. Studying fission yeast meiosis

There are multiple approaches available to study fission yeast meiosis. Depending on the experiment to perform, different levels of synchronicity of the meiotic cultures are necessary – reaching from asynchronous over semi-synchronous to highly synchronous.

If meiotic events can be studied by analyzing single cells or screening for cells that are at the correct meiotic stage is possible, asynchronous and semi-synchronous meiotic cultures are best suitable. This is the case for experiments such as live cell imaging or immunofluorescence (IF). Zygotic meiosis can be induced by mixing h^+ and h^- cells or a homothallic h^{90} strain and starve them either in liquid culture or on an solid agar plates lacking nitrogen (Ekwall & Thon, 2017). Due to the fact that conjugation and mating between cells will happen at different rates, the resulting meiotic culture will have cells at all different meiotic stages. To circumvent the issue with timing of conjugation, one can use diploid fission yeast cells that are heterozygous for the mating-type (h^+/h^-) and do not need to fuse anymore to start the meiotic program. Even though *S. pombe* haploids are healthier, it is possible to create and select diploids by crosses or protoplast fusion and returning them to nutrient-rich medium before they fully commit to the meiotic program (Ekwall & Thon, 2017). Meiosis initiated from diploid cells is called azygotic meiosis but except for differently shaped asci, no differences between zygotic and azygotic meiosis are known (Smith, 2009). These approaches of inducing meiosis can be easily coupled with mutations that arrest at different stages of the meiotic program, similar to the *cdc* mutants of the mitotic cell cycle.

Experiments that rely on homogenous cell cultures or cellular lysates to study (molecular) biological events during meiotic progression, exploit the Mei3-Pat1-Mei2 pathway (section 2.2.1). These three proteins play such a crucial role in regulating entry into meiosis, that overexpression or inactivation of the respective protein can induce ectopic meiosis independent of ploidy and nutrient condition (Iino & Yamamoto, 1985; McLeod et al., 1987; Nurse, 1985; Watanabe et al., 1997). The approach that is nowadays most commonly used to generate highly synchronous meiotic cultures,

leans on inhibiting Pat1 activity in diploid strains homozygous for the mating-type (h^+/h^+ or h^-/h^-). Generally, mitotic cultures are grown in rich medium and arrested in G_1-phase by nitrogen starvation. Since the diploids used in this approach are not heterozygous for the mating-type locus, they cannot induce expression of *mei3* and will not commit to meiosis on their own. Controlled inactivation of Pat1 triggers the start of meiosis and the cell culture will progress through the sexual program in a synchronous manner. A temperature-sensitive (ts) mutant of the *pat1* allele, *pat1-114*, was commonly used to inactive Pat1 by shifting the cultures to 34°C (Yamashita et al., 2017b). However, even though meiosis achieved by using Pat1-ts is highly comparable to wild-type meiosis, carrying out the sexual cell cycle at elevated temperatures reflects non-physiological conditions. The drawbacks of high temperatures and the lack of mating-type pheromones leads to issues with chromosome segregation and heat shock responses. To tackle these problems analogue-sensitive (as) Pat1 mutants, expressing the mating-pheromone *mat-Pc*, were created in which meiosis can be induced at physiological temperatures by addition of an ATP-analogue to achieve synchronous meiosis most similar to wild-type meiosis (Figure 6) (Cipak et al., 2012, 2014; Guerra-Moreno et al., 2012).

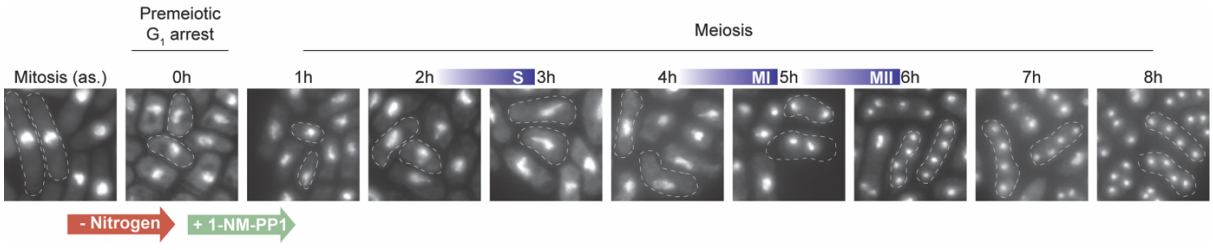

Figure 6. Synchronizing fission yeast meiosis using the Pat1-as system.
Diploid h^-/h^- *pat1-as/pat1-as mat-Pc* cells are arrested in premeiotic G_1-phase by nitrogen starvation. Addition of the ATP-analogue 1-NM-PP1 inhibits Pat1 and thus triggers the onset of meiosis in these G_1 arrested cells. Premeiotic S-phase (S) takes place within 2h and the meiotic divisions, meiosis I (MI) and meiosis II (MII), occur after 4h and 5h, respectively.

3. Heterochromatin

In many eukaryotes, heterochromatin can be found at permanently silenced genomic regions, such as repetitive elements, telomeres, and centromeres. In certain tissues or during differentiation, even loci containing genes can be conditionally silenced by means of heterochromatin. This chapter will deal with the characterization of heterochromatin, introduce the proteins necessary for establishing heterochromatic regions, and explain the underlying principles of chromatin regulation.

3.1. Histones and chromatin structure

The blueprint of eukaryotic life is basically made up by an alternating sequence of four nucleotides, which is stored inside the nucleus of the cell in the form of DNA. There, DNA molecules do not exist as naked nucleic acids but are rather organized into a higher-level structure called chromatin. On the lowest level, chromatin consists of repeating units of nucleosomes which are histone protein complexes bound by 145-147 base pairs (bp) of DNA. The octameric nucleosome core, also called core particle, is built from two copies of each histone protein (H2A, H2B, H3, and H4) and contains exposed histone tails that emanate the nucleosome core (Figure 7).

These highly basic N-terminal histone tails, which are well conserved from yeast to human, are involved in interacting with other nucleosomes and are often targeted for post-translational modifications (PTMs) (Bannister & Kouzarides, 2011; Kornberg, 1977; Luger et al., 1997). Core particles are connected with each other via short and highly accessible linker DNA, giving chromatin a “knobby”, beaded primary structure as seen by electron microscopy (Olins & Olins, 1974). Further compaction of oligonucleosomes, similar to secondary and tertiary structures of RNA and proteins, results in the formation of chromatin fibers and eventually in the structures that we

know as chromosomes (Baldi et al., 2020; Luger & Hansen, 2005). This phenomenon of chromatin compaction is the reason why it is possible for a DNA fiber of 2 m to fit into the nucleus of a cell, measuring merely 5-10 µm in diameter.

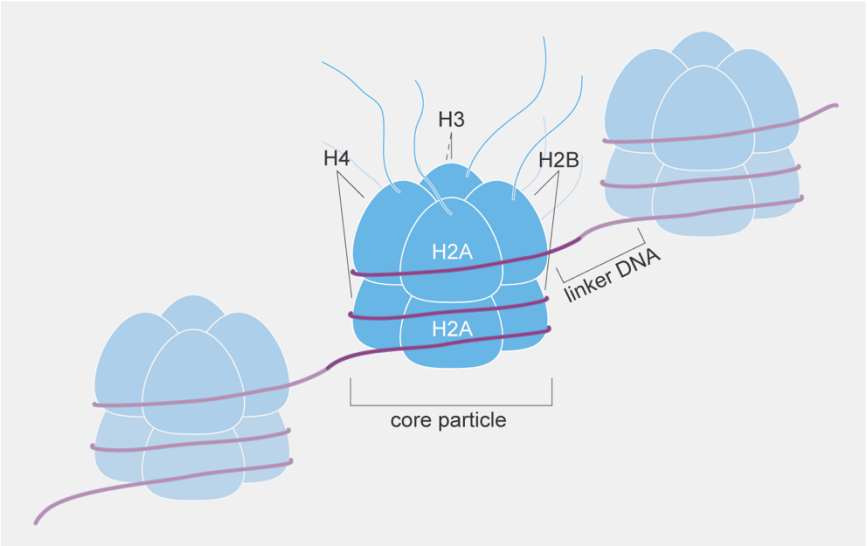

Figure 7. Schematic illustration of the nucleosome composition in *S. pombe*.
The nucleosome core particle consist of eight histone molecules, which contain highly basic and exposed N-terminal tails. 145-147 bp of protected DNA are wound around the core particle to form the nucleosome and highly accessible linker DNA connects repeating units of nucleosomes with each other.

However, besides having an impact on the size and topology of DNA, chromatin is heavily involved in other biological processes, such as DNA replication, chromosome segregation, and gene expression (Bannister & Kouzarides, 2011; Kornberg & Lorch, 1999). The physical properties and characteristics of chromatin can be regulated in multiple ways. One way is by affecting DNA accessibility via nucleosome density, positioning, and turnover. Instead of evicting the whole core particle, it is also possible for individual histone proteins to be replaced by histone variants, containing different properties. Further the DNA can undergo chemical modification directly (e.g. DNA methylation) or the N-terminal histone tails can be modified post-translationally (Bannister & Kouzarides, 2011; Jiang & Pugh, 2009; Moore et al., 2013; Weber & Henikoff, 2014). The complete description of these

chemical modifications are also referred to as the epigenome, even though not all of them are indeed inherited to next generations (Bernstein et al., 2007).

Depending on the effect that all of the aforementioned factors have on chromatin states, chromatin can be subdivided into two classes. When talking about transcriptionally active, gene-rich, and accessible chromatin, people refer to euchromatin. On the contrary, the transcriptionally inactive and condensed state was termed heterochromatin (section 3.7 and 3.8). The silent heterochromatin is typically associated with methylation of H3K9, hypoacetylated nucleosomes, and recruitment of different members of the HP1 family (Grewal & Jia, 2007).

3.2. Histone tail modifications

The initial observation that histones can be acetylated and methylated was made in the 1960s. However, it took more than two decades to identify the enzymes responsible for said modifications and to decipher the biological role modified histone tails play in mediating chromatin regulation (Allfrey et al., 1964; Brownell et al., 1996; Luger et al., 1997; Rea et al., 2000).

Over the last couple of decades more than 60 different histone residues were shown to be modified and a steadily increasing amount of histone PTMs are still being reported. This is due to the advance of chromatin immunoprecipitation (ChIP), mass spectrometry (MS), and genomics technology which facilitates our ability to identify and quantify histone modifications. By now there is quite a large library of detected histone modifications, of which a lot are understudied or not studied at all concerning their physiological function (Zhao & Garcia, 2015). Generally speaking, there are at least eight distinct classes of histone modifications, of which acetylation, phosphorylation, and methylation are the most prominent ones (Kouzarides, 2007).

One would think that with the immense amount of information and studies available, we can by now easily map or predict histone modifications to their regulatory function. However, the reality shows us that any given modification has the ability to act either activating or repressing and that the context of the modification plays a crucial role on the regulatory outcome. For instance, methylation of H3K4 and H3K36 is predominantly enriched at active genes whereas methylation of H3K9, H3K27, and H4K20 marks regions for silencing (Xhemalce et al., 2011). Concerning transcription regulation, as a rule of thumb, acetylation, phosphorylation, methylation, and ubiquitination have been associated with activation. The latter, methylation and ubiquitination, together with sumoylation, trigger a repressive response (Kouzarides, 2007). The underlying principle how histone PTMs affect chromatin states is based either on changing the charge of the histone tails or by recruiting downstream, non-histone, effector proteins. By masking the positive charges on histones or by actively introducing negative charges, such as acetylation of H4K16 or phosphorylation of H3S10, electrostatic interactions between the histone tail and the DNA are disrupted (Allfrey et al., 1964; Sauvé et al., 1999; Shogren-Knaak et al., 2006). Thus, chromatin unfolds and gets less compact which is accompanied by increased accessibility for the transcription machinery or TFs in general. The other mode of action is based on presenting a binding site for so-called histone “reader” proteins which can bind to the modified histone residues directly and thereby initiate specific downstream responses. Acetylated lysines (Lys, K) can be bound by bromodomain-containing proteins whereas phosphorylated serines (Ser, S) are recognized by a class of 14-3-3 proteins. Methylation on lysine residues serves as a binding platform for PHD domains or chromo-like domains, such as chromodomains (CD), tudor, and MBT (Bannister & Kouzarides, 2011).

3.3. H3K9 methylation

Characteristic features of heterochromatin in metazoans are hypoacetylation of histones, (co-)transcriptional gene silencing, and high levels of H3K9 and H3K27 methylation. In the fission yeast *S. pombe*, the distribution and architecture of heterochromatic regions are very similar to the ones of higher eukaryotes. However, *S. pombe* lacks homologs of the polycomb group proteins responsible for H3K27 methylation (Kouzarides, 2007; Schuettengruber & Cavalli, 2009). Therefore, H3K9 methylation is the main repressive histone modification in *S. pombe* and earned its name as the “hallmark of heterochromatin”.

Generally, H3K9 methylation is associated with transcriptional silencing and formation of heterochromatin. However, the classical view of heterochromatin regarding its repressive nature might be outdated in some aspects. By now, we are quite aware that heterochromatin is not transcriptionally silent *per se*. Basal levels of transcription take place at several heterochromatic regions and different degrees of H3K9 methylation result in different levels of repressiveness. (Azzalin et al., 2007; Bühler et al., 2006; Dümpelmann et al., 2019; Jih et al., 2017; Volpe et al., 2002). Ironically, little transcriptional activity of heterochromatin is even needed to sustain the silent chromatin state in fission yeast, where initiation and maintenance of heterochromatin depends on nascent transcripts arising from the pericentromeric repeats (section 3.9.1)(Kato et al., 2005; Volpe et al., 2002).

Methylation of lysine residues within histones is catalyzed by a family of enzymes called histone lysine methyltransferases (HKMTs) (Xhemalce et al., 2011). Due to the lack of reported demethylases and the relatively long half-life of methylated histones, it was thought for a long time that this PTM would be a stable and irreversible modification. In the early 1970s, the hypothesis was that, to get rid of the methylation

mark, the modified histone had to be replaced with an unmodified one (Bannister et al., 2002). It was not until the year 2004 that this over 30 year old belief was overturned with the discovery of the first histone lysine demethylases (HKDMs), LSD1 (Shi et al., 2004). Since then many more HKDMs have been reported, playing important roles in counteracting HKMTase activity (Xhemalce et al., 2011). The levels of methylated lysine residues on histones are precisely balanced and changes of this equilibrium have been linked to the various forms of cancer, neuronal diseases, and regulation of lifespan (Greer & Shi, 2012).

3.4. The family of SET-domain containing methyltransferases

The characterization of the first HKMTs, namely human and mouse SUV39H1 and Suv39h1 in the year 2000 by the laboratory of Thomas Jenuwein marked a critical point in advancing our understanding around the topic of H3K9 methylation (Rea et al., 2000). By now many more HKMTs from all different eukaryotes including plants, fungi, insects, nematodes, and vertebrates are known and most of the reported HKMTs were shown to modify lysines that reside in the unstructured and exposed histone tail (Shinkai, 2007). The common denominator of these methyltransferases is the presence of a well conserved 130-140 amino acid SET-domain, which forms the catalytic core of these enzymes. The folding structure and amino acid sequence of the preceding pre-SET and the following post-SET regions determine the position of the methyl donor and the peptide-binding cleft. Thus, the correct transfer of the methyl group from the cofactor S-adenosyl-L-methionine (SAM) to the ε-amino group of the target lysine is ensured (Dillon et al., 2005; Xhemalce et al., 2011). HKMTs are highly specific enzymes regarding their substrate lysine and the degree of methylation they catalyze, which can range from mono-methylation all the way to tri-methylation (me1

- me3) of lysine residues (Figure 8). Among the HKMTs, some lack the ability to catalyze all three methylation states and are only able to generate one or two of these states. The product specificity rises from a single amino acid residue within the SET-domain, termed switch position. A combination of multiple sequence alignment (MSA) of different SET-domain containing methyltransferases from several species and site-directed mutagenesis revealed that the presence of either phenylalanine (Phe, F) or tyrosine (Tyr, Y) critically dictates the degree of methylation (Collins et al., 2005; Dillon et al., 2005). Phe at the switch position, such as in *Neurospora crassa* Dim-5 or mammalian SUV39H1/2, allows di- and tri-methylation of H3K9, whereas Tyr, like in *Arabidopsis thaliana* SUVH4/KYP, only allows for catalysis of H3K9me1/me2 (Figure 9) (Collins et al., 2005; Jih et al., 2017).

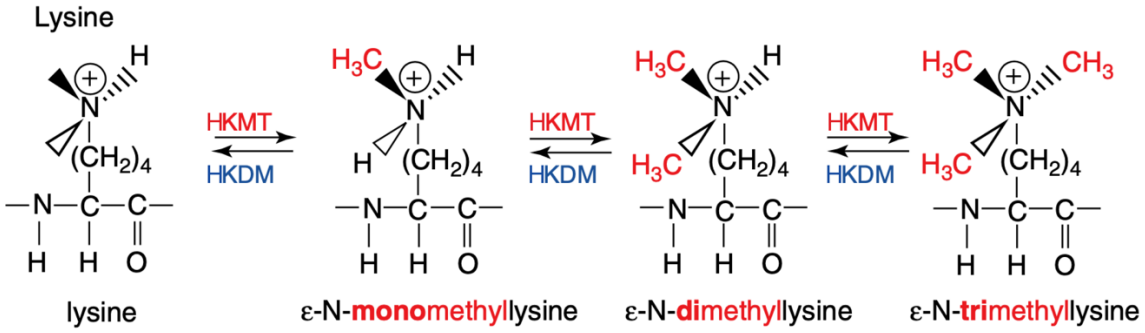

Figure 8. Schematic (de-)methylation reaction of a histone lysine residue by a HKDM or a HKMT.
Lysine residues are methylated on the ε-amino group by HKMTs and demethylated by HKDMs. Depending on the switch position of the HKMT, either mono-, di-, or, tri-methylation can be catalyzed. Figure adapted from Xhemalce et al., 2011.

3.5. Clr4, the *S. pombe* H3K9 methyltransferase

The fission yeast *S. pombe* has only one HKMT responsible for methylating lysine 9 of histone H3, namely Cryptic loci regulator 4 (Clr4). Clr4 is a 490 amino acid protein, consisting of a N-terminal CD and C-terminal SET-domain that shares high sequence similarity with the class of SET-domain containing SUV39 methyltransferases (Figure 9) (Ivanova et al., 1998; Nakayama et al., 2001). The

switch position within the SET-domain of Clr4 is occupied by a Phe (F449), thus allowing Clr4 to catalyze H3K9me2 as well as H3K9me3 (Collins et al., 2005; Nakayama et al., 2001). Replacing the switch position residue with Tyr (F449Y) turns Clr4 to a di-methyltransferase exclusively (Jih et al., 2017).

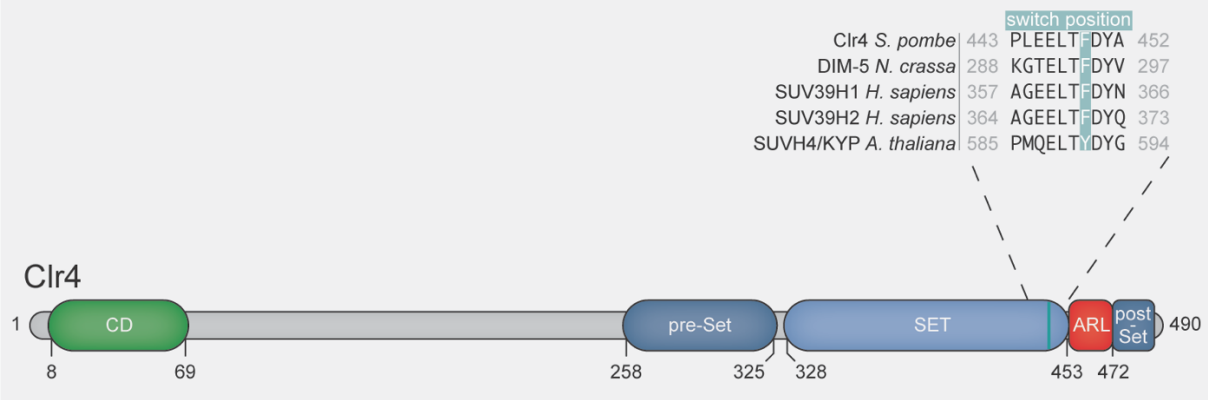

Figure 9. Domain organization of the *S. pombe* HKMT Clr4.

Clr4 is a 490 amino acid protein, consisting of a N-terminal CD and a C-terminal SET-domain. The SET-domain is flanked by the pre-SET region at its N-terminal end and is connected to the post-SET region at its C-terminal end via an autoregulatory loop (ARL) (bottom). Ten amino acids surrounding the switch position within the SET-domain of different HKMTs are shown (top).

In vivo, Clr4 is associated with multiple proteins to form the Clr4 methyltransferase complex (CLRC) consisting of Rik1, Raf1, Raf2, Pip1, and the fission yeast E3 ubiquitin ligase Cul4 (Hong et al., 2005; Horn et al., 2005; Jia et al., 2005; Kuscu et al., 2014). Part of CLRC strongly resembles the human Cullin-RING ubiquitin ligases 4 complex (CRL), whose function is to bridge E2-ubiquitin-conjugating enzymes to their respective substrates. Why Clr4 forms a multi protein complex with E3 ubiquitin ligase activity is not well understood. However, the CLRC complex plays a major role in targeting and subsequent spreading of Clr4s methyltransferase activity along heterochromatic repeats, explaining why deletion of CLRC subunits results in depletion of H3K9 methylation (Hong et al., 2005; Horn et al., 2005; K. Zhang et al., 2008).

3.5.1. The autoregulatory loop of Clr4

Recently, a 18 amino acid stretch between the SET- and post-SET domains of Clr4 was shown to function as an autoregulatory loop (ARL) (Iglesias et al., 2018). This loop possesses the intrinsic ability to fold and span over Clr4s catalytic pocket depending on the methylation state of two lysine residues, sitting at the beginning and end of the ARL (K455 and K472). A combination of *in vitro* methylation assays and crystal structures revealed that Clr4 has the ability to methylate these lysine residues itself, thus inducing an automethylation-mediated conformational switch. In a non-methylated state, the ARL autoinhibits Clr4 activity by occupying the active site and hindering substrate recognition. Upon automethylation, the ARL undergoes a conformational transition which exposes the catalytic pocket and thereby increases Clr4 methyltransferase activity (Figure 10). Site-directed mutagenesis demonstrated that cells mimicking hypoactive (autoinhibited) and hyperactive (automethylated) states, indeed exhibit altered H3K9 methylation levels (Iglesias et al., 2018). However, whether Clr4 undergoes automethylation *in vivo*, or whether $Clr4^{K455}$ and $Clr4^{K472}$ are methylated inside the cell, still needs to be shown.

Interestingly, phosphoproteomic screens in *S. pombe* revealed multiple phosphorylation sites on Clr4 that map to serine residues in the CD and ARL (Carpy et al., 2014; Kettenbach et al., 2015; Swaffer et al., 2018). Even though it is known that PTMs, particularly phosphorylation, can regulate protein activity in a fast and reversible manner, the biological relevance of these phosphorylation events have not been studied at all and its effect on the ARL have remained enigmatic (Olsen et al., 2006).

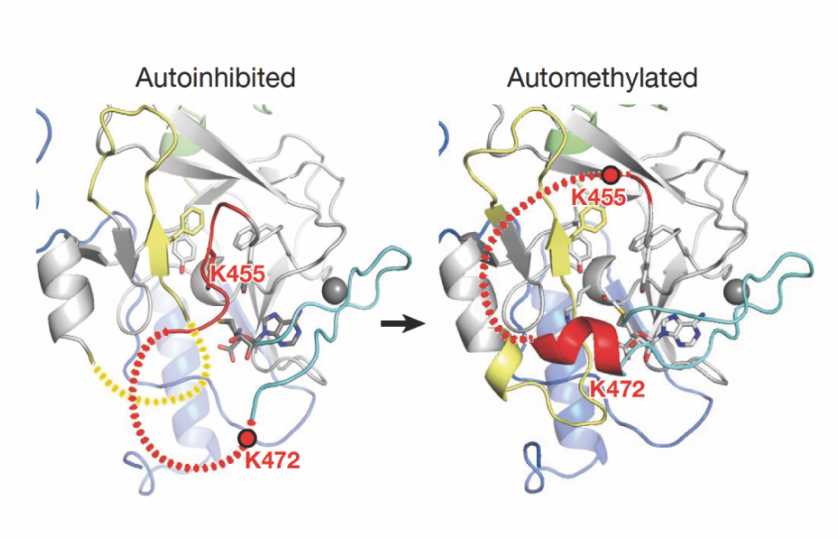

Figure 10. Close-up crystal structure view of Clr4's active site in the autoinhibited and automethylated state.

Upon automethylation of the lysine residues, K455 and K472, which span the ARL (red loop) Clr4 undergoes a conformational switch that exposes the active site. Further, the methylation-induced structural rearrangements stabilize the SET insertion domain (yellow) which is unstructured in the autoinhibited form of Clr4; grey domain = SET-domain; turquoise domain = post-SET. Figure adapted from Iglesias et al., 2018.

3.6. The heterochromatin protein 1 homolog Swi6

As described in section 3.2, besides changing electrostatic interactions between histones and the DNA, histone tail modifications can serve as a binding platform for chromatin binding proteins. So does H3K9 methylation for the family of heterochromatin protein 1 (HP1) proteins.

The presence of HP1 proteins was first discovered in the late 1980s, when James and Elgin detected a predominantly heterochromatin-associated protein by IF using monoclonal antibodies in *Drosophila melanogaster* (*D. melanogaster*) (James & Elgin, 1986). Since then, study of these heterochromatin-associated proteins attracted a lot of attention and by now we know that this family of chromosomal proteins are conserved from yeast to human and play crucial roles in heterochromatin formation and gene repression (Grewal & Jia, 2007). Most organisms evolved to have multiple homologs of HP1 proteins, such as HP1α, HP1β, and HP1γ in mammals or Swi6 and

Chp2 in *S. pombe* (Fanti & Pimpinelli, 2008). This points towards the existence of species-specific functions and nonoverlapping pathways of HP1 proteins. Whereas Swi6 interacts with a variety of different nuclear proteins to regulate chromatin remodeling, DNA replication, and centromere structure, Chp2 associates with the Snf2/histone deacetylase repressor complex (SHREC) to facilitate H3K14 deacetylation and induces transcriptional gene silencing that way (Motamedi et al., 2008; Sugiyama et al., 2007). Despite their functional differences, the overall domain structure of HP1 proteins is highly conserved. HP1s contain a N-terminal CD and a C-terminal chromo shadow domain (CSD), which are connected by a flexible hinge region. The CD directly binds to methylated H3K9 residues, while the CSD is involved in homodimerization and protein-protein interactions (Bannister et al., 2001; Brasher et al., 2000; Cowieson et al., 2000). Comparison of *in vitro* binding constants for three out of the four CD-containing proteins in *S. pombe* (Chp1, Swi6, and Clr4) revealed that Chp1 has the highest and Swi6 the lowest affinity towards methylated H3 peptides (Schalch et al., 2009). Introduction of E80V and V82E point mutations into the CD of Swi6 increases its binding affinity drastically by making it more similar to the high affinity CD of Chp1 (Chp1-like-CD). However, what holds true across all of the CD-containing proteins is their overall preference in binding more tightly to tri-methylated than to di-methylated H3 peptides (Schalch et al., 2009).

In contrast to the CD and the CSD, the hinge region is known to have nucleic acid binding capacity (Muchardt et al., 2002). Keller and colleagues have shown that the flexible hinge of Swi6 binds to RNAs arising from heterochromatic regions, which mediates transfer of said RNAs to Cid14 priming them for the RNA degradation process (Keller et al., 2012). Notably, binding of RNA to the hinge of Swi6 triggers a conformational change in the CD, causing it to dissociate from heterochromatin.

Therefore, association of Swi6 with methylated H3K9 *in vivo* is highly dynamic and also necessary for its role in heterochromatic gene silencing.

3.7. Constitutive Heterochromatin in *S. pombe*

Large, repetitive DNA sequences have to be continuously repressed to ensure genome integrity by preventing aberrant events, such as unwanted recombination, chromosome loss, chromosome segregation defects, and many more (Allshire et al., 1995; Saksouk et al., 2015). These permanently heterochromatic regions are thought to exist at the same genomic location in every cell (type). Due to their static nature, these regions are referred to as constitutive heterochromatin.

In the genome of the fission yeast *S. pombe*, multiple regions are classified as constitutive heterochromatin, such as the centromeres and telomeres of all three chromosomes, the mating type locus on chromosome II, and the rDNA repeats on both ends of chromosome III (Figure 11) (Cam et al., 2005). In the following parts of my introduction, I would like to concentrate on describing the structure and pathways relevant for centromeric heterochromatin, as this region turned out to be the focal point of my PhD study. However, it is noteworthy that there is a big overlap between the aforementioned loci, concerning the factors that are essential for initiation and maintenance of heterochromatin.

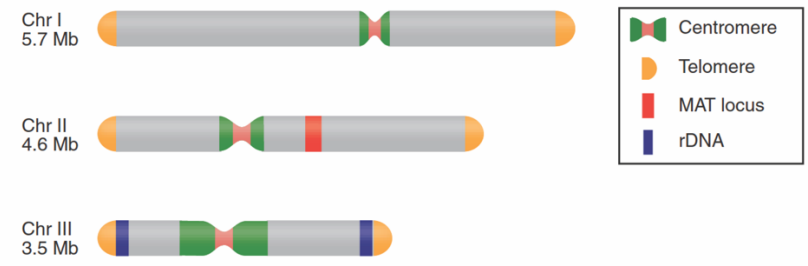

Figure 11. Distribution of constitutive heterochromatin across the three *S. pombe* chromosomes.
Constitutive heterochromatin can be found at the telomeres and centromeres of all three fission yeast chromosomes. Additionally, the mating-type locus on chromosome II and the rDNA repeats on both ends of chromosome III are silenced permanently. Figure adapted from Allshire & Ekwall, 2015.

The central functional structure of all centromeres is the central core (*cnt*), where homologous chromosomes attach during meiotic recombination and kinetochores assemble to allow proper mitotic and meiotic chromosome segregation (Ding et al., 1993; Yokobayashi et al., 2003). This is not just the case for the three centromeres of *S. pombe* but also true for metazoans in general. Both sides of the *cnt* are made up with repetitive sequences called innermost (*imr*) and outermost (*omr*) repeats (Figure 12). The *omr*s are composed of an alternating sequence of tandem repeats (*cendg/cendh*), which exhibit strong silencing capabilities and little transcriptional activity (Allshire et al., 1995). Interference with pathways that ensure maintenance of centromeric heterochromatin results in accumulation of sense and antisense RNA Pol II transcripts from these *cendg/cendh* repeats (Verdel & Moazed, 2005; Volpe et al., 2002). Unique inverted repeats (*IRC*), cluster of tRNA genes, and long non-coding RNAs can cap off the pericentromeric repeats at both ends and help to prevent illegitimate spreading of heterochromatin, acting as “barriers” or boundary elements (Cam et al., 2005; Keller et al., 2013; Scott et al., 2006; Takahashi et al., 1991).

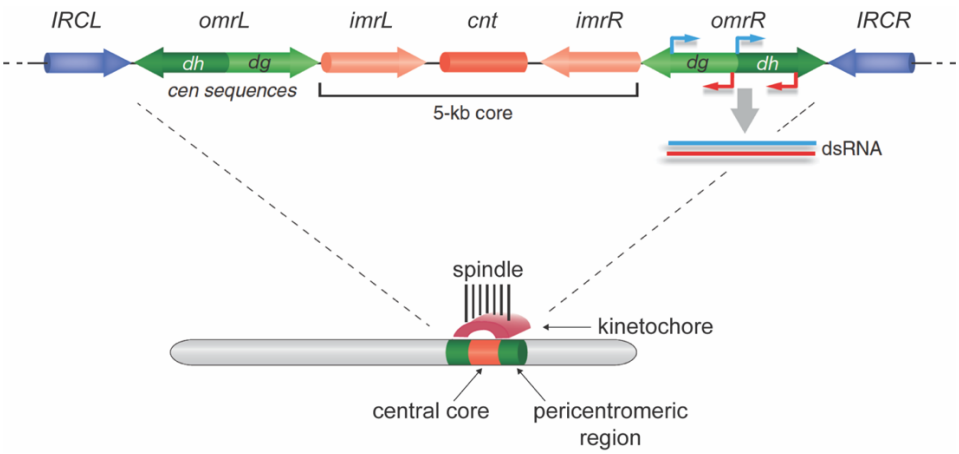

Figure 12. Schematic illustration of a close-up view of *S. pombe* centromere organization.
The *cnt* is void of H3K9 methylation and acts as a platform for kinetochore assembly and spindle attachment. Heterochromatic pericentromeric *cendg* and *cendh* repeats flank the *cnt*. Even though they are heterochromatic, these repeats show basal levels of bidirectional transcription. Figure adapted from Martienssen & Moazed, 2015.

3.8. Facultative heterochromatin in *S. pombe*

In contrast to constitutive heterochromatin, there are gene-rich loci that are conditionally silenced in a subset of cell types or during differentiation. Depending on cellular signals the underlying chromatin state can change and thus influence gene activity. Therefore, these regions were termed developmentally regulated or facultative heterochromatin (Trojer & Reinberg, 2007). The probably most prominent case of facultative heterochromatin regulating gene expression, is the X-linked dosage compensation in female mammalian cells. There, one X chromosome is subjected to inactivation by silencing, thus ensuring equal gene expression of X-linked gene products between the two sexes (Heard & Disteche, 2006).

A decade ago, facultative heterochromatin islands were reported to exist in the fission yeast *S. pombe*, which predominantly coincide with meiotic genes (Figure 13) (Hiriart et al., 2012; Zofall et al., 2012). These facultative islands are regulated by the RNA degradation machinery and the putative HKDM Epe1, that either maintain or disassemble them, respectively. Paradoxically, several meiotic genes are transcribed during vegetative growth. To prevent inappropriate expression of these meiotic transcripts, they undergo selective degradation via the RNA degradation machinery which further promotes the initiation of facultative heterochromatin at those sites. (Harigaya et al., 2006; Zofall et al., 2012). Nascent transcripts emanating from these loci contain a unique *cis*-acting determinant of selective removal (DSR) element, marking them for nuclear exosome-mediated degradation (Harigaya et al., 2006). The DSR element is bound by the specialized RNA-binding protein Mmi1 which bridges these transcripts to the RNA-degradation machinery via Red1 (Zofall et al., 2012). Before the transcripts are processed by the exosome, nucleation of heterochromatin is thought to happen by recruitment of HKMTase activity in the form of CLRC (Hiriart

et al., 2012; Zofall et al., 2012). Once cells enter the meiotic program, the heterochromatic state of these facultative islands is reversed in an Epe1-dependent manner.

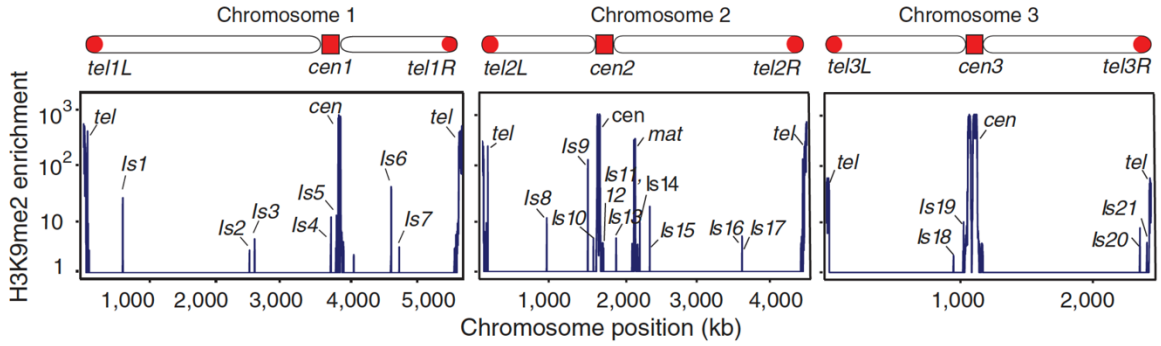

Figure 13. Facultative heterochromatin islands in wild-type *S. pombe*.
Besides the classical constitutive heterochromatin regions, *S. pombe* supposedly contains multiple facultative heterochromatin islands (*Is1-Is21*) at ectopic sites. Figure adapted from Zofall et al., 2012.

In my experience, detection of these heterochromatic islands is not as straightforward as stated in some reports. I analyzed an array of different, as wild-type annotated, *S. pombe* strains, which revealed that there are wild-type strains in circulation that do and do not contain these facultative islands (see discussion). This observation can also be made when comparing different, published, genome-wide wild-type H3K9me2 ChIP data sets, suggesting that detection of these islands is not completely reproducible (Cam et al., 2005; Zofall et al., 2012). Interestingly, these observations indicate that the *S. pombe* genome contains many heterochromatin nucleation sites outside of constitutive heterochromatin but when or why heterochromatin is being assembled at those loci is not fully understood yet.

3.9. RNA interference and the different forms of gene silencing

To initiate formation of constitutive heterochromatin at pericentromeric repeats and to maintain the heterochromatic state, *S. pombe* heavily relies on a functional RNA interference (RNAi) pathway. RNAi is a conserved silencing mechanism that is

present in most eukaryotes and was first described in the late 1990s in the nematode *Caenorhabditis elegans* (Fire et al., 1998). Initially it was regarded as a phenomenon where exogenous double-stranded RNA (dsRNA) can induce silencing of complementary (reporter) genes. Over time, the definition of RNAi changed and by now describes a gene silencing mechanism that is induced by different classes of small non-coding RNAs that associate with an Argonaute (Ago) family protein (Martienssen & Moazed, 2015). In principle, the source of small RNAs is provided by the endonuclease Dicer, which processes dsRNA into 20-24 nt fragments. Subsequently, these small RNAs can be loaded onto Argonaute-containing effector complexes that are thereby specifically guided to complementary transcripts by base pairing (Verdel & Moazed, 2005).

There are multiple routes the RNAi pathway can take to eventually induce a silent state in the fission yeast (Martienssen & Moazed, 2015): (1) RNAi can trigger modification of histones and thereby effect nucleosome structure and stability, inducing heterochromatin formation directly. This hampers transcription and is therefore generally referred to as transcriptional gene silencing (TGS); (2): RNAi can prime target transcripts for degradation in the cytoplasm or block translation of mRNAs, which is called post-transcriptional gene silencing (PTGS); (3) RNAi can mediate degradation of nascent transcripts from heterochromatic domains, in a process known as co-transcriptional gene silencing (CTGS).

3.9.1. Formation of constitutive heterochromatin at centromeres

When talking about RNAi-mediated transcriptional gene silencing and heterochromatin formation, *S. pombe* can be regarded as one of the pioneers since it was heavily involved in elucidating basic principles of the nowadays known

mechanisms. This is partly due to the fact that, just like for Clr4, *S. pombe* contains only a single gene for each of the key proteins involved in the RNAi pathway, namely Ago (*ago1*$^{+}$), Dicer (*dcr1*$^{+}$), and the RNA-dependent RNA polymerase (RdRP, *rdp1*$^{+}$) (Holoch & Moazed, 2015a). It became apparent rather early that an intact RNAi machinery is essential for centromeric H3K9 methylation and transcriptional silencing of pericentromeric repeats (Volpe et al., 2002). Our current understanding of the RNAi-mediated heterochromatin formation implies a tight interplay between RNAi and H3K9 methylation, in which these two pathways depend on each other and create a strong self-reinforcing positive feedback loop (Holoch & Moazed, 2015a).

In a first step, RNA Pol II-dependent transcripts of the *cendg*/*cendh* repeats are used as a template by the RdRP complex (RDRC) to synthesize dsRNA (Figure 14) (Colmenares et al., 2007; Kato et al., 2005). Dsh1 couples the *S. pombe* Dicer homolog Dcr1 to RDRC, thus bringing its RNase III activity close to the generated dsRNA (Kawakami et al., 2012). The dsRNA is eventually cleaved by Dcr1 into small interfering RNAs (siRNAs) which are then loaded onto Ago1 with the help of the Argonaute siRNA chaperone (ARC) complex (Buker et al., 2007; Colmenares et al., 2007; Holoch & Moazed, 2015b). In addition to facilitate loading of Ago1, ARC also represses its slicer activity, prohibiting maturation of the siRNA by blocking the release of the passenger strand. Besides Ago1, ARC contains the proteins Arb1 and Arb2, which are replaced by Tas3 and the CD protein Chp1 once Ago1 has bound the double-stranded siRNA, creating the RNA-induced transcriptional silencing (RITS) complex (Buker et al., 2007; Verdel et al., 2004). Subsequently, siRNA-bound Ago1 guides the RITS complex to new sites of RNA Pol II transcription, where it binds directly to nascent centromeric transcripts via base pairing and sequence complementarity of the guide siRNA (Shimada et al., 2016). Physical interaction of the

RITS complex with Hrr1, a subunit of RDRC, recruits Rdp1-activity towards these transcripts, triggering new cycles of dsRNA synthesis and in turn siRNA generation by Dcr1 (Motamedi et al., 2004). Hence, the pool of available siRNA is steadily increased which results in an amplification of the heterochromatin formation cycle. At the same time, this pathway degrades heterochromatic transcripts and thereby contributes to the repression of heterochromatin (CTGS).

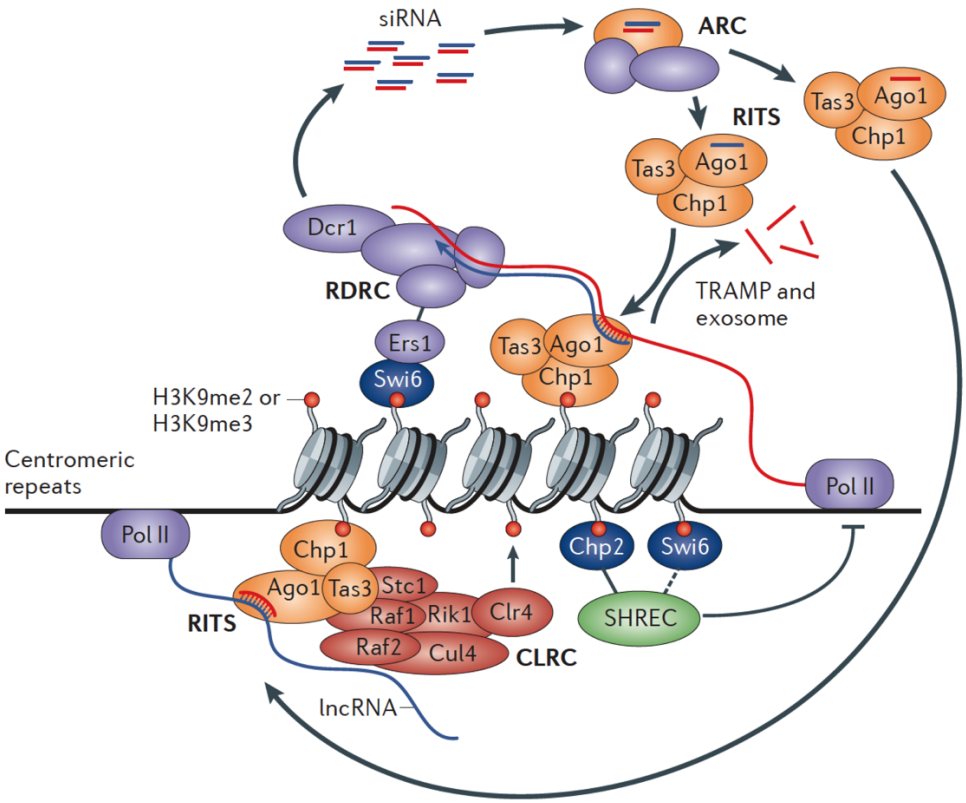

Figure 14. Self-reinforcing feedback loop ensures RNAi-mediated heterochromatin formation in *S. pombe*. The key steps of RNAi-mediated heterochromatin formation at *S. pombe* centromeres are explained in the main text. The black arrows visualize the interplay of the RNAi machinery and CLRC to, first, amplify the heterochromatin formation cycle and, second, repress the centromeric repeats by CTGS. Figure adapted from Holoch & Moazed, 2015a.

The RITS complex engages with many more effector proteins as well as various histone modifying enzymes to regulate CTGS and TGS. As a matter of fact, artificially tethering RITS to nascent transcripts of active genes is already sufficient to trigger

H3K9 methylation, Swi6 binding, and CTGS, emphasizing its role in orchestrating heterochromatin formation (Bühler et al., 2006). Stc1, a bridging protein, links the RITS complex to CLRC and thus brings Clr4s HKMTase activity in close proximity to centromeric chromatin causing methylation of H3K9 and subsequent binding of Swi6 (Bannister et al., 2001; Bayne et al., 2010; Nakayama et al., 2001). Deposition of H3K9 methylation does not only attract Swi6 but also the other CD-containing proteins including, in addition to Clr4 itself, Chp1 and Chp2. Clr4s affinity towards methylated H3K9 is essential for silencing and enhances its binding to chromatin (Ivanova et al., 1998). Similarly, having affinity towards methylated H3K9, by means of Chp1, is a great benefit for the RITS complex. Chp1 secures binding of RITS on chromatin and said binding affinity is essential for heterochromatin maintenance (Partridge et al., 2002; Schalch et al., 2009). As already touched upon, Chp2 plays a key role in TGS as part of SHREC by deacetylating H3K14 and thereby reducing RNA Pol II levels and binding of TFs in general (section 3.6).

3.10. The role of H3K9 methylation in genome stability and disease

The main reason why aberrant H3K9 methylation levels have an effect on genome integrity and thus are responsible for several diseases, is its impact on heterochromatin as a structural component in biological events. In most cases, it boils down to the functional state of the centromeres which is why loss of silencing mutants, such as RNAi components and defective Clr4, exhibit elevated chromosome loss as well as mitotic and meiotic segregation defects (Allshire et al., 1995; Bernard et al., 2001; Ekwall et al., 1996; Nonaka et al., 2002). The same holds true for *D. melanogaster*, mouse, and human cells, speaking for the conserved importance of heterochromatin (and heterochromatin proteins) in genome stability (Kellum & Alberts,

1995; Melcher et al., 2000; Peters et al., 2001). The family of HP1 proteins are the link between centromeric heterochromatin and faithful chromosome segregation. Swi6 does not only physically bridge between the centromere and mitosis-specific (Rad21) and meiosis-specific (Rec8) cohesin complexes but also ensures the correct temporal attachment of sister chromatids during meiotic divisions (Bernard et al., 2001; Kitajima et al., 2004; Nonaka et al., 2002).

Consequences of chromosome segregation errors are fatal and lead to cells containing the incorrect number of chromosomes which is referred to as aneuploidy. Aneuploidy can be traced back to issues during microtubule - kinetochore attachment or chromosome cohesion defects, where sister chromatid cohesion is either lost prematurely or persists too long (Gordon et al., 2012). In the human female, the first meiotic division is particularly error-prone, which makes aneuploidy the leading known cause for miscarriages or mental retardation (Hassold & Hunt, 2001).

Aberrant H3K9 methylation can also lead to certain forms of cancer and correlates with increased cancer recurrence and poor survival. Additionally, mutations in the human H3K9 HKMT EHMT1 have been linked to intellectual disability and neuronal diseases (Greer & Shi, 2012).

4. Aim of this thesis

As can be inferred from the introductory part of my thesis, by now we have in-depth knowledge about heterochromatin initiation and maintenance in mitotic *S. pombe*. Further, we are quite aware of the factors that are downstream of H3K9 methylation and the important biological processes or physiological roles that they are connected to. This part holds true for mitosis as well as meiosis. Despite that, genome-wide studies of H3K9 methylation, and the epigenome in general, was so far limited to

mitotic cells only and the sexual life cycle remained heavily understudied. A possible explanation for the lack of such studies could be, that combination of ChIP experiments with sexually differentiating *S. pombe* was regarded as too elaborate, since cells initiate meiosis at different rates without the use of a special synchronization protocol. Otherwise, the resulting ChIP would never be representative of the actual meiotic stage but rather reflect the average signal of an asynchronous meiotic cell population. During my PhD, I wanted to take it upon me and try to combine ChIP-seq with synchronized meiotic fission yeast cultures, to generate the first genome-wide H3K9me2 and H3K9me3 data sets during fission yeast meiosis.

Moreover, up until recently H3K9me2 and H3K9me3 were used interchangeably when talking about gene silencing and heterochromatin. Recent studies in mutant Clr4 strains however revealed that these two histone marks can form functionally distinct heterochromatin domains (Jih et al., 2017). But whether partitioning of heterochromatin into H3K9me2 and H3K9me3 domains really happens, and what physiological role these domains would have, remains unclear. Therefore, I got really excited when I discovered that there actually exists a condition when *S. pombe* contains predominantly H3K9me3 nucleosomes during early meiosis. This opened up the opportunity for me to investigate the role of exclusively tri-methylated H3K9 domains in a physiological context as well as the underlying regulation behind the H3K9 methylation switch.

RESULTS

1. Cdc2-dependent phosphorylation of Clr4 controls a H3 methylation switch that is essential for gametogenesis

---

Cdk1-dependent phosphorylation of Clr4^{Suv39H} controls a histone H3 methylation switch that is essential for gametogenesis

T. Kuzdere, V. Flury, T. Schalch, V. Iesmantavicius, D. Hess & M. Bühler

Nature Structural & Molecular Biology, in revision

The entire unpublished manuscript can be found in the appendix section.

Summary

Combination of ChIP-seq with a synchronization protocol for fission yeast meiosis allowed me to map H3K9me2 and H3K9me3 to the *S. pombe* genome during mitosis, premeiotic G_1 arrest, and the meiotic program at hourly intervals. When comparing the distribution of the two heterochromatic histone marks in *clr4*$^+$/*clr4*$^+$ cells, I did not detect *de novo* formation of facultative heterochromatin during sexual differentiation. However, H3K9 methylation levels at constitutive heterochromatin regions, such as (sub-) telomeres, mating-type locus, and centromeres, changed drastically between mitosis and early meiosis. More precisely, H3K9me2 was lost 1h into meiosis whereas H3K9me3 signal increased anticorrelatively. Both histone marks started to go back to initial, mitotic, levels after 2h into meiosis. Intrigued by the unanticipated switch to H3K9me3 at the onset of meiosis and the role of constitutive heterochromatin, especially centromeres, in genome stability I was curious to see what would happen if cells went through meiosis without the ability to tri-methylate

H3K9. It turned out, that the H3K9me3-depleted *clr4*^{F449Y}/ *clr4*^{F449Y} strain had troubles segregating chromosomes during the first meiotic division, even though mitotic chromosome segregation was not affected. In a series of rescue experiments, I convincingly showed that highest binding affinity of Swi6 was needed at the onset of meiosis to ensure its proper subnuclear localization and to prevent said chromosome segregation defects during meiosis I. *In vivo*, strongest binding of Swi6 to centromeric repeats can only be achieved by completely tri-methylating centromeric nucleosomes at H3K9, fitting well with the H3K9 methylation switch that I observed in early meiosis. In an attempt to figure out how the methylation activity of Clr4 might be regulated from catalyzing predominantly H3K9me2 to H3K9me3, I discovered that Clr4 is differentially phosphorylated in its ARL (S458) during the mitotic and meiotic program. Clr4^{S458} was dephosphorylated during early meiosis (0h-1h) and became gradually phosphorylated after 2h into the meiotic program, correlating well with the timing of the H3K9 methylation switch. Lastly, I performed a small-scale candidate screen in order to identify the kinase that is involved in modifying Clr4. Surprisingly, phosphorylation of Clr4 critically depends on the key cell cycle regulator Cdc2. Inhibition of Cdc2 activity in mitotic cells showed decreased H3K9me2 and increased H3K9me3 levels, mimicking the H3K9 methylation switch that naturally occurs at the onset of meiosis.

In summary, I was the first to profile the two repressive histone marks, H3K9me2 and H3K9me3, genome-wide during fission yeast meiosis. Further, my PhD work described the first physiologically relevant difference between these two methylation states and revealed that plasticity of constitutive heterochromatin during meiotic progression is required to ensure faithful chromosome segregation during meiosis I. This safeguarding mechanism involves the conserved proteins Cdc2 (CDK1), Clr4, and Swi6 which suggests that the regulation of constitutive

heterochromatin during meiosis in humans could be regulated in a similar way. If this holds true, my findings could have key implications for understanding genetic disorders associated with aberrant chromosome segregation resulting in aneuploidy, such as Down syndrome or certain forms of cancer.

Contributions

This manuscript contains the results of my PhD project. The initial idea to study epigenetic regulation during fission yeast meiosis came from Marc Bühler and Valentin Flury, before I joined the laboratory. In constant discussion with Marc, I further developed the project on my own. I performed all the experiments and analyzed the generated data. Here, I would like to highlight that I implemented and further optimized the synchronization protocol to make it compatible with ChIP-seq. Vytautas Iesmantavicius and Daniel Hess, members of the Protein Analysis Facility at the FMI, analyzed the Clr4 IP-MS data and Thomas Schalch from the LISCB performed the recombinant Clr4-Cdk1/Cyclin B *in vitro* kinase assays.

2. Additional data

2.1. Facultative heterochromatin islands in *S. pombe*

Reports have shown that several DSR-containing meiotic genes are actively transcribed in mitotically growing cells (Harigaya et al., 2006). To prevent aberrant expression of these meiotic transcripts, they undergo selective degradation via Mmi1, Red1, and the nuclear exosome which additionally promotes assembly of facultative heterochromatin at those loci (Harigaya et al., 2006; Hiriart et al., 2012; Zofall et al., 2012).

RESULTS

My H3K9me2 ChIP-seq data in mitotic *clr4*$^{+}$*/clr4*$^{+}$ cells does not show enrichment of H3K9me2 outside of constitutive heterochromatin regions. In addition, as already hinted to in my introduction, inconsistencies in detecting these heterochromatic islands can be seen by comparing different, published H3K9me2 datasets. To figure out if the irreproducibility of detecting the facultative heterochromatin islands is due to technical differences or arises from elsewhere, I set out and compared H3K9me2 levels in multiple different wild-type *S. pombe* strains by ChIP-qPCR. Three of the wild-type strains I used were the original isolates from Urs Leupold, 968 *h*^{90}, 972 *h*$^{-}$, and 975 *h*$^{+}$. I selected primers against two out of the three most enriched facultative islands, *mei4*$^{+}$ (*Island 9)* and *mcp7*$^{+}$ (*Island 1*), and compared the H3K9me2 signal in each wild-type strain against the enrichment at the pericentromeric repeats, *cendh* (Figure 15) (Zofall et al., 2012). The experiment was done in parallel, including a *clr4*Δ strain which was used as a background control. The H3K9me2 enrichments at the centromeric repeats were comparable between all wild-type strains. However, only spb594 showed high levels of H3K9me2 at *mei4*$^{+}$ and *mcp7*$^{+}$ whereas the other wild-type strains (spb64, spb65, and spb66) displayed none or marginal enrichments over background, *clr4*Δ, level.

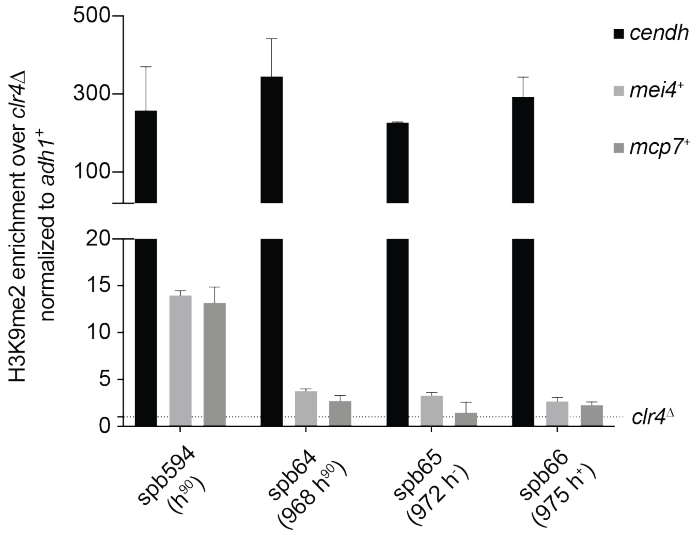

Figure 15. H3K9me2 levels at facultative heterochromatin islands in different wild-type *S. pombe* strains. ChIP-qPCR experiment to assess H3K9me2 levels at *cendh*, *mei4*$^{+}$, and *mcp7*$^{+}$ in vegetatively growing wild-type cells. ChIP enrichments were normalized to *adh1*$^{+}$ and are shown relative to *clr4*Δ cells; Error bars, s.d.; *n* = 3 independent biological replicates.

2.2. Site-directed mutagenesis of Clr4 ARL

The biological relevance of specific phosphorylation events can be dissected by site-directed mutagenesis (Dissmeyer & Schnittger, 2011). For that, the phosphorylated target residue is substituted with either a phospho-mimetic or a non-phosphorylatable amino acid, which in most cases implies the use of aspartate (Asp, D) or alanine (Ala, A), respectively. To test if the phosphorylation state of Clr4^{S458} directly influences its HKMTase activity, I replaced S458 of 3xFLAG-Clr4 with D or A, trying to mimic a constantly phosphorylated or non-phosphorylated Clr4^{S458}. Following that, I assessed H3K9me2 and H3K9me3 levels at pericentromeric repeats (*cendh*) in those mutant Clr4 strains (*3xFLAG-clr4*^{S458A} and *3xFLAG-clr4*^{S458D}) and compared the enrichments to an unaltered wild-type *3xFLAG-clr4*$^{+}$ strain (Figure 16). The experiment was done in parallel and total H3 ChIP levels were used to normalize the H3K9 methylation enrichments. Both *3xFLAG-clr4*^{S458A} and *3xFLAG-clr4*^{S458D} showed slight downregulation of H3K9me3 at *cendh*, compared to wild-type *3xFLAG-clr4*$^{+}$.

Regarding H3K9me2, only non-phosphorylatable Clr4^{S458A} displayed increased enrichments, whereas wild-type and phospho-mimetic Clr4^{S458D} featured the same levels.

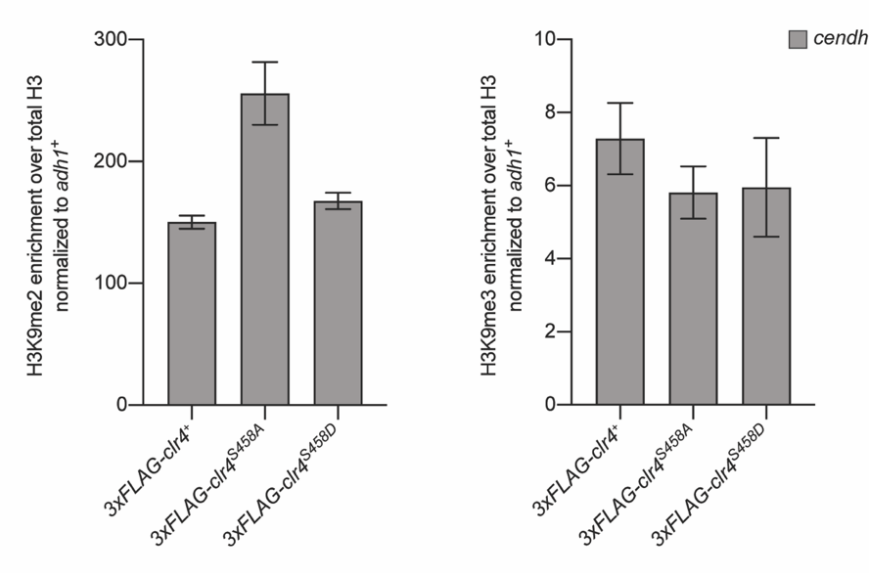

Figure 16. H3K9 methylation levels in phospho-mimetic and non-phosphorylatable Clr4^{S458} mutants.
ChIP-qPCR experiments to assess H3K9me2 and H3K9me3 levels at *cendh* in vegetatively growing cells. H3K9 methylation enrichments of phospho-mimetic Clr4^{S458D} and non-phosphorylatable Clr4^{S458A} mutants were compared to wild-type Clr4 (*3xFlag-clr4*$^{+}$). ChIP enrichments were normalized to *adh1*$^{+}$ and are shown relative to total H3 levels; Error bars, s.d.; *n* = 2 independent biological replicates.

DISCUSSION

Chromatin states and centromere organization are key for (C)TGS and ensuring genome integrity. Given that the meiotic program is accompanied by large chromosomal rearrangements, undergoes immense transcriptional changes, and heavily depends on functional centromeric domains to perform meiotic divisions, I find it surprising that we are still in the dark when it comes to the meiosis-specific epigenome. This lack of knowledge is due to the technical difficulty of generating epigenetic maps in sexually differentiating cells. The results presented in this thesis provide the first source of global histone PTM distribution during *S. pombe* meiosis. With my work, I demonstrate that constitutive heterochromatin exhibits a dynamic H3K9 methylation landscape when transitioning from the mitotic to the meiotic life cycle. My data suggests a safeguarding mechanism, in which Cdc2-dependent regulation of Clr4 activity and highest binding affinity of Swi6 are needed for reductional segregation of chromosomes during the first meiotic division. I showed that dephosphorylation of Clr4 correlates with increased tri-methylation of H3K9 at constitutive heterochromatin. Notably, H3K9me3 appears to be predominant at centromeric domains during early meiosis and these domains function as the best binding site for CD-containing proteins in terms of affinity. These observations highlight the role of heterochromatin plasticity during sexual differentiation and reveal the first physiologically relevant difference between H3K9me2 and H3K9me3 containing chromatin domains.

H3K9 methylation dynamics at constitutive heterochromatin during meiosis

One of the most exciting observations of my PhD work is that H3K9 methylation levels at constitutive heterochromatin undergo drastic changes when cells enter the

meiotic program. Such global changes between samples can hint towards technical issues impacting the effectiveness of ChIP experiments, like crosslinking efficiency and chromatin shearing (Wiehle & Breiling, 2016). Further, the non-inherently quantitative nature of the ChIP-seq method makes comparisons between different ChIP samples tricky, as standard reads per million (RPM) normalization displays the ChIP signal merely as a percentage of all mapped reads, making it prone to background signal levels (Orlando et al., 2014). To rule out the above-mentioned technical issues and to permit direct comparison between ChIP-seq samples, a defined amount of exogenous spike-in chromatin can be used to normalize signals of each sample to internal controls instead to the total mapped reads. Growing fission yeast cells and synchronizing meiotic progression to generate H3K9me2, H3K9me3, and total histone H3 ChIP-seq libraries in triplicates at ten hourly intervals is quite elaborate. Reducing every non-essential step in this long series of experiments helps to make it more manageable and, more importantly, minimizes potential sources of errors. Hence, I decided to test and apply mESC spike-in normalization only to the pair of samples exhibiting the most drastic changes: asynchronous mitotic and early meiotic cells (1h). Independent of the normalization method, RPM or internal spike-in control, H3K9me2 was lost and H3K9me3 was increased significantly when comparing mitotic to early meiotic cells. Therefore, I reasoned that mESC spike-in normalization can be omitted for this experiment and standard RPM normalization is sufficient to compare H3K9 methylation levels between the different time points. Another good indicator, albeit not an ultimate proof, that the observed differences in H3K9 methylation during meiotic progression are real, is the fact that the changes in H3K9me2 and H3K9me3 levels anticorrelate and do not show the same trend, be it down – or upregulation. This holds true for early meiosis (0h-1h) when H3K9me2 is

depleted and H3K9me3 is enriched and 2h into the meiotic time course when cells start to re-establish the initial, mitotic H3K9me2/H3K9me3 ratio. Anticorrelated behavior of the two methylation states, more precisely accumulation of H3K9me2 when the transition to H3K9me3 is interfered with, can be observed in different Clr4 mutants, such as *clr4*^{F449Y} and *clr4*^{W31G}, in the absence of the AAA-ATPase Abo1, and with an instable version of the E2-ubiquitin-conjugating enzyme Ubc4 (Dong et al., 2020; Jih et al., 2017; Kim et al., 2021). Further, *clr4*^{F449Y}/*clr4*^{F449Y} cells show steady H3K9me2 levels when being forced through meiosis and do not mimic the loss of said histone mark at the onset of meiosis. Taken together, this suggests that the depletion of H3K9me2 at constitutive heterochromatin during early meiosis is a consequence of Clr4s tri-methylation activity and thus goes hand in hand with increased H3K9me3 at those sites.

What I unfortunately could not address yet during my PhD work is how the initial, mitotic H3K9me2/H3K9me3 ratio is re-established so rapidly after 2h into meiosis. The intriguing part here is the quick time window in which the methylation switch is reversed. This excludes mechanism linked to nucleosome exchange and suggests that the methylation mark itself is targeted for removal. Therefore, the obvious mechanism to consider would be demethylation of the tri-methyl mark by a HKDM. H3K9me3 at constitutive heterochromatin is not lost all at once but declines rather gradually, coinciding with a progressive appearance of di-methylated H3K9 nucleosomes. Therefore, I argue either for a single demethylation step from H3K9me3 to H3K9me2 or a model in which complete demethylation of H3K9me3 is coupled to subsequent *de novo* di-methylation by Clr4. Overexpression of the anti-silencing factor Epe1, a JmjC domain-containing putative H3K9 demethylase, was shown to be involved in reducing H3K9me3 levels *in vivo* (Bao et al., 2019). Even though a direct

proof of its demethylase activity is still lacking, genetic evidence hints towards Epe1 being a HKDM (Ragunathan et al., 2015; Trewick et al., 2007). Epe1 is brought to heterochromatic regions by direct interaction with Swi6, which fits with my data where Epe1 recruitment would be enhanced due to hyper-tri-methylated H3K9 during early meiosis. (Zofall & Grewal, 2006). Deletion of Epe1 results in increased levels of H3K9 methylation as well as illegitimate spreading across heterochromatin boundaries. Hence, it is not so easy to test the involvement of Epe1 in re-establishing the mitotic H3K9me2/H3K9me3 ratio after the methylation switch has taken place, without starting with an already messed up H3K9 methylation state. Therefore, I suggest to create diploid Pat1-as cells with conditionally depletable Epe1, using for instance the auxin-inducible degron system (Epe1-AID), instead of an *epe1*Δ strain (Zhang et al., 2022). I propose, to arrest *pat1-as2/pat1-as2 epe1-AID/epe1-AID* cells in premeiotic G_1-phase by nitrogen starvation to induce the transition from H3K9me2 to H3K9me3 at constitutive heterochromatin. In a next step, I would start the meiotic program by inhibiting Pat1-as and simultaneously initiate degradation of Epe1-AID. This should allow to test if Epe1 is involved in demethylating H3K9me3 2h into meiosis, with the least pleiotropic effects possible.

Facultative heterochromatin in different wild-type *S. pombe* strains

My H3K9 methylation ChIP-seq data points towards the fact that the wild-type *S. pombe* genome does not feature ectopic heterochromatin outside of the constitutively silenced regions – not during mitosis nor during any stage of meiosis. This might come as a surprise to some readers, since several published reports describe the presence of facultative heterochromatin islands at meiotic genes in vegetatively growing cells, which disassemble when meiosis is initiated.

DISCUSSION

As elucidated before, I noticed early into my PhD work that published genome-wide H3K9me2 datasets differ frequently, regarding the detection of these facultative islands. This raised the question to me whether the irreproducibility of mapping H3K9me2 to these sites is based on a technical issue or arises from genomic differences of the strains used. My results demonstrate, that we have wild-type *S. pombe* strains in circulation that differ from the originally isolated strains (968 h^{90}, 972 h^{-}, and 975 h^{+}) with regard to their H3K9me2 levels outside of constitutive heterochromatin (Leupold, 1950). I assume that Leupold's yeast isolates served as founder cells for probably all studies in *S. pombe*, ensuring reproducibility and consistency of generated data due to the isogenic nature of the created strains. However, with the increasing amount of laboratories all around the globe that work with the fission yeast and the generous attitude of sharing generated strains, tracing back the origins of each strain is quite difficult. Same holds true for the wild-type strain spb594, which we obtained from the Nakayama group (RIKEN, Japan) that harbors the facultative heterochromatin islands. Therefore, I speculate that this strain, or one of its previous parental lines, acquired an enabling mutation somewhere in the pathway regulating the formation of ectopic heterochromatin.

Initiation of ectopic heterochromatin assembly is under constant negative regulation. In the absence of the anti-silencing factor Epe1, cells exhibit twice as many ectopic heterochromatin sites and H3K9 methylation spreads across multiple islands compared to *epe1*$^{+}$ strains (Zofall et al., 2012). Further, interfering with the intact exosome RNA degradation machinery causes several additional euchromatic loci, termed heterochromatin domains (HOODs), to become heterochromatic in a RNAi-dependent manner (Yamanaka et al., 2013). Formation of several of these HOODs can also be mediated by certain environmental conditions, such as low temperature

or glucose depletion (Yamanaka et al., 2013). In general, it seems that there is a tendency for the initiation of ectopic heterochromatin whenever the physiological balance between positive and negative regulators of heterochromatin formation is interfered with, either by mutations or exogenous stimuli. Wang and colleagues demonstrated that deletion of Epe1 or Mst2, a H3K14 acetyltransferase, triggers formation of ectopic heterochromatin in otherwise “island-free” *S. pombe* (Figure 17) (Wang et al., 2015). I made similar observations by enhancing the binding properties of Swi6 towards methylated H3K9 beyond its physiological affinity. In very severe cases of aberrant heterochromatin formation and deleterious heterochromatin spreading, cells take advantage of the lack of negative regulators and mitigate the formation of ectopic heterochromatin by silencing the *clr4*$^{+}$ locus itself (Iglesias et al., 2018; Wang et al., 2015). These examples demonstrate that multiple sites in the fission yeast genome have the potential to be theoretically H3K9me2 but methylation is kept in check by several regulatory pathways. Many of these loci are probably still silenced on a regular basis in wild-type cells but the methylation mark is immediately turned over by Epe1.

I propose to sequence and compare the genomic DNA (gDNA) of multiple different “facultative heterochromatin – containing” wild-type *S. pombe* strains to the gDNA of the original fission yeast isolates from Urs Leupold. Spontaneous single nucleotide polymorphisms (SNPs) in genes encoding for regulators of heterochromatin formation could be the reason why there are wild-type strains in circulation that differ in the genome-wide distribution of H3K9me2.

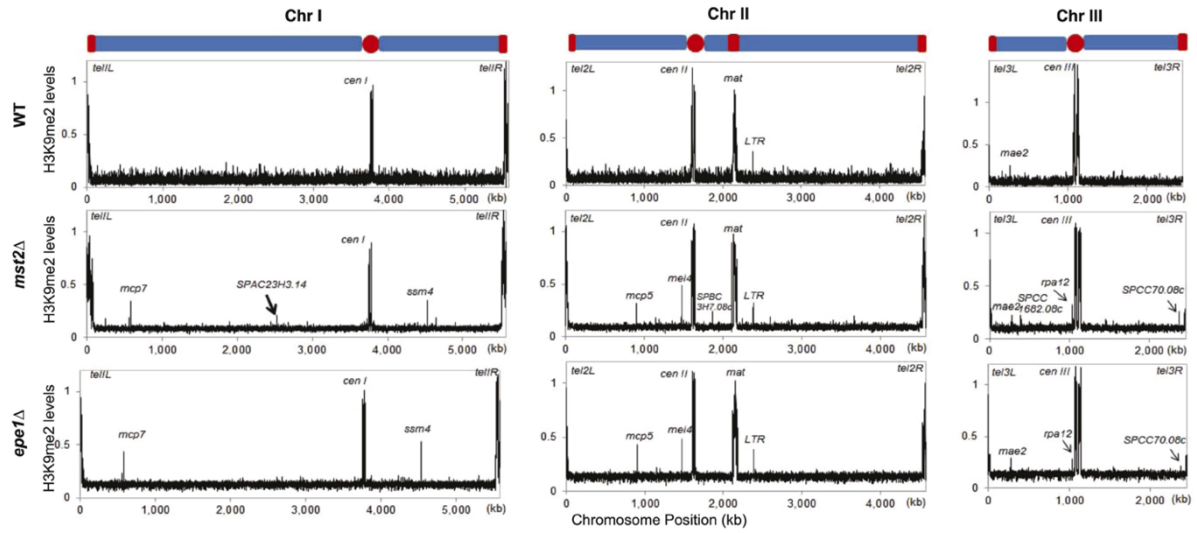

Figure 17. Mst2 and Epe1 counteract the formation of ectopic H3K9me2 sites in the *S. pombe* genome. Genome-wide ChIP-chip data showing the distribution of H3K9me2 in wild-type (WT), *mst2*Δ, and *epe1*Δ cells. Outside of constitutive heterochromatin, no facultative heterochromatin is detected in wild-type *S. pombe* cells. Deletion of Mst2 or Epe1 results in the formation of facultative heterochromatin islands at genes like *mei4*$^{+}$, *mcp7*$^{+}$, and *ssm4*$^{+}$. Figure adapted from Wang et al., 2015.

The role of pericentromeric H3K9me3 in chromosome segregation

Up until recently, H3K9me2 and H3K9me3 were used interchangeably when talking about fission yeast heterochromatin and silencing. The work of Jih and colleagues in 2017, introduced the tools to study the different degrees of H3K9 methylation in the fission yeast *S. pombe* which revealed unique roles for H3K9me2 and H3K9me3 domains in heterochromatin function (Jih et al., 2017). However, these two methylation states usually coexist in wild-type cells and the presence of exclusively di- or tri-methylated H3K9 was only detected in mutant backgrounds so far. Consequently, the relevance as well as the physiological role of uniformly di- or tri-methylated H3K9 domains have remained enigmatic.

To the best of my knowledge, my results reveal the first condition in which constitutive heterochromatin is solely marked by H3K9me3 in wild-type fission yeast cells, namely during premeiotic G_1 arrest and early meiosis. The reason why this hyper-tri-methylated H3K9 state has not been described before might be due to the

intense focus of epigeneticists on the mitotic lifecycle, thus neglecting the genome-wide analysis of histone PTMs during sexual differentiation. My PhD work does not only show the existence of purely H3K9me3 constitutive heterochromatin, it additionally demonstrates the relevance of predominantly tri-methylated H3K9 at centromeric repeats during meiosis. Cells that lack the ability to catalyze H3K9me3 (*clr4*^{F449Y}) display chromosome segregation phenotypes similar to H3K9 methylation depleted cells (*clr4*Δ), albeit only during the first meiotic division and not during mitosis. The missing link between H3K9 methylation and chromosome segregation is the structural HP1 protein, Swi6, which recruits mitotic as well as meiotic cohesin complexes to the pericentromeric repeats to ensure sister chromatid cohesion and proper kinetochore function (Bernard et al., 2001; Kitajima et al., 2004; Nonaka et al., 2002; Yamagishi et al., 2008; Yokobayashi et al., 2003). Combined data from the Moazed laboratory and my own work show that Swi6 localization and enrichment in mitotic and meiotic *clr4*^{F449Y} cells is drastically reduced in comparison to *clr4*$^{+}$ cells, which can be explained by the different *in vitro* binding affinities towards H3K9me2 and H3K9me3 peptides, 10.28 µM and 3.34 µM respectively (Jih et al., 2017; Schalch et al., 2009). However, the amount of Swi6 recruited in H3K9me2-only *clr4*^{F449Y} cells is sufficient to ensure faithful mitotic chromosome segregation and growth in the presence of the microtubule destabilizing drug TBZ, whereas *swi6*Δ cells show lagging chromosomes and increased sensitivity towards TBZ (Allshire et al., 1995; Ekwall et al., 1996). On the other hand, my results reveal that the levels of Swi6 that are recruited to the centromere by H3K9me2 alone do not suffice to allow accurate division during meiosis I, unless the CD of Swi6 is mutated to a Chp1-like-CD, increasing its binding affinity towards H3K9me2 immensely (1.07 µM) (Schalch et al., 2009). These observations mean two things: (1) During mitosis, *S. pombe* cells can cope with the

lack of H3K9me3. Interfering with Clr4's tri-methylation activity increases H3K9me2 at centromeric repeats almost two-fold in comparison to a wild type. These high amounts of H3K9me2 can recruit enough levels of Swi6 to fulfill all necessary functions to uphold faithful mitotic chromosome segregation; (2): During the first meiotic division *clr4*^{F449Y} phenocopies a *clr4*Δ, indicating the existence of a H3K9me3-dependent function which cannot be compensated by high levels of H3K9me2 and the therewith associated levels of Swi6. The fact that high affinity Swi6$^{Chp1\text{-}like\text{-}CD}$ rescues the meiotic segregation phenotype of a *clr4*^{F449Y} strain supports the idea that highest binding affinity of fission yeast HP1 is crucial during early meiosis, which can only be achieved by completely tri-methylating H3K9 at pericentromeric repeats. This raises the question in what aspect mitotic chromosome segregation differs from segregating chromosome during meiosis I. The answer to this question might help to explain why these two processes vary so drastically in their tolerance to pericentromeric Swi6 levels.

The key difference between the mitotic and the first meiotic division lies in the composition of the cohesin complexes and the way they control the orientation of kinetochores towards the spindle pole(s) to allow either equational (mitosis) or reductional (meiosis I) segregation of chromosomes (Figure 18). The mitotic cohesin subunit Rad21 ensures, besides chromatid cohesion, bipolar attachment of microtubules to sister kinetochores by facing them towards the opposite spindle poles. Before premeiotic S-phase, Rad21 is replaced by the meiotic cohesin subunit Rec8 at pericentromeric repeats, causing monopolar attachment of sister kinetochores during meiosis I (Watanabe & Nurse, 1999; Yokobayashi et al., 2003). Rec8 in *A. thaliana* and maize fulfill similar roles in directing monopolar attachment during meiosis I (Chelysheva et al., 2005; Yu & Dawe, 2000). My data suggest that part of the

chromosome segregation defects in *clr4*^{F449Y} result from bipolar attachment during meiosis I, reminiscent of Rec8-depleted cells. In absence of Rec8, Rad21 persists at centromeres during meiosis I but fails to establish monopolar attachment, resulting in equational instead of reductional segregation. Both cohesin complexes are recruited to the centromere in a Clr4-Swi6-dependent manner. However, these processes were studied in either *clr4*$^{+}$ or *clr4*Δ strains, since generating H3K9me2-only cells was not possible previously. Therefore, in light of my data, I would like to propose a mechanism in which recruitment of Rec8 during early meiosis critically depends on H3K9me3-Swi6 whereas the mitotic cohesin counterpart, Rad21, can be sufficiently recruited by H3K9me2-Swi6 alone. This would explain why H3K9me3 is dispensable for mitotic but not the first meiotic division and link the H3K9me3 shift at pericentromeric repeats at the onset of meiosis to the first meiotic division. In ongoing experiments, I am currently trying to see if the high affinity Swi6$^{\text{Chp1-like-CD}}$ can re-establish monopolar attachment in H3K9me3-depleted *clr4*^{F449Y} cells.

Even though Kitajima and colleagues report the dependency of Rec8 on Clr4 and Swi6 to be recruited to pericentromeric repeats, they notice a pool of Rec8 which associates with the central core independent of H3K9 methylation. Interestingly, this population of central core bound Rec8 is sufficient to ensure intact monopolar attachment in the absence of H3K9 methylation, hence no errors during meiosis I are detected in *clr4*Δ and *swi6*Δ strains (Kitajima et al., 2003). At first glance, this seems contradictory to my proposed model where Clr4 and Swi6 are vital for the first meiotic division. However, I think there is a big difference between cells that lack H3K9 methylation completely and cells that are only void of H3K9me3 (Figure 18).

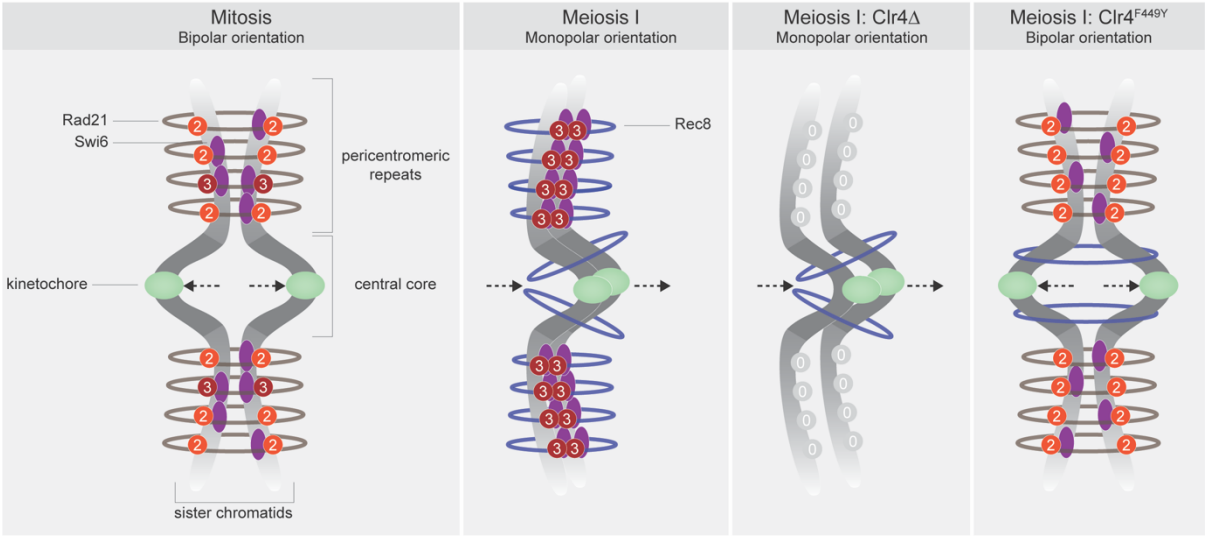

Figure 18. Mitotic and meiotic cohesin recruitment to centromeres dependent on H3K9 methylation levels. Mitosis: During mitosis, the mitotic cohesin Rad21 is recruited to pericentromeric repeats mainly by H3K9me2-Swi6. Binding of Rad21 causes bipolar orientation of kinetochores and subsequent equational segregation of chromosomes; Meiosis I: During early meiosis, H3K9me2 is converted to H3K9me3. This strong affinity binding site recruits high levels of Swi6 and thus the meiotic cohesin Rec8 to pericentromeric repeats. At the central core, Rec8 is additionally recruited in a H3K9 methylation-independent manner during early meiosis. Binding of the meiotic cohesin complex leads to monopolar orientation and reductional chromosome segregation. In H3K9 methylation-depleted cells (*clr4Δ)* the pericentromeric repeats are void of any cohesin complexes. The levels of central core-bound Rec8 are sufficient to ensure proper reductional segregation during meiosis I. My data suggests that in early meiotic H3K9me3-depleted cells (*clr4*^{F449Y}) pericentromeric repeats are coated with H3K9me2-Swi6-Rad21. The function of the mitotic cohesin complex overwrites the action of central core-bound Rec8 and thus enforces bipolar orientation of kinetochores during meiosis I.

In both cases, the H3K9 methylation-independent fraction of Rec8 will be present at the central core, which can compensate for the lack of pericentromeric Rec8 in a *clr4*Δ or *swi6*Δ cell. In the case of *clr4*^{F449Y}, pericentromeric repeats will be covered with fully di-methylated H3K9 nucleosomes which fail to attract Rec8 but not the mitotic cohesin subunit Rad21. I assume that the function of pericentromeric Rad21 will outcompete the role of central core bound Rec8 and enforce bipolar attachment of kinetochores, resulting in equational instead of reductional meiosis I. To test this hypothesis, I recommend to perform live-cell imaging experiments with Rad21-GFP and Rec8-mCherry in *clr4*$^{+}$, *clr4*Δ, and *clr4*^{F449Y} strains with either wild-type Swi6 or

Swi6$^{Chp1\text{-}like\text{-}CD}$ to see which cohesin subunits localize to pericentromeric repeats during meiosis I depending on the degree of H3K9 methylation.

Rec8 and its essential role as a subunit of the meiosis-specific cohesin complex is conserved from yeast to mammals. Even though its function in maintaining cohesion between sister chromatids during meiosis I up until the beginning of meiosis II is very similar in different species, mechanisms evoking around its recruitment and dissociation from chromatin varies quite a bit (Lee et al., 2003). Recruitment of *A. thaliana* Rec8 and mitotic cohesin in MEFs, and thus most likely also the meiotic counterparts, to pericentromeric repeats were shown to be unaltered in the absence of the species-specific HKMTs (Koch et al., 2008; Lambing et al., 2020). Therefore, it is possible that in higher eukaryotes other heterochromatic marks or pericentromeric features, which are not present in *S. pombe*, did evolve to recruit cohesin complexes, such as H3K27 methylation or DNA methylation. But even if H3K9 methylation, or more precisely the transition of H3K9me2 to H3K9me3 at the onset of meiosis, is not a universal trigger for the recruitment of meiotic cohesin complexes to pericentromeric repeats, maybe the underlying mechanism, in temporally enriching for the respective recruiting mark, is.

Temporal H3K9 methylation switch as a recruiting mechanism

The proposal that temporal enrichment of histone PTMs is used for fast and reversible recruitment of downstream “reader” proteins, by creating short-lived, high affinity binding sites, is an interesting idea that poses some questions. In my case, where a transition of H3K9me2 to H3K9me3 is used to strengthen Swi6 binding to pericentromeric regions at the onset of meiosis, one could ask why pericentromeric repeats do not always consist of just H3K9me3 nucleosomes, or why Swi6 did not

simply evolve to have a higher affinity towards H3K9me2 rather than requiring a change from H3K9me2 to H3K9me3 for efficient recruitment?

As demonstrated by Jih and colleagues, exclusively di-methylated H3K9 domains are associated with transcriptionally permissive heterochromatin and allow for RNAi-CTGS to take place (Figure 19). On the other hand, H3K9me3 is linked to classical TGS precisely because of efficient recruitment of Swi6 (Jih et al., 2017). Without the ability to constantly generate pericentromeric transcripts, synthesize dsRNA, and thereby amplify the siRNA pool, the positive feedback loop that upholds heterochromatin would be eventually disrupted. For example, my data reveals that constitutive heterochromatin regions that are not backed up by the RNAi machinery, such as the telomeres, are completely disassembled in *clr4*^{F449Y}. Instead of being recruited to heterochromatin by both, the function of its CD and RITS, it seems that Clr4's dependency on its affinity towards H3K9me3 is the critical step in binding to telomeres. Even its recruitment via the shelterin complex in form of Taz1 and Ccq1 seems to be insufficient in the presence of only H3K9me2 with no underlying amplification loop (Kanoh et al., 2005; Sugiyama et al., 2007). This foreshadows how prone centromeres would be to perturbations if *S. pombe* cells were able to catalyze H3K9me3 only, thereby consisting of just transcriptionally inert heterochromatin, omitting CTGS, and lacking any form of backup mechanism.

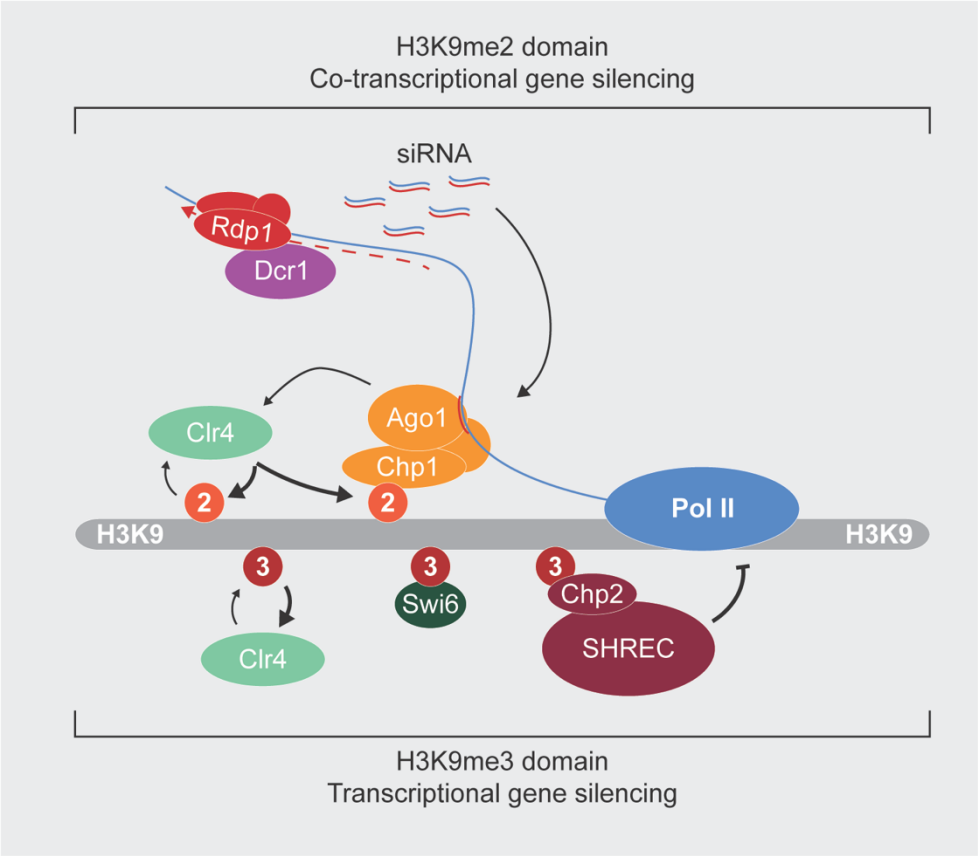

Figure 19. The degree of H3K9 methylation dictates the mechanism of transcriptional gene silencing. H3K9me2 domains allow heterochromatin to be actively transcribed due to inefficient binding of the fission yeast HP1 homologs Swi6 and Chp2. Transcriptionally permissive heterochromatin is established in a RNAi-mediated manner and the nascent pericentromeric transcripts are degraded by CTGS. H3K9me3 domains, on the other hand, are capable of inducing TGS by recruiting high levels of Swi6 and Chp2, which in turn guides effector complexes, such as SHREC, directly to chromatin. Therefore, H3K9me3-coated pericentromeric repeats are regarded as transcriptionally inert.

As stated before, another way for *S. pombe* to increase Swi6 binding, without the need of the tri-methylation switch, could be achieved by tweaking its affinity towards H3K9me2, similar to the mutant Swi6$^{\text{Chp1-like-CD}}$. However, my results indicate that increasing Swi6's affinity towards methylated H3K9 beyond physiological levels does not only result in strong pericentromeric enrichments, it also causes ectopic binding at many sites distributed over the genome. These ectopic Swi6$^{\text{Chp1-like-CD}}$ peaks can cause the formation of facultative heterochromatin in vegetatively growing cells, reminiscent of the situation observed in exosome deletion mutants, *epe1*Δ, *mst2*Δ, and

hyperactive Clr4 mutants (Iglesias et al., 2018; Wang et al., 2015; Yamanaka et al., 2013). As discussed above, this phenomenon typically indicates a disbalance between positive and negative regulators of heterochromatin formation and can have severe effects on the viability of the fission yeast if these facultative heterochromatin domains spread and thus silence essential genes (Iglesias et al., 2018; Wang et al., 2015). Therefore, it is desirable to have a rather low affinity Swi6 protein, as this would firstly prevent unwanted formation of facultative heterochromatin in regions with potential nucleation sites, and secondly provide the organism a means to recruit effector proteins conditionally through modulation of the H3K9 methylation state in a fast and reversible manner.

Role of Clr4 phosphorylation in controlling the H3K9 methylation switch

Post-translational protein modifications are key in regulating protein features in response to extra- and intracellular signals. PTMs can direct protein localization, facilitate protein-protein interaction, steer conformational changes, and regulate enzymatic activities. One of the most abundant PTM is protein phosphorylation which is known to alter protein function in a fast and reversible manner due to the interplay between specific kinases and phosphatases (Ardito et al., 2017; Olsen et al., 2006). Kinases are especially important in signal transduction pathways, where receptor tyrosine kinases such as EGFR are involved in translating extracellular cues into intracellular signals, and during the cell cycle where a kinase network centering around Cdc2 (Cdk1) is essential for the progression and directionality of cell cycle transitions (Moser & Russell, 2000; Seet et al., 2006).

Interestingly, my results reveal the dynamic nature of Clr4^{S458} phosphorylation during the meiotic program which critically depends on the activity of the cell cycle

regulator, Cdc2. Clr4^{S458} phosphorylation is lost during premeiotic G_1 arrest and early meiosis and is subsequently re-established 2h into meiosis. Correlating with the phosphorylation status of Clr4, Cdc2 activity is inhibited in G_1-phase by the CKI Rum1 and continuous inactivation of Cdc2 is essential for initiation of sexual differentiation and early meiosis (Benito et al., 1998). The main cue for *S. pombe* to exit the mitotic life cycle and to enter premeiotic G_1 arrest is nitrogen starvation. This external signal stabilizes Rum1 until the start of premeiotic S-phase, after which Rum1 gets degraded resulting in Cdc2 reactivation (Daga et al., 2003; Stern & Nurse, 1998). The time window of Cdc2 inactivation, loss of Clr4 phosphorylation, and simultaneous gain of H3K9me3 fit extremely well together. These observations would provide a likely mechanism for the H3K9 methylation switch occurring at the onset of meiosis. Yet, so far this is only supported by the correlations described and more direct experimental evidence is needed to strengthen the above-mentioned hypothesis. *In vitro* kinase assays, performed in a collaborative effort together with Thomas Schalch, of recombinant Clr4 and human CDK1/Cyclin B indicate that Clr4 can be a direct substrate of the conserved family of CDKs. This claim is further underlined with my results that show complete loss of Clr4^{S458} phosphorylation in conditionally inactivated *cdc2-as* cells *in vivo*. Inhibition of Cdc2-as activity in mitotically growing fission yeast cells does not only lead to the loss of Clr4 phosphorylation but also to reduced H3K9me2 and increased H3K9me3 levels at pericentromeric repeats, mimicking the H3K9 methylation switch naturally occurring at the onset of meiosis. I am aware of the fact that inhibition of Cdc2 activity *in vivo* can cause heavy stress and secondary effects, as cell division is blocked within one cycle (Dischinger et al., 2008). However, changes in Clr4 phosphorylation levels and the switch in H3K9 methylation activity is rather fast and can be detected within 3h. Together with the *in vitro* kinase data and

the conserved minimal consensus sequence preference of Cdc2 (S/T-P), which matches for Clr4^{S458}, this argues for a causal relationship between Cdc2 activity and Clr4 phosphorylation and not for side effects due to cell cycle arrest or interference with other misregulated targets of Cdc2 (Songyang et al., 1994). It would be advantageous to know if a protein phosphatase is involved in removing Clr4^{S458} phosphorylation or if phosphorylated Clr4 is degraded as a whole by the proteasome when Cdc2 in inhibited. Deletion of the responsible phosphatase would provide me another tool to study the role of constitutively phosphorylated Clr4 during the cell cycle and the therewith associated consequences during meiosis. Hence, I started a small-scale candidate phosphatase deletion screen in the *cdc2-as* strain to see if I can find a condition that prohibits removal of Clr4^{S458} phosphorylation upon Cdc2-as inhibition. Candidate phosphatases were selected either due to their role in antagonizing CDK activity or their physical association with heterochromatin (Iglesias et al., 2020; Mochida & Hunt, 2012).

Interestingly, Cdk1-dependent phosphorylation of the proline-directed serine within the SET- and the post-SET domains of Clr4 appears to be conserved in the mammalian system. That is, SUV39H1^{S391}, analogous to Clr4^{S458}, is phosphorylated by CDK2 in human (HeLa and HEK293) and mouse (NIH3T3) cells (Aagaard et al., 2000; Firestein et al., 2000; Park et al., 2014). The position of the proline-directed serine in the mammalian Clr4 homologs is intriguing since its resides, just like in Clr4, within the ARL (Iglesias et al., 2018; Wu et al., 2010). The ARL was shown to boost HKMTase activity in the fission yeast by undergoing a conformational switch when K455 and K472 of the loop are substituted with methylation-mimicking amino acids (Iglesias et al., 2018). Whereas *in vivo* methylation events of these lysine residues in *S. pombe* are not reported so far, my work describes the presence of a differentially

phosphorylated serine residue within this loop. Several protein kinases rely on a mechanism similar to Clr4 in which an activation loop (A-loop) blocks access to the active site. Upon (auto)phosphorylation of said loop, its autoinhibitory character is lifted and the kinase activity is enhanced significantly. This phosphorylation-induced conformational change is referred to as a "phosphorylation-sensitive switch" (Adams, 2003). Bearing my data in mind, I speculate that Clr4's enzymatic activity, which is in part stimulated by automethylation of the ARL, underlies an additional layer of regulation, namely that of a phosphorylation-sensitive switch. However, in the aforementioned example of protein kinases, a gain of enzymatic activity is achieved by phosphorylation of the A-loop whereas an increase in Clr4 activity correlates with dephosphorylation of the ARL. Many phosphorylation events, independent of their localization on the protein, have also the capability to fulfil inhibitory roles, as seen by phosphorylation of Cdc2 at Tyr15 by Wee1 and Mik1. Logically, dephosphorylation of these residues leads to activation of protein function, again, as demonstrated with dephosphorylation of Cdc2 by Cdc25 (Lundgren et al., 1991).

One underlying principle of the phosphorylation-sensitive switch is stabilization of the phosphorylated A-loop with positively charged side chains using electrostatic interactions (Hubbard, 1997). Therefore, it is conceivable that phosphorylation does not *per se* push unstructured loops away from the active site but that phosphorylation could also move unstructured loops towards the catalytic pocket, depending on the surrounding electrostatic interactions. Further, *in silico* modeling has shown that phosphorylation of X-SP-X motifs, such as in Clr4 ARL (S458-P459), influences *cis/trans* isomerization of the peptidyl-prolyl bond, providing another possible mechanism how phosphorylation of Clr4^{S458} can induce a conformational switch (Hamelberg et al., 2005). Unfortunately, crystal structures of Clr4 are not complete

and densities around the SET- and post-SET domains are missing, probably due to the difficulties of crystalizing the unstructured ARL (Figure 20). The most complete crystal structures are missing the majority of the ARL, more specifically residues 460-472 and 455-468 (PDB ID: 6BOX and 6BP4, respectively), making it almost impossible to conclude anything about potential (electrostatic) interactions and configuration of the S458-P459 backbone in phosphorylated and dephosphorylated Clr4^{S458}. Additionally, recombinant Clr4 is not phosphorylated which raises the question to what degree these structures reflect the *in vivo* Clr4 conformation. Iglesias and colleagues drew their conclusion about ARL structure from the positioning of K455 and the most C-terminal residues of the ARL only (Iglesias et al., 2018). Trying to take a guess, there are two arginine (Arg, R) residues that could help the ARL to block the active site by stabilizing phosphorylated S458, one within the SET-domain (R406) and one in the post-SET region (R474) (Figure 20). However, there is no other option but to solve and compare the structures of phosphorylated and dephosphorylated Clr4 to see if the ARL indeed undergoes a phosphorylation-sensitive switch and if so, how the induced conformational change looks like. For a structural biochemist this should be a straight-forward experiment, since purification and crystallization conditions for Clr4 are readily available. Further, my data shows that *in vitro* generation of non-phosphorylated and phosphorylated Clr4 at S458 by CDK1/Cyclin B is highly efficient and specific. These experiments will be key to explain how the different phosphorylation states of Clr4 could influence its di- or tri-methylation preference.

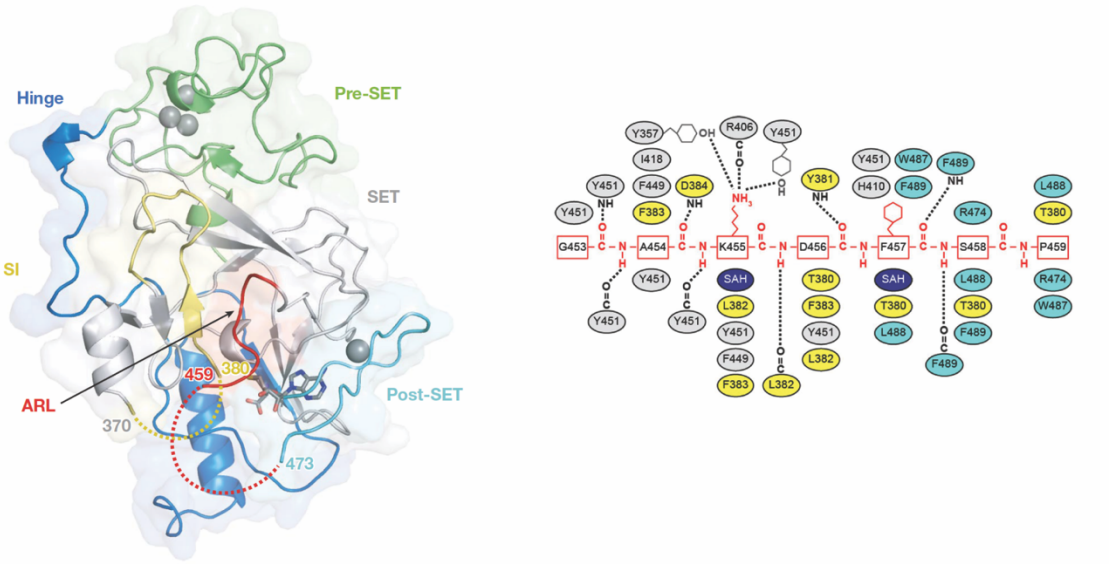

Figure 20. Crystal structure of autoinhibited Clr4 and detected amino acid interactions with the ARL. The dotted line within the ARL (red loop) shows the residues which could not be crystallized. Only the very N-terminal part of the ARL is included in the Clr4 structure (left). Amino acids emerging from the SET-domain (grey), SET insertion domain (yellow), and the post-SET domain (turquoise) which are likely to contact the ARL are indicated here (right); blue domain = hinge; green domain = pre-SET. Figure adapted from Iglesias et al., 2018.

An indispensable tool to decipher the biological role of specific phosphorylation events is the use of phospho-mimetic and non-phosphorylatable amino acid substitutions in target proteins (Dissmeyer & Schnittger, 2011). In the case of serine, the negatively charged amino acid aspartate is commonly used to mimic a constitutively phosphorylated residue, whereas its substitution with alanine mimics a dephosphorylated state. Unfortunately, it is not a given that phospho-mimetics can replace the function of phosphate groups in a cellular context, which is also reflected by the fact that phospho-specific antibodies do not recognize phospho-mimetic substitutions. Moreover, it is rather rare that non-phosphorylatable substitutions reflect the characteristics of an unphosphorylated serine properly, which can be usually neglected if the residue is within a highly ordered domain but might become problematic if the substituted residue lies in an exposed, unstructured loop. Therefore,

the viability of these substitutions has to be proven empirically for each target residue and inconclusive results have to be expected.

Assuming that phosphorylated and non-phosphorylated Clr4^{S458} are mimicked properly with the respective D and A mutations, my H3K9 methylation data implies that there is no difference in tri-methylation activity between the two phosphorylation states. However, di-methylation activity is stimulated in non-phosphorylatable Clr4^{S458A} which is contradictory to the observations made in the conditionally inhibited Cdc2-as system where loss of phosphorylation correlates with H3K9me3. As mentioned before, a good indicator for a genuine change in H3K9 methylation activity is anticorrelation of the gained vs the lost marked e.g. increase in di-methylation and decrease in tri-methylation or *vice versa*, which is not the case for these amino acid substitutions. One explanation which would fit with my ChIP data, is that non-phosphorylatable Clr4 causes hypermethylation, similar to automethylated Clr4 (Iglesias et al., 2018). In this scenario, the high levels of H3K9me3 would be immediately turned over to H3K9me2 by Epe1, thus masking an increase in Clr4's tri-methylation activity and exhibiting increased H3K9me2 levels instead. To test this hypothesis, I suggest to check H3K9me2 and H3K9me3 levels in *clr4^{S458A} epe1*Δ cells and compare the enrichments to *clr4^{+} epe1^{+}* and *clr4^{+} epe1*Δ.

Otherwise, the possibility exists that substitution of the polar S458 residue with a non-polar alanine disrupts important interaction sites within Clr4 and thereby influences ARL structure and positioning. This could potentially result in changes in HKMTase activity independent of mimicking a non-phosphorylatable state. To address this question, Thomas Schalch and I have started to look into Clr4s HKMTase activity using *in vitro* methyltransferase assays. However, these experiments were just performed once so far and the data is too preliminary to draw any conclusions from.

Knowing the respective *in vitro* methylation kinetics of the different Clr4^{S458} versions (D, A, phosphorylated, and non-phosphorylated) would provide me confidence to either use, and study the effect of the amino acid substitutions *in vivo*, or to declare them as malfunctioning. Independent of that, the *in vitro* methylation assay with phosphorylated and non-phosphorylated Clr4^{S458} should ultimately reveal if phosphorylation of the ARL affects Clr4's H3K9 methylation activity directly or indirectly.

Phosphoregulation of the SUV family of H3K9 methyltransferases

In early 2000, Aagaard and colleagues predicted multiple potential phosphorylation sites on the human Clr4 homolog, SUV39H1 (Aagaard et al., 2000). Four of these phosphorylation sites cluster in the C-terminal part of SUV39H1, which also contains the aforementioned S391 that is analogues to Clr4^{S458}. One phosphorylation site is proposed to be at the beginning of the SET-domain and three around the N-terminal CD (Figure 21). Due to the important enzymatic function of the SET-domain, investigation of the C-terminal phosphorylation events attracted most attention so far, but in general not much is known about phosphoregulation of the SUV family of H3K9 methyltransferases. However, studies in *D. melanogaster* examined N-terminal phosphorylation of Su(VAR)3-9^{S191} but failed to show influence of said phosphorylation event on its HKMTase activity. Instead it was postulated that the N-terminus of Su(VAR)3-9 acts as a platform in which phosphorylation might regulate potential interactions (Boeke et al., 2010).

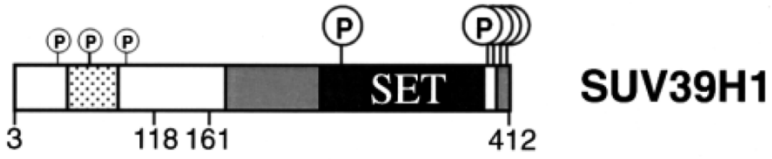

Figure 21. Schematic illustration of potential phosphorylation sites on human SUV39H1.
Phospho-amino acid analysis of transiently transfected FLAG-SUV39H1 HeLa cells revealed the presence of eight potential phosphorylation sites. Three of these phosphorylation sites map around the N-terminal CD of SUV39H1 (dotted box). The other five sites are localized at the C-terminus of the protein, one at the beginning and the rest proceeding the SET-domain.

The proline-directed S391 of mouse and human Suv39h1 and SUV39H1, respectively, is known to be a direct target of CDK2 and is preferentially phosphorylated during the G_1/S transition of the mitotic cell cycle (Firestein et al., 2000; Park et al., 2014). Phosphorylation levels of SUV39H1^{S391} are stable from S- until the end of M-phase, when CDK2 is biologically active, but do not impact the methyltransferase activity of the HKMT. Instead, S391 phosphorylation causes SUV39H1 to dissociate from heterochromatin which in turn leads to a decrease in H3K9me3 levels (Park et al., 2014). Even though these observations are quite interesting and would provide a potential explanation for the correlation between H3K9 methylation and phosphorylation of Clr4 in *S. pombe*, one has to be careful with the reported ChIP data for SUV39H1 binding and H3K9 methylation. Park and colleagues concluded these results from experiments using (sometimes even overexpressed) phospho-mimetic (S391E) and non-phosphorylatable (S391A) SUV39H1 in asynchronous Hela cells. My preliminary data indicates that site-directed mutagenesis of the proline-directed serine within the SET- and post-SET domains might cause pleiotropic effects. I would have liked them to look for endogenous SUV39H1 binding and H3K9 methylation levels during synchronized mitosis, similar to their phosphorylation assay. Inspired by this, I suggest to check Clr4 phosphorylation levels

during synchronized fission yeast mitosis to see, if phosphorylation of Clr4^{S458} oscillates throughout the mitotic cell cycle depending on Cdc2 activity. Further, I propose to simultaneously monitor binding of 3xFLAG-Clr4 to heterochromatin and to examine H3K9me2 and H3K9me3 levels. Additionally, I recommend to look at 3xFLAG-Clr4 enrichments during synchronized meiosis and test the hypothesis if HKMTs of the SUV family indeed have the tendency to dissociate from chromatin upon phosphorylation.

Taken together, studies of mammalian Suv39h1/SUV39H1 indicate that phosphorylation of the proline-directed serine in the ARL does not stimulate catalytic activity of the HKMTs directly. Instead, there is evidence that H3K9me3 levels are regulated by either controlling, as mentioned before, the binding affinity of SUV39H1 or the abundance of SUV39H1 protein levels. It was shown that phosphorylation of S391 recruits the conserved peptidyl-prolyl *cis/trans* isomerase Pin1 which binds SUV39H1 and promotes ubiquitin-mediated degradation (Khanal et al., 2013). The underlying mode of action how Pin1 marks phosphorylated proteins for ubiquitination by E3 ligases goes back to its ability to induce prolyl isomerization of the peptide bond (Liou et al., 2011). The thereby induced conformational shift establishes the correct conformation needed for SUV39H1 to be recognized as an E3 ubiquitin ligase substrate (Khanal et al., 2013). Combining these results with my observations, creates a very interesting hypothesis which could explain how the H3K9me2 to H3K9me3 shift at the onset of meiosis is regulated if phosphorylation of Clr4^{S458} does not directly influence HKMTase activity. In this speculative model, Clr4^{S458} phosphorylation would constantly lead to Pin1 recruitment and thereby change ARL conformation, ultimately leading to E3-mediated proteasomal degradation (Figure 22). Translation of new Clr4 and steady turn-over of phosphorylated Clr4 would create an equilibrium that dictates

H3K9 methylation levels. During premeiotic G_1 arrest, inhibition of Cdc2 prevents phosphorylation of newly synthesized Clr4 thus prohibiting Pin1 binding and rearrangement of the ARL. Without the phosphorylation-sensitive switch happening, ubiquitination of Clr4 is not possible and its protein levels accumulate which in turn leads to an increase in H3K9me3. Once Cdc2 activity is restored 2h into meiosis, the ARL of Clr4 gets phosphorylated inducing the Pin1-mediated degradation pathway again.

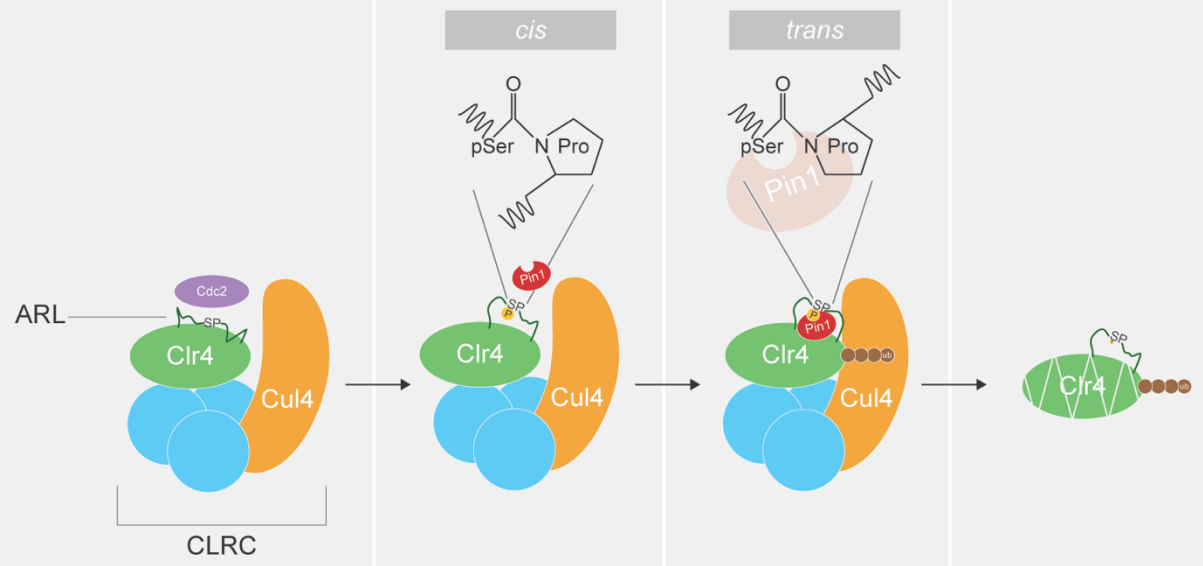

Figure 22. Hypothetical model of Pin1-mediated proteasomal degradation of Clr4.
Non-phosphorylated Clr4^{S458} has a specific conformation which protects it from being recognized by the E3 ubiquitin ligase Cul4. Upon phosphorylation of Clr4^{S458}, the peptidyl-prolyl isomerase Pin1 recognizes and binds the dipeptide "- pSer - Pro -" and thus induces a phosphorylation-sensitive switch. This remodeling step of the ARL renders Clr4 sensitive to poly-ubiquitination by Cul4, which targets it for degradation by the proteasome.

If it holds true that Clr4 is permanently degraded except during the G_1-phase, it would finally explain why Clr4 and the E3 ubiquitin ligase Cul4 share the same complex, namely CLRC. The close proximity of these two enzymes circumvents an additional recruitment mechanism and makes sure that Clr4 protein levels can be changed rapidly, simply by tweaking its phosphorylation status.

Kim and colleagues recently reported in a preprint that Cul4 associates with the E2-ubiquitin-conjugating enzyme Ubc4 and that this interaction leads to ubiquitination of Clr4 (Kim et al., 2021). This study was mainly focusing on mono-ubiquitination of Clr4 and how this PTM affects the dynamics of the HKMT by changing its liquid-liquid phase separation properties. To detect ubiquitinated Clr4 the authors had to inhibit the proteasome, explaining why I did not see any higher molecular weight forms of Clr4 in my IPs (Figure 23). Interestingly the preprint data indicates that, in addition to mono-ubiquitination, poly-ubiquitinated Clr4 can be stabilized when the proteasome is hampered with, which just partly depends on the E2-ubiquitin-conjugating enzyme Ubc4.

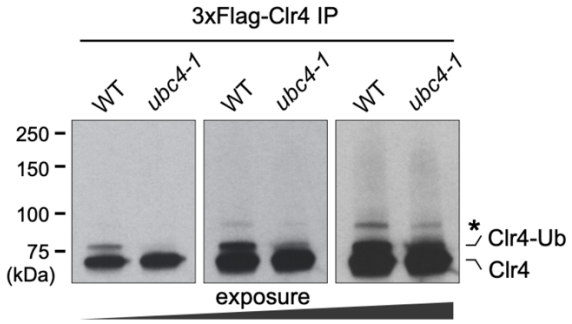

Figure 23. Inhibition of the proteasome stabilizes ubiquitinated Clr4.
Multiple higher molecular weight 3xFLAG-Clr4 species can be detected when wild-type *S. pombe* cells are treated with a proteasome inhibitor prior to cell lysis. These shifts in molecular weight are due to ubiquitination of Clr4 and depend to some degree on the E2-ubiquitin-conjugating enzyme Ubc4. Besides mono-ubiquitination (Clr4-Ub) also poly-ubiquitinated Clr4 (*) is detected under these conditions. Figure adapted from Kim et al., 2021.

In light of the aforementioned findings, I strongly suggest to look for poly-ubiquitination in mitotic and early meiotic cells (phosphorylated and non-phosphorylated Clr4^{S458}, respectively). If the hypothesis holds true and phosphorylation of Clr4^{S458} is a trigger for E3 ubiquitin ligase-mediated degradation, one would expect differential ubiquitination in cells treated with the proteasome inhibitor MG-132.

My Clr4 IP-MS data reveals, that Pin1 does not co-IP with Clr4. Assuming Pin1's role in regulating SUV39H1 protein levels is conserved in *S. pombe*, this suggests that the interaction between the two proteins is either too transient or that Pin1-bound Clr4 is degraded rapidly. To test both of these assumptions, I propose to use a crosslinking IP-MS approach or to probe for Pin1 in proteasome inhibited Clr4 IPs, respectively. Further, analysis of Pin1-depleted cells will reveal if it is involved in regulation of Clr4 protein half-life. Therefore, I recommend to monitor protein levels of phosphorylated and non-phosphorylated Clr4^{S458} and to ChIP H3K9 methylation in mitotic *pin1*Δ cells.

Conclusion

Within my PhD work, I provided the first genome-wide H3K9 methylation maps during the sexual life cycle of *S. pombe*. I discovered that a temporal methylation switch at constitutive heterochromatin safeguards the first meiotic division by ensuring sufficient binding of fission yeast HP1 to pericentromeric repeats. This early meiotic H3K9 methylation switch is negatively regulated by the cyclin-dependent kinase Cdc2 which constantly phosphorylates the fission yeast SUV family HKMT Clr4 at S458 and thus dampens its tri-methylation activity. Artificial inhibition of Cdc2 activity in mitotic cells leads to accumulation of dephosphorylated Clr4^{S458} which is accompanied by elevated H3K9me3 levels. During meiotic commitment, Cdc2 activity is inhibited in a physiological context by the CKI Rum1. The consequences on Clr4's phosphorylation state and on H3Kme3 enrichments are identical to the ones observed in conditionally inactivated Cdc2 cells. However, within the scope of my thesis I could not decisively test if phosphorylation of Clr4 at S458 directly regulates the H3K9me2 to H3K9me3 transition. Observations made with the human Clr4 homolog suggest that

phosphorylation of Clr4^{S458} could influence H3K9 methylation levels by regulating its protein half-life instead of directly affecting catalysis. To ultimately answer this question, *in vitro* methylation assays and structural studies of phosphorylated and non-phosphorylated Clr4 are inevitable. Further, the structure of phosphorylated Clr4^{S458} should be solved in absence and presence of Pin1. With the aforementioned experiments, one should be able to answer if Clr4 ARL undergoes a phosphorylation-sensitive switch and if this switch is dependent on the peptidyl-prolyl isomerase Pin1 or not. Additionally, the combination of crystal structures and *in vitro* methylation kinetics will reveal whether the conformational change is altering Clr4s intrinsic catalytic activity or rather bridges it to proteasomal degradation.

Interestingly, the majority of the proteins I studied within this PhD thesis are conserved from yeast to human. Therefore, it is not too far-fetched to assume that parts of the regulatory pathway described here in my thesis are conserved as well. However, if phosphoregulation of SUV39H1 also controls faithful division of chromosomes during meiosis in humans remains to be investigated.

I find it fascinating that the master regulator of the cell cycle targets a HKMT to alter the structure of constitutive heterochromatin during the highly specialized meiotic program. Further, these changes in constitutive heterochromatin, more precisely H3K9 methylation and HP1 binding, ensure faithful segregation of the genome during the first meiotic division. The cue for the fission yeast *S. pombe* to initiate meiosis are environmental changes and exogenous stimuli, such as nitrogen deprivation. These signals initiate inhibition of Cdc2 and thus the cascade which eventually results in fast and reversible changes of the epigenome. The link between environmental cues and changes of the epigenome is a very intriguing one, which has been fascinating epigeneticists for a long time. Maybe there are more environmental stimuli that effect

key cell cycle regulators (or other downstream factors) similar to what I described in my PhD thesis, causing modulation of the epigenetic landscape and thereby facilitate epigenetic adaptation.

ACKNOWLEDGMENTS

First and foremost, I thank Marc for being probably the best boss and mentor I could have asked for. I am very grateful that I got the opportunity to pursue my PhD in his lab. He always supported me and my ideas and gave me the freedom to drive my project in whatever direction I wanted. I give Marc great credit for his high spirit, trust, and genuine honesty. His passion for science is unparalleled and his contagious enthusiasm helped me more than once to overcome signs of frustration. But to put it in football terms: "The best ability is availability". Hence, I would like to emphasize my appreciation for his open door policy, constant discussions without needing to schedule a meeting, immediate responses, and quick corrections. I learned a lot from being around Marc and I greatly enjoyed our conversations, be it scientific or personal. Along the same line, I am grateful for the excellent advice, great discussions, and immense support I got from the members of my thesis committee, Helge Grosshans and Viesturs Simanis.

Something that I will miss for sure is the crazy everyday life and the wonderful atmosphere in the lab. The biggest “THANK YOU” goes to all current and former lab members for making the Bühler lab such a special place, creating memorable moments, and letting me be who I am ;). I would like to thank Yuki and Motty for keeping the place running so smoothly and for looking after everyone. Again, huge thanks to Yuki (because one cannot appreciate her efforts enough!) for being so supportive and cheerful. I really hope she knows how valuable she is to everyone’s success. I am especially grateful to Vale for supervising me in the beginning and teaching me the fundamental yeast techniques. It was a blast to work together with him! Furthermore, I would like to thank Merle for all the fun and serious conversations we had and for becoming such a great friend. Cheers to my big Bros Lucas and Matyas

with whom I, luckily, overlapped the most during my time in the lab – I wish them nothing but the best for their new chapters. Also, I am very thankful to Fabio for his valuable input and help with data analysis.

I could not have achieved nearly as much during my PhD without the awesome facilities here at FMI. Thanks to Functional Genomics, Proteomics and Protein Analysis, FAIM, FACS, IT, and the Media Kitchen for all their work and contribution. I would like to specially thank Elida for coordinating the PhD program and taking care of all the administrative formalities!

The majority of my leisure time I spent together with my team mates from Freespeed Basel: Monday, Tuesday, and Thursday practices plus the gym sessions, meetings, team events, the crazy trips, tournaments, and championships. I still remember the day I arrived in Basel and went to my first practice like it was yesterday. It immediately felt like home and I am honored that I eventually got the chance to be part of such a great family. I am privileged to call every one of the squad my dear friend. I will never forget the experiences that I made with all these guys – literally blood, sweat, and tears. A very special bond. The won national titles, the defeats, the tough practices, and the injuries. Everything and everyone shaped me in one way or another and I am very grateful for that. It was not always easy for me to manage my scientific passion and my love for Ultimate time-wise, but I am sure that both benefitted from each other! Props to the Juhns for keeping me young and special kisses to #27 Cäspi and #11 Gilles, thanks for being such great friends. Freespeed Love #14.

Here, I would also like to spend a few words to highlight multiple different things that accompanied me throughout my PhD journey and thus “contributed significantly” to my work: (1) Shout-out to Radiohead, Alt-J, Caspian, and (often explicit) German rap music for making the awfully late and long time courses more enjoyable, boosting

my mood when needed, and assisting me during the thesis-writing process; (2) Big ups to the NFL and fantasy football in sparking my passion for watching sports again; (3) Props to my plant collection for distracting me just enough to help me clear my mind during stressful times.

Lastly, I would like to thank my family for their continuous support and unconditional love: my parents, Züby, Sümy, and Buddy as well as Harald and Henni. Words will never be able to describe how grateful I am for my parents. I know that they faced immense challenges throughout their lives and sacrificed a whole lot to make it possible for me to receive a good education. Ich danke euch für alles, Mama und Papa. All of this work would not have been possible without Vera, her never-ending support, understanding, and unparalleled kindheartedness. Çok teşekkür ederim aşkım.

REFERENCES

Aagaard, L., Schmid, M., Warburton, P., & Jenuwein, T. (2000). Mitotic phosphorylation of SUV39H1, a novel component of active centromeres, coincides with transient accumulation at mammalian centromeres. Journal of Cell Science, 113(5), 817–829. https://doi.org/10.1242/jcs.113.5.817

Adams, J. A. (2003). Activation Loop Phosphorylation and Catalysis in Protein Kinases: Is There Functional Evidence for the Autoinhibitor Model? Biochemistry, 42(3), 601–607. https://doi.org/10.1021/bi020617o

Allfrey, V. G., Faulkner, R., & Mirsky, A. E. (1964). Acetylation and methylation of histones and their possible role in the regulation of RNA synthesis. Proceedings of the National Academy of Sciences of the United States of America, 51(5), 786–794.

Allshire, R. C., & Ekwall, K. (2015). Epigenetic Regulation of Chromatin States in Schizosaccharomyces pombe. Cold Spring Harbor Perspectives in Biology, 7(7), a018770. https://doi.org/10.1101/cshperspect.a018770

Allshire, R. C., Nimmo, E. R., Ekwall, K., Javerzat, J. P., & Cranston, G. (1995). Mutations derepressing silent centromeric domains in fission yeast disrupt chromosome segregation. Genes & Development, 9(2), 218–233. https://doi.org/10.1101/gad.9.2.218

Andric, V., & Rougemaille, M. (2021). Long Non-Coding RNAs in the Control of Gametogenesis: Lessons from Fission Yeast. Non-Coding RNA, 7(2), 34. https://doi.org/10.3390/ncrna7020034

Ardito, F., Giuliani, M., Perrone, D., Troiano, G., & Lo Muzio, L. (2017). The crucial role of protein phosphorylation in cell signaling and its use as targeted therapy (Review). International Journal of Molecular Medicine, 40(2), 271–280. https://doi.org/10.3892/ijmm.2017.3036

Azzalin, C. M., Reichenbach, P., Khoriauli, L., Giulotto, E., & Lingner, J. (2007). Telomeric Repeat–Containing RNA and RNA Surveillance Factors at Mammalian

Chromosome Ends. Science, 318(5851), 798–801. https://doi.org/10.1126/science.1147182

Baldi, S., Korber, P., & Becker, P. B. (2020). Beads on a string—Nucleosome array arrangements and folding of the chromatin fiber. Nature Structural & Molecular Biology, 27(2), 109–118. https://doi.org/10.1038/s41594-019-0368-x

Bannister, A. J., & Kouzarides, T. (2011). Regulation of chromatin by histone modifications. Cell Research, 21(3), 381–395. https://doi.org/10.1038/cr.2011.22

Bannister, A. J., Schneider, R., & Kouzarides, T. (2002). Histone Methylation: Dynamic or Static? Cell, 109(7), 801–806. https://doi.org/10.1016/S0092-8674(02)00798-5

Bannister, A. J., Zegerman, P., Partridge, J. F., Miska, E. A., Thomas, J. O., Allshire, R. C., & Kouzarides, T. (2001). Selective recognition of methylated lysine 9 on histone H3 by the HP1 chromo domain. Nature, 410(6824), 120–124. https://doi.org/10.1038/35065138

Bao, K., Shan, C.-M., Moresco, J., Yates, J., & Jia, S. (2019). Anti-silencing factor Epe1 associates with SAGA to regulate transcription within heterochromatin. Genes & Development, 33(1–2), 116–126. https://doi.org/10.1101/gad.318030.118

Bayne, E. H., White, S. A., Kagansky, A., Bijos, D. A., Sanchez-Pulido, L., Hoe, K.-L., Kim, D.-U., Park, H.-O., Ponting, C. P., Rappsilber, J., & Allshire, R. C. (2010). Stc1: A Critical Link between RNAi and Chromatin Modification Required for Heterochromatin Integrity. Cell, 140(5), 666–677. https://doi.org/10.1016/j.cell.2010.01.038

Benito, J., Martin-Castellanos, C., & Moreno, S. (1998). Regulation of the G1 phase of the cell cycle by periodic stabilization and degradation of the p25rum1 CDK inhibitor. The EMBO Journal, 17(2), 482–497. https://doi.org/10.1093/emboj/17.2.482

Bernard, P., Maure, J.-F., Partridge, J. F., Genier, S., Javerzat, J.-P., & Allshire, R. C. (2001). Requirement of Heterochromatin for Cohesion at Centromeres. Science, 294(5551), 2539–2542. https://doi.org/10.1126/science.1064027

REFERENCES

Bernstein, B. E., Meissner, A., & Lander, E. S. (2007). The Mammalian Epigenome. Cell, 128(4), 669–681. https://doi.org/10.1016/j.cell.2007.01.033

Boeke, J., Regnard, C., Cai, W., Johansen, J., Johansen, K. M., Becker, P. B., & Imhof, A. (2010). Phosphorylation of SU(VAR)3–9 by the Chromosomal Kinase JIL-1. PLOS ONE, 5(4), e10042. https://doi.org/10.1371/journal.pone.0010042

Brasher, S. V., Smith, B. O., Fogh, R. H., Nietlospach, D., Thiru, A., Nielsen, P. R., Broadhurst, R. W., Ball, L. J., Murzina, N. V., & Laue, E. D. (2000). The structure of mouse HP1 suggests a unique mode of single peptide recognition by the shadow chromo domain dimer. The EMBO Journal, 19(7), 1587–1597. https://doi.org/10.1093/emboj/19.7.1587

Brownell, J. E., Zhou, J., Ranalli, T., Kobayashi, R., Edmondson, D. G., Roth, S. Y., & Allis, C. D. (1996). Tetrahymena Histone Acetyltransferase A: A Homolog to Yeast Gcn5p Linking Histone Acetylation to Gene Activation. Cell, 84(6), 843–851. https://doi.org/10.1016/S0092-8674(00)81063-6

Bühler, M., Verdel, A., & Moazed, D. (2006). Tethering RITS to a Nascent Transcript Initiates RNAi- and Heterochromatin-Dependent Gene Silencing. Cell, 125(5), 873–886. https://doi.org/10.1016/j.cell.2006.04.025

Buker, S. M., Iida, T., Bühler, M., Villén, J., Gygi, S. P., Nakayama, J.-I., & Moazed, D. (2007). Two different Argonaute complexes are required for siRNA generation and heterochromatin assembly in fission yeast. Nature Structural & Molecular Biology, 14(3), 200–207. https://doi.org/10.1038/nsmb1211

Cam, H. P., Sugiyama, T., Chen, E. S., Chen, X., FitzGerald, P. C., & Grewal, S. I. S. (2005). Comprehensive analysis of heterochromatin- and RNAi-mediated epigenetic control of the fission yeast genome. Nature Genetics, 37(8), 809–819. https://doi.org/10.1038/ng1602

Carpy, A., Krug, K., Graf, S., Koch, A., Popic, S., Hauf, S., & Macek, B. (2014). Absolute Proteome and Phosphoproteome Dynamics during the Cell Cycle of Schizosaccharomyces pombe (Fission Yeast). Molecular & Cellular Proteomics, 13(8), 1925–1936. https://doi.org/10.1074/mcp.M113.035824

REFERENCES

Chelysheva, L., Diallo, S., Vezon, D., Gendrot, G., Vrielynck, N., Belcram, K., Rocques, N., Márquez-Lema, A., Bhatt, A. M., Horlow, C., Mercier, R., Mézard, C., & Grelon, M. (2005). AtREC8 and AtSCC3 are essential to the monopolar orientation of the kinetochores during meiosis. Journal of Cell Science, 118(20), 4621–4632. https://doi.org/10.1242/jcs.02583

Cipak, L., Hyppa, R. W., Smith, G. R., & Gregan, J. (2012). ATP analog-sensitive Pat1 protein kinase for synchronous fission yeast meiosis at physiological temperature. Cell Cycle, 11(8), 1626–1633. https://doi.org/10.4161/cc.20052

Cipak, L., Polakova, S., Hyppa, R. W., Smith, G. R., & Gregan, J. (2014). Synchronized fission yeast meiosis using an ATP analog–sensitive Pat1 protein kinase. Nature Protocols, 9(1), 223–231. https://doi.org/10.1038/nprot.2014.013

Collins, R. E., Tachibana, M., Tamaru, H., Smith, K. M., Jia, D., Zhang, X., Selker, E. U., Shinkai, Y., & Cheng, X. (2005). In Vitro and in Vivo Analyses of a Phe/Tyr Switch Controlling Product Specificity of Histone Lysine Methyltransferases *. Journal of Biological Chemistry, 280(7), 5563–5570. https://doi.org/10.1074/jbc.M410483200

Colmenares, S. U., Buker, S. M., Buhler, M., Dlakić, M., & Moazed, D. (2007). Coupling of double-stranded RNA synthesis and siRNA generation in fission yeast RNAi. Molecular Cell, 27(3), 449–461.

Costello, G., Rodgers, L., & Beach, D. (1986). Fission yeast enters the stationary phase G0 state from either mitotic G1 or G2. Current Genetics, 11(2), 119–125. https://doi.org/10.1007/BF00378203

Coudreuse, D., & Nurse, P. (2010). Driving the cell cycle with a minimal CDK control network. Nature, 468(7327), 1074–1079. https://doi.org/10.1038/nature09543

Cowieson, N. P., Partridge, J. F., Allshire, R. C., & McLaughlin, P. J. (2000). Dimerisation of a chromo shadow domain and distinctions from the chromodomain as revealed by structural analysis. Current Biology, 10(9), 517–525. https://doi.org/10.1016/S0960-9822(00)00467-X

REFERENCES

Daga, R. R., Bolaños, P., & Moreno, S. (2003). Regulated mRNA Stability of the Cdk Inhibitor Rum1 Links Nutrient Status to Cell Cycle Progression. Current Biology, 13(23), 2015–2024. https://doi.org/10.1016/j.cub.2003.10.061

Dillon, S. C., Zhang, X., Trievel, R. C., & Cheng, X. (2005). The SET-domain protein superfamily: Protein lysine methyltransferases. Genome Biology, 6(8), 227. https://doi.org/10.1186/gb-2005-6-8-227

Ding, R., McDonald, K. L., & McIntosh, J. R. (1993). Three-dimensional reconstruction and analysis of mitotic spindles from the yeast, Schizosaccharomyces pombe. Journal of Cell Biology, 120(1), 141–151. https://doi.org/10.1083/jcb.120.1.141

Dischinger, S., Krapp, A., Xie, L., Paulson, J. R., & Simanis, V. (2008). Chemical genetic analysis of the regulatory role of Cdc2p in the S. pombe septation initiation network. Journal of Cell Science, 121(6), 843–853. https://doi.org/10.1242/jcs.021584

Dissmeyer, N., & Schnittger, A. (2011). Use of Phospho-Site Substitutions to Analyze the Biological Relevance of Phosphorylation Events in Regulatory Networks. Plant Kinases, 93–138. https://doi.org/10.1007/978-1-61779-264-9_6

Dong, W., Oya, E., Zahedi, Y., Prasad, P., Svensson, J. P., Lennartsson, A., Ekwall, K., & Durand-Dubief, M. (2020). Abo1 is required for the H3K9me2 to H3K9me3 transition in heterochromatin. Scientific Reports, 10(1), 6055. https://doi.org/10.1038/s41598-020-63209-y

Dümpelmann, L., Mohn, F., Shimada, Y., Oberti, D., Andriollo, A., Lochs, S., & Bühler, M. (2019). Inheritance of a Phenotypically Neutral Epimutation Evokes Gene Silencing in Later Generations. Molecular Cell, 74(3), 534-541.e4. https://doi.org/10.1016/j.molcel.2019.02.009

Egel, R. (1971). Physiological aspects of conjugation in fission yeast. Planta, 98(1), 89–96. https://doi.org/10.1007/BF00387025

Ekwall, K., Nimmo, E. R., Javerzat, J.-P., Borgstrom, B., Egel, R., Cranston, G., & Allshire, R. (1996). Mutations in the fission yeast silencing factors clr4+ and rik1+

disrupt the localisation of the chromo domain protein Swi6p and impair centromere function. Journal of Cell Science, 109(11), 2637–2648.

Ekwall, K., & Thon, G. (2017). Setting up Schizosaccharomyces pombe Crosses/Matings. Cold Spring Harbor Protocols, 2017(7), pdb.prot091694. https://doi.org/10.1101/pdb.prot091694

Fantes, P. A., & Hoffman, C. S. (2016). A Brief History of Schizosaccharomyces pombe Research: A Perspective Over the Past 70 Years. Genetics, 203(2), 621–629. https://doi.org/10.1534/genetics.116.189407

Fanti, L., & Pimpinelli, S. (2008). HP1: A functionally multifaceted protein. Current Opinion in Genetics & Development, 18(2), 169–174. https://doi.org/10.1016/j.gde.2008.01.009

Fire, A., Xu, S., Montgomery, M. K., Kostas, S. A., Driver, S. E., & Mello, C. C. (1998). Potent and specific genetic interference by double-stranded RNA in Caenorhabditis elegans. Nature, 391(6669), 806–811. https://doi.org/10.1038/35888

Firestein, R., Cui, X., Huie, P., & Cleary, M. L. (2000). Set Domain-Dependent Regulation of Transcriptional Silencing and Growth Control by SUV39H1, a Mammalian Ortholog ofDrosophila Su(var)3-9. Molecular and Cellular Biology. https://doi.org/10.1128/MCB.20.13.4900-4909.2000

Fisher, D., & Nurse, P. (1996). A single fission yeast mitotic cyclin B p34cdc2 kinase promotes both S-phase and mitosis in the absence of G1 cyclins. The EMBO Journal, 15(4), 850–860.

Forsburg, S. L., & Nurse, P. (1991). Cell cycle regulation in the yeasts Saccharomyces cerevisiae and Schizosaccharomyces pombe. Annual Review of Cell Biology, 7(1), 227–256.

Gordon, D. J., Resio, B., & Pellman, D. (2012). Causes and consequences of aneuploidy in cancer. Nature Reviews Genetics, 13(3), 189–203. https://doi.org/10.1038/nrg3123

REFERENCES

Greer, E. L., & Shi, Y. (2012). Histone methylation: A dynamic mark in health, disease and inheritance. Nature Reviews Genetics, 13(5), 343–357. https://doi.org/10.1038/nrg3173

Grewal, S. I. S., & Jia, S. (2007). Heterochromatin revisited. Nature Reviews Genetics, 8(1), 35–46. https://doi.org/10.1038/nrg2008

Guerra-Moreno, A., Alves-Rodrigues, I., Hidalgo, E., & Ayté, J. (2012). Chemical genetic induction of meiosis in Schizosaccharomyces pombe. Cell Cycle, 11(8), 1621–1625. https://doi.org/10.4161/cc.20051

Hamelberg, D., Shen, T., & McCammon, J. A. (2005). Phosphorylation Effects on cis/trans Isomerization and the Backbone Conformation of Serine−Proline Motifs: Accelerated Molecular Dynamics Analysis. Journal of the American Chemical Society, 127(6), 1969–1974. https://doi.org/10.1021/ja0446707

Harigaya, Y., Tanaka, H., Yamanaka, S., Tanaka, K., Watanabe, Y., Tsutsumi, C., Chikashige, Y., Hiraoka, Y., Yamashita, A., & Yamamoto, M. (2006). Selective elimination of messenger RNA prevents an incidence of untimely meiosis. Nature, 442(7098), 45–50. https://doi.org/10.1038/nature04881

Hartwell, L. H., Culotti, J., Pringle, J. R., & Reid, B. J. (1974). Genetic Control of the Cell Division Cycle in Yeast. Science, 183(4120), 46–51.

Hartwell, L. H., Mortimer, R. K., Culotti, J., & Culotti, M. (1973). Genetic control of the cell division cycle in yeast: V. Genetic analysis of cdc mutants. Genetics, 74(2), 267–286. https://doi.org/10.1093/genetics/74.2.267

Hassold, T., & Hunt, P. (2001). To err (meiotically) is human: The genesis of human aneuploidy. Nature Reviews Genetics, 2(4), 280–291. https://doi.org/10.1038/35066065

Hayles, J., & Nurse, P. (2018). Introduction to Fission Yeast as a Model System. Cold Spring Harbor Protocols, 2018(5), pdb.top079749. https://doi.org/10.1101/pdb.top079749

REFERENCES

Heard, E., & Disteche, C. M. (2006). Dosage compensation in mammals: Fine-tuning the expression of the X chromosome. Genes & Development, 20(14), 1848–1867. https://doi.org/10.1101/gad.1422906

Hiriart, E., Vavasseur, A., Todeschini, L., Yamashita, A., Gilquin, B., Lambert, E., Perot, J., Shichino, Y., Nazaret, N., Boyault, C., Laucher, J., Perazza, D., Yamamoto, M., & Verdel, A. (2012). Mmi1 RNA surveillance machinery directs RNAi complex RITS to specific meiotic genes in fission yeast. The EMBO Journal, 31(10), 2296–2308. https://doi.org/10.1038/emboj.2012.105

Holoch, D., & Moazed, D. (2015a). RNA-mediated epigenetic regulation of gene expression. Nature Reviews Genetics, 16(2), 71–84. https://doi.org/10.1038/nrg3863

Holoch, D., & Moazed, D. (2015b). Small-RNA loading licenses Argonaute for assembly into a transcriptional silencing complex. Nature Structural & Molecular Biology, 22(4), 328–335. https://doi.org/10.1038/nsmb.2979

Hong, E.-J. E., Villén, J., & Moazed, D. (2005). A Cullin E3 Ubiquitin Ligase Complex Associates with Rik1 and the Clr4 Histone H3-K9 Methyltransferase and is Required for RNAi-Mediated Heterochromatin Formation. RNA Biology, 2(3), 106–111. https://doi.org/10.4161/rna.2.3.2131

Horn, P. J., Bastie, J.-N., & Peterson, C. L. (2005). A Rik1-associated, cullin-dependent E3 ubiquitin ligase is essential for heterochromatin formation. Genes & Development, 19(14), 1705–1714. https://doi.org/10.1101/gad.1328005

Hubbard, S. R. (1997). Crystal structure of the activated insulin receptor tyrosine kinase in complex with peptide substrate and ATP analog. The EMBO Journal, 16(18), 5572–5581. https://doi.org/10.1093/emboj/16.18.5572

Iglesias, N., Currie, M. A., Jih, G., Paulo, J. A., Siuti, N., Kalocsay, M., Gygi, S. P., & Moazed, D. (2018). Automethylation-induced conformational switch in Clr4 (Suv39h) maintains epigenetic stability. Nature, 560(7719), 504–508. https://doi.org/10.1038/s41586-018-0398-2

REFERENCES

Iglesias, N., Paulo, J. A., Tatarakis, A., Wang, X., Edwards, A. L., Bhanu, N. V., Garcia, B. A., Haas, W., Gygi, S. P., & Moazed, D. (2020). Native Chromatin Proteomics Reveals a Role for Specific Nucleoporins in Heterochromatin Organization and Maintenance. Molecular Cell, 77(1), 51-66.e8. https://doi.org/10.1016/j.molcel.2019.10.018

Iino, Y., & Yamamoto, M. (1985). Mutants of Schizosaccharomyces pombe which sporulate in the haploid state. Molecular and General Genetics MGG, 198(3), 416–421. https://doi.org/10.1007/BF00332932

Ishiguro, T., Tanaka, K., Sakuno, T., & Watanabe, Y. (2010). Shugoshin–PP2A counteracts casein-kinase-1-dependent cleavage of Rec8 by separase. Nature Cell Biology, 12(5), 500–506. https://doi.org/10.1038/ncb2052

Ivanova, A. V., Bonaduce, M. J., Ivanov, S. V., & Klar, A. J. S. (1998). The chromo and SET domains of the Clr4 protein are essential for silencing in fission yeast. Nature Genetics, 19(2), 192–195. https://doi.org/10.1038/566

James, T. C., & Elgin, S. C. (1986). Identification of a nonhistone chromosomal protein associated with heterochromatin in Drosophila melanogaster and its gene. Molecular and Cellular Biology. https://doi.org/10.1128/mcb.6.11.3862-3872.1986

Jia, S., Kobayashi, R., & Grewal, S. I. S. (2005). Ubiquitin ligase component Cul4 associates with Clr4 histone methyltransferase to assemble heterochromatin. Nature Cell Biology, 7(10), 1007–1013. https://doi.org/10.1038/ncb1300

Jiang, C., & Pugh, B. F. (2009). Nucleosome positioning and gene regulation: Advances through genomics. Nature Reviews Genetics, 10(3), 161–172. https://doi.org/10.1038/nrg2522

Jih, G., Iglesias, N., Currie, M. A., Bhanu, N. V., Paulo, J. A., Gygi, S. P., Garcia, B. A., & Moazed, D. (2017). Unique roles for histone H3K9me states in RNAi and heritable silencing of transcription. Nature, 547(7664), 463–467. https://doi.org/10.1038/nature23267

REFERENCES

Kanoh, J., Sadaie, M., Urano, T., & Ishikawa, F. (2005). Telomere Binding Protein Taz1 Establishes Swi6 Heterochromatin Independently of RNAi at Telomeres. Current Biology, 15(20), 1808–1819. https://doi.org/10.1016/j.cub.2005.09.041

Kato, H., Goto, D. B., Martienssen, R. A., Urano, T., Furukawa, K., & Murakami, Y. (2005). RNA Polymerase II Is Required for RNAi-Dependent Heterochromatin Assembly. Science, 309(5733), 467–469. https://doi.org/10.1126/science.1114955

Kato, T., Okazaki, K., Murakami, H., Stettler, S., Fantes, P. A., & Okayama, H. (1996). Stress signal, mediated by a Hogl-like MAP kinase, controls sexual development in fission yeast. FEBS Letters, 378(3), 207–212. https://doi.org/10.1016/0014-5793(95)01442-X

Kawakami, K., Hayashi, A., Nakayama, J., & Murakami, Y. (2012). A novel RNAi protein, Dsh1, assembles RNAi machinery on chromatin to amplify heterochromatic siRNA. Genes & Development, 26(16), 1811–1824. https://doi.org/10.1101/gad.190272.112

Keller, C., Adaixo, R., Stunnenberg, R., Woolcock, K. J., Hiller, S., & Bühler, M. (2012). HP1Swi6 Mediates the Recognition and Destruction of Heterochromatic RNA Transcripts. Molecular Cell, 47(2), 215–227. https://doi.org/10.1016/j.molcel.2012.05.009

Keller, C., Kulasegaran-Shylini, R., Shimada, Y., Hotz, H.-R., & Bühler, M. (2013). Noncoding RNAs prevent spreading of a repressive histone mark. Nature Structural & Molecular Biology, 20(8), 994–1000. https://doi.org/10.1038/nsmb.2619

Kellum, R., & Alberts, B. M. (1995). Heterochromatin protein 1 is required for correct chromosome segregation in Drosophila embryos. Journal of Cell Science, 108(4), 1419–1431.

Kelly, M., Burke, J., Smith, M., Klar, A., & Beach, D. (1988). Four mating-type genes control sexual differentiation in the fission yeast. The EMBO Journal, 7(5), 1537–1547. https://doi.org/10.1002/j.1460-2075.1988.tb02973.x

REFERENCES

Kettenbach, A. N., Deng, L., Wu, Y., Baldissard, S., Adamo, M. E., Gerber, S. A., & Moseley, J. B. (2015). Quantitative Phosphoproteomics Reveals Pathways for Coordination of Cell Growth and Division by the Conserved Fission Yeast Kinase Pom1*. Molecular & Cellular Proteomics, 14(5), 1275–1287. https://doi.org/10.1074/mcp.M114.045245

Khanal, P., Kim, G., Lim, S.-C., Yun, H.-J., Lee, K. Y., Choi, H.-K., & Choi, H. S. (2013). Prolyl isomerase Pin1 negatively regulates the stability of SUV39H1 to promote tumorigenesis in breast cancer. The FASEB Journal, 27(11), 4606–4618. https://doi.org/10.1096/fj.13-236851

Kim, H.-S., Roche, B., Bhattacharjee, S., Todeschini, L., Chang, A.-Y., Hammell, C., Verdel, A., & Martienssen, R. A. (2021). Clr4SUV39H1 and Bdf2BRD4 ubiquitination mediate transcriptional silencing via heterochromatic phase transitions (p. 2021.01.08.425919). https://doi.org/10.1101/2021.01.08.425919

Kitajima, T. S., Kawashima, S. A., & Watanabe, Y. (2004). The conserved kinetochore protein shugoshin protects centromeric cohesion during meiosis. Nature, 427(6974), 510–517. https://doi.org/10.1038/nature02312

Kitajima, T. S., Yokobayashi, S., Yamamoto, M., & Watanabe, Y. (2003). Distinct Cohesin Complexes Organize Meiotic Chromosome Domains. Science, 300(5622), 1152–1155. https://doi.org/10.1126/science.1083634

Koch, B., Kueng, S., Ruckenbauer, C., Wendt, K. S., & Peters, J.-M. (2008). The Suv39h–HP1 histone methylation pathway is dispensable for enrichment and protection of cohesin at centromeres in mammalian cells. Chromosoma, 117(2), 199–210. https://doi.org/10.1007/s00412-007-0139-z

Kornberg, R. D. (1977). Structure of chromatin. Annual Review of Biochemistry, 46(1), 931–954.

Kornberg, R. D., & Lorch, Y. (1999). Twenty-Five Years of the Nucleosome, Fundamental Particle of the Eukaryote Chromosome. Cell, 98(3), 285–294. https://doi.org/10.1016/S0092-8674(00)81958-3

Kouzarides, T. (2007). Chromatin Modifications and Their Function. Cell, 128(4), 693–705. https://doi.org/10.1016/j.cell.2007.02.005

Krapp, A., Hamelin, R., Armand, F., Chiappe, D., Krapp, L., Cano, E., Moniatte, M., & Simanis, V. (2019). Analysis of the S. pombe Meiotic Proteome Reveals a Switch from Anabolic to Catabolic Processes and Extensive Post-transcriptional Regulation. Cell Reports, 26(4), 1044-1058.e5. https://doi.org/10.1016/j.celrep.2018.12.075

Kuscu, C., Zaratiegui, M., Kim, H. S., Wah, D. A., Martienssen, R. A., Schalch, T., & Joshua-Tor, L. (2014). CRL4-like Clr4 complex in Schizosaccharomyces pombe depends on an exposed surface of Dos1 for heterochromatin silencing. Proceedings of the National Academy of Sciences, 111(5), 1795–1800. https://doi.org/10.1073/pnas.1313096111

Lambing, C., Tock, A. J., Topp, S. D., Choi, K., Kuo, P. C., Zhao, X., Osman, K., Higgins, J. D., Franklin, F. C. H., & Henderson, I. R. (2020). Interacting Genomic Landscapes of REC8-Cohesin, Chromatin, and Meiotic Recombination in Arabidopsis. The Plant Cell, 32(4), 1218–1239. https://doi.org/10.1105/tpc.19.00866

Lee, J., Iwai, T., Yokota, T., & Yamashita, M. (2003). Temporally and spatially selective loss of Rec8 protein from meiotic chromosomes during mammalian meiosis. Journal of Cell Science, 116(13), 2781–2790. https://doi.org/10.1242/jcs.00495

Lee, M. G., & Nurse, P. (1987). Complementation used to clone a human homologue of the fission yeast cell cycle control gene cdc2. Nature, 327(6117), 31–35. https://doi.org/10.1038/327031a0

Leupold, U. (1950). The inheritance of homothally and heterothally in S. Pombe. Comptes rendus des Travaux du Laboratoire Carlsberg, 24, 381–480.

Li, P., & McLeod, M. (1996). Molecular Mimicry in Development: Identification of ste11+ As a Substrate and mei3+ As a Pseudosubstrate Inhibitor of ran1+ Kinase. Cell, 87(5), 869–880. https://doi.org/10.1016/S0092-8674(00)81994-7

REFERENCES

Liou, Y.-C., Zhou, X. Z., & Lu, K. P. (2011). Prolyl isomerase Pin1 as a molecular switch to determine the fate of phosphoproteins. Trends in Biochemical Sciences, 36(10), 501–514. https://doi.org/10.1016/j.tibs.2011.07.001

Luger, K., & Hansen, J. C. (2005). Nucleosome and chromatin fiber dynamics. Current Opinion in Structural Biology, 15(2), 188–196. https://doi.org/10.1016/j.sbi.2005.03.006

Luger, K., Mäder, A. W., Richmond, R. K., Sargent, D. F., & Richmond, T. J. (1997). Crystal structure of the nucleosome core particle at 2.8 Å resolution. Nature, 389(6648), 251–260. https://doi.org/10.1038/38444

Lundgren, K., Walworth, N., Booher, R., Dembski, M., Kirschner, M., & Beach, D. (1991). Mik1 and wee1 cooperate in the inhibitory tyrosine phosphorylation of cdc2. Cell, 64(6), 1111–1122. https://doi.org/10.1016/0092-8674(91)90266-2

Maeda, T., Mochizuki, N., & Yamamoto, M. (1990). Adenylyl cyclase is dispensable for vegetative cell growth in the fission yeast Schizosaccharomyces pombe. Proceedings of the National Academy of Sciences, 87(20), 7814–7818. https://doi.org/10.1073/pnas.87.20.7814

Martienssen, R., & Moazed, D. (2015). RNAi and Heterochromatin Assembly. Cold Spring Harbor Perspectives in Biology, 7(8), a019323. https://doi.org/10.1101/cshperspect.a019323

Martin-Castellanos, C., Labib, K., & Moreno, S. (1996). B-type cyclins regulate G1 progression in fission yeast in opposition to the p25rum1 cdk inhibitor. The EMBO Journal, 15(4), 839–849.

Mata, J., & Bahler, J. (2006). Global roles of Ste11p, cell type, and pheromone in the control of gene expression during early sexual differentiation in fission yeast. Proceedings of the National Academy of Sciences, 103(42), 15517–15522. https://doi.org/10.1073/pnas.0603403103

REFERENCES

Mata, J., Lyne, R., Burns, G., & Bähler, J. (2002). The transcriptional program of meiosis and sporulation in fission yeast. Nature Genetics, 32(1), 143–147. https://doi.org/10.1038/ng951

McLeod, M., & Beach, D. (1986). Homology between the ran1+ gene of fission yeast and protein kinases. The EMBO Journal, 5(13), 3665–3671. https://doi.org/10.1002/j.1460-2075.1986.tb04697.x

McLeod, M., & Beach, D. (1988). A specific inhibitor of the ran1+ protein kinase regulates entry into meiosis in Schizosaccharomyces pombe. Nature, 332(6164), 509–514. https://doi.org/10.1038/332509a0

McLeod, M., Stein, M., & Beach, D. (1987). The product of the mei3+ gene, expressed under control of the mating-type locus, induces meiosis and sporulation in fission yeast. The EMBO Journal, 6(3), 729–736.

Melcher, M., Schmid, M., Aagaard, L., Selenko, P., Laible, G., & Jenuwein, T. (2000). Structure-Function Analysis of SUV39H1 Reveals a Dominant Role in Heterochromatin Organization, Chromosome Segregation, and Mitotic Progression. 20, 14.

Mitchison, J. M., & Nurse, P. (1985). Growth in cell length in the fission yeast Schizosaccharomyces pombe. Journal of Cell Science, 75(1), 357–376. https://doi.org/10.1242/jcs.75.1.357

Mochida, S., & Hunt, T. (2012). Protein phosphatases and their regulation in the control of mitosis. EMBO Reports, 13(3), 197–203. https://doi.org/10.1038/embor.2011.263

Mondesert, O., McGowan, C. H., & Russell, P. (1996). Cig2, a B-type cyclin, promotes the onset of S in Schizosaccharomyces pombe. Molecular and Cellular Biology, 16(4), 1527–1533. https://doi.org/10.1128/MCB.16.4.1527

Moore, L. D., Le, T., & Fan, G. (2013). DNA Methylation and Its Basic Function. Neuropsychopharmacology, 38(1), 23–38. https://doi.org/10.1038/npp.2012.112

REFERENCES

Moreno, S., Hayles, J., & Nurse, P. (1989). Regulation of p34cdc2 protein kinase during mitosis. Cell, 58(2), 361–372. https://doi.org/10.1016/0092-8674(89)90850-7

Moser, B. A., & Russell, P. (2000). Cell cycle regulation in Schizosaccharomyces pombe. Current Opinion in Microbiology, 3(6), 631–636. https://doi.org/10.1016/S1369-5274(00)00152-1

Motamedi, M. R., Hong, E.-J. E., Li, X., Gerber, S., Denison, C., Gygi, S., & Moazed, D. (2008). HP1 Proteins Form Distinct Complexes and Mediate Heterochromatic Gene Silencing by Nonoverlapping Mechanisms. Molecular Cell, 32(6), 778–790. https://doi.org/10.1016/j.molcel.2008.10.026

Motamedi, M. R., Verdel, A., Colmenares, S. U., Gerber, S. A., Gygi, S. P., & Moazed, D. (2004). Two RNAi Complexes, RITS and RDRC, Physically Interact and Localize to Noncoding Centromeric RNAs. Cell, 119(6), 789–802. https://doi.org/10.1016/j.cell.2004.11.034

Muchardt, C., Guilleme, M., Seeler, J.-S., Trouche, D., Dejean, A., & Yaniv, M. (2002). Coordinated methyl and RNA binding is required for heterochromatin localization of mammalian HP1α. EMBO Reports, 3(10), 975–981. https://doi.org/10.1093/embo-reports/kvf194

Murray, A. W. (2004). Recycling the Cell Cycle: Cyclins Revisited. Cell, 116(2), 221–234. https://doi.org/10.1016/S0092-8674(03)01080-8

Nakayama, J., Rice, J. C., Strahl, B. D., Allis, C. D., & Grewal, S. I. (2001). Role of histone H3 lysine 9 methylation in epigenetic control of heterochromatin assembly. Science, 292(5514), 110–113.

Nonaka, N., Kitajima, T., Yokobayashi, S., Xiao, G., Yamamoto, M., Grewal, S. I. S., & Watanabe, Y. (2002). Recruitment of cohesin to heterochromatic regions by Swi6/HP1 in fission yeast. Nature Cell Biology, 4(1), 89–93. https://doi.org/10.1038/ncb739

Norbury, C. J., & Nurse, P. (1989). Control of the higher eukaryote cell cycle by p34cdc2 homologues. Biochimica et Biophysica Acta (BBA) - Reviews on Cancer, 989(1), 85–95. https://doi.org/10.1016/0304-419X(89)90036-X

Nurse, P. (1975). Genetic control of cell size at cell division in yeast. Nature, 256(5518), 547–551. https://doi.org/10.1038/256547a0

Nurse, P. (1985a). Cell cycle control genes in yeast. Trends in Genetics, 1, 51–55. https://doi.org/10.1016/0168-9525(85)90023-X

Nurse, P. (1985b). Mutants of the fission yeast Schizosaccharomyces pombe which alter the shift between cell proliferation and sporulation. Molecular and General Genetics MGG, 198(3), 497–502. https://doi.org/10.1007/BF00332946

Nurse, P., & Bissett, Y. (1981). Gene required in G1 for commitment to cell cycle and in G2 for control of mitosis in fission yeast. Nature, 292(5823), 558–560. https://doi.org/10.1038/292558a0

Nurse, P., & Thuriaux, P. (1977). Controls over the timing of DNA replication during the cell cycle of fission yeast. Experimental Cell Research, 107(2), 365–375. https://doi.org/10.1016/0014-4827(77)90358-5

Nurse, P., & Thuriaux, P. (1980). Regulatory genes controlling mitosis in the fission yeast Schizosaccharomyces Pombe. Genetics, 96(3), 627–637. https://doi.org/10.1093/genetics/96.3.627

Nurse, P., Thuriaux, P., & Nasmyth, K. (1976). Genetic control of the cell division cycle in the fission yeast Schizosaccharomyces pombe. Molecular and General Genetics MGG, 146(2), 167–178. https://doi.org/10.1007/BF00268085

Olins, A. L., & Olins, D. E. (1974). Spheroid chromatin units (v bodies). Science, 183(4122), 330–332.

Olsen, J. V., Blagoev, B., Gnad, F., Macek, B., Kumar, C., Mortensen, P., & Mann, M. (2006). Global, In Vivo, and Site-Specific Phosphorylation Dynamics in Signaling Networks. Cell, 127(3), 635–648. https://doi.org/10.1016/j.cell.2006.09.026

REFERENCES

Orlando, D. A., Chen, M. W., Brown, V. E., Solanki, S., Choi, Y. J., Olson, E. R., Fritz, C. C., Bradner, J. E., & Guenther, M. G. (2014). Quantitative ChIP-Seq Normalization Reveals Global Modulation of the Epigenome. Cell Reports, 9(3), 1163–1170. https://doi.org/10.1016/j.celrep.2014.10.018

Page, S. L., & Hawley, R. S. (2003). Chromosome Choreography: The Meiotic Ballet. Science, 301(5634), 785–789. https://doi.org/10.1126/science.1086605

Park, S. H., Yu, S. E., Chai, Y. G., & Jang, Y. K. (2014). CDK2-dependent phosphorylation of Suv39H1 is involved in control of heterochromatin replication during cell cycle progression. Nucleic Acids Research, 42(10), 6196–6207. https://doi.org/10.1093/nar/gku263

Partridge, J. F., Scott, K. S. C., Bannister, A. J., Kouzarides, T., & Allshire, R. C. (2002). Cis-Acting DNA from Fission Yeast Centromeres Mediates Histone H3 Methylation and Recruitment of Silencing Factors and Cohesin to an Ectopic Site. Current Biology, 12(19), 1652–1660. https://doi.org/10.1016/S0960-9822(02)01177-6

Peters, A. H. F. M., O'Carroll, D., Scherthan, H., Mechtler, K., Sauer, S., Schöfer, C., Weipoltshammer, K., Pagani, M., Lachner, M., Kohlmaier, A., Opravil, S., Doyle, M., Sibilia, M., & Jenuwein, T. (2001). Loss of the Suv39h Histone Methyltransferases Impairs Mammalian Heterochromatin and Genome Stability. Cell, 107(3), 323–337. https://doi.org/10.1016/S0092-8674(01)00542-6

Ragunathan, K., Jih, G., & Moazed, D. (2015). Epigenetic inheritance uncoupled from sequence-specific recruitment. Science, 348(6230).

Rea, S., Eisenhaber, F., O'Carroll, D., Strahl, B. D., Sun, Z.-W., Schmid, M., Opravil, S., Mechtler, K., Ponting, C. P., Allis, C. D., & Jenuwein, T. (2000). Regulation of chromatin structure by site-specific histone H3 methyltransferases. Nature, 406(6796), 593–599. https://doi.org/10.1038/35020506

Roberts, K., Alberts, B., Johnson, A., Walter, P., & Hunt, T. (2002). Molecular biology of the cell. New York: Garland Science, 32(2).

REFERENCES

Russell, P., & Nurse, P. (1987). Negative regulation of mitosis by wee1+, a gene encoding a protein kinase homolog. Cell, 49(4), 559–567. https://doi.org/10.1016/0092-8674(87)90458-2

Saksouk, N., Simboeck, E., & Déjardin, J. (2015). Constitutive heterochromatin formation and transcription in mammals. Epigenetics & Chromatin, 8(1), 3. https://doi.org/10.1186/1756-8935-8-3

Sakuno, T., & Watanabe, Y. (2009). Studies of meiosis disclose distinct roles of cohesion in the core centromere and pericentromeric regions. Chromosome Research, 17(2), 239–249. https://doi.org/10.1007/s10577-008-9013-y

Sato, M., Kakui, Y., & Toya, M. (2021). Tell the Difference Between Mitosis and Meiosis: Interplay Between Chromosomes, Cytoskeleton, and Cell Cycle Regulation. Frontiers in Cell and Developmental Biology, 9, 660322. https://doi.org/10.3389/fcell.2021.660322

Sauvé, D. M., Anderson, H. J., Ray, J. M., James, W. M., & Roberge, M. (1999). Phosphorylation-induced Rearrangement of the Histone H3 NH2-terminal Domain during Mitotic Chromosome Condensation. Journal of Cell Biology, 145(2), 225–235. https://doi.org/10.1083/jcb.145.2.225

Schalch, T., Job, G., Noffsinger, V. J., Shanker, S., Kuscu, C., Joshua-Tor, L., & Partridge, J. F. (2009). High-Affinity Binding of Chp1 Chromodomain to K9 Methylated Histone H3 Is Required to Establish Centromeric Heterochromatin. Molecular Cell, 34(1), 36–46. https://doi.org/10.1016/j.molcel.2009.02.024

Schuettengruber, B., & Cavalli, G. (2009). Recruitment of Polycomb group complexes and their role in the dynamic regulation of cell fate choice. Development, 136(21), 3531–3542. https://doi.org/10.1242/dev.033902

Scott, K. C., Merrett, S. L., & Willard, H. F. (2006). A Heterochromatin Barrier Partitions the Fission Yeast Centromere into Discrete Chromatin Domains. Current Biology, 16(2), 119–129. https://doi.org/10.1016/j.cub.2005.11.065

Seet, B. T., Dikic, I., Zhou, M.-M., & Pawson, T. (2006). Reading protein modifications with interaction domains. Nature Reviews Molecular Cell Biology, 7(7), 473–483. https://doi.org/10.1038/nrm1960

Shi, Y., Lan, F., Matson, C., Mulligan, P., Whetstine, J. R., Cole, P. A., Casero, R. A., & Shi, Y. (2004). Histone Demethylation Mediated by the Nuclear Amine Oxidase Homolog LSD1. Cell, 119(7), 941–953. https://doi.org/10.1016/j.cell.2004.12.012

Shimada, Y., Mohn, F., & Bühler, M. (2016). The RNA-induced transcriptional silencing complex targets chromatin exclusively via interacting with nascent transcripts. Genes & Development, 30(23), 2571–2580. https://doi.org/10.1101/gad.292599.116

Shinkai, Y. (2007). Regulation And Function Of H3K9 Methylation. In T. K. Kundu, R. Bittman, D. Dasgupta, H. Engelhardt, L. Flohe, H. Herrmann, A. Holzenburg, H.-P. Nasheuer, S. Rottem, M. Wyss, & P. Zwickl (Eds.), Chromatin and Disease (pp. 341–354). Springer Netherlands. https://doi.org/10.1007/1-4020-5466-1_15

Shogren-Knaak, M., Ishii, H., Sun, J.-M., Pazin, M. J., Davie, J. R., & Peterson, C. L. (2006). Histone H4-K16 acetylation controls chromatin structure and protein interactions. Science, 311(5762), 844–847.

Simanis, V., & Nurse, P. (1986). The cell cycle control gene cdc2+ of fission yeast encodes a protein kinase potentially regulated by phosphorylation. Cell, 45(2), 261–268. https://doi.org/10.1016/0092-8674(86)90390-9

Smith, G. R. (2009). Genetic Analysis of Meiotic Recombination in Schizosaccharomyces pombe. In S. Keeney (Ed.), Meiosis: Volume 1, Molecular and Genetic Methods (pp. 65–76). Humana Press. https://doi.org/10.1007/978-1-59745-527-5_6

Songyang, Z., Blechner, S., Hoagland, N., Hoekstra, M. F., Piwnica-Worms, H., & Cantley, L. C. (1994). Use of an oriented peptide library to determine the optimal substrates of protein kinases. Current Biology, 4(11), 973–982. https://doi.org/10.1016/S0960-9822(00)00221-9

REFERENCES

Stern, B., & Nurse, P. (1998). Cyclin B Proteolysis and the Cyclin-dependent Kinase Inhibitor rum1p Are Required for Pheromone-induced G 1 Arrest in Fission Yeast. Molecular Biology of the Cell, 9(6), 1309–1321. https://doi.org/10.1091/mbc.9.6.1309

Sugimoto, A., Iino, Y., Maeda, T., Watanabe, Y., & Yamamoto, M. (1991). Schizosaccharomyces pombe ste11+ encodes a transcription factor with an HMG motif that is a critical regulator of sexual development. Genes & Development, 5(11), 1990–1999. https://doi.org/10.1101/gad.5.11.1990

Sugiyama, T., Cam, H. P., Sugiyama, R., Noma, K., Zofall, M., Kobayashi, R., & Grewal, S. I. S. (2007). SHREC, an Effector Complex for Heterochromatic Transcriptional Silencing. Cell, 128(3), 491–504. https://doi.org/10.1016/j.cell.2006.12.035

Swaffer, M. P., Jones, A. W., Flynn, H. R., Snijders, A. P., & Nurse, P. (2018). Quantitative Phosphoproteomics Reveals the Signaling Dynamics of Cell-Cycle Kinases in the Fission Yeast Schizosaccharomyces pombe. Cell Reports, 24(2), 503–514. https://doi.org/10.1016/j.celrep.2018.06.036

Takahashi, K., Murakami, S., Chikashige, Y., Niwa, O., & Yanagida, M. (1991). A large number of tRNA genes are symmetrically located in fission yeast centromeres. Journal of Molecular Biology, 218(1), 13–17. https://doi.org/10.1016/0022-2836(91)90867-6

Trewick, S. C., Minc, E., Antonelli, R., Urano, T., & Allshire, R. C. (2007). The JmjC domain protein Epe1 prevents unregulated assembly and disassembly of heterochromatin. The EMBO Journal, 26(22), 4670–4682. https://doi.org/10.1038/sj.emboj.7601892

Trojer, P., & Reinberg, D. (2007). Facultative Heterochromatin: Is There a Distinctive Molecular Signature? Molecular Cell, 28(1), 1–13. https://doi.org/10.1016/j.molcel.2007.09.011

Verdel, A., Jia, S., Gerber, S., Sugiyama, T., Gygi, S., Grewal, S. I. S., & Moazed, D. (2004). RNAi-Mediated Targeting of Heterochromatin by the RITS Complex. Science, 303(5658), 672–676. https://doi.org/10.1126/science.1093686

Verdel, A., & Moazed, D. (2005). RNAi-directed assembly of heterochromatin in fission yeast. FEBS Letters, 579(26), 5872–5878. https://doi.org/10.1016/j.febslet.2005.08.083

Volpe, T. A., Kidner, C., Hall, I. M., Teng, G., Grewal, S. I., & Martienssen, R. A. (2002). Regulation of heterochromatic silencing and histone H3 lysine-9 methylation by RNAi. Science, 297(5588), 1833–1837.

Wang, J., Reddy, B. D., & Jia, S. (2015). Rapid epigenetic adaptation to uncontrolled heterochromatin spreading. ELife, 4, e06179. https://doi.org/10.7554/eLife.06179

Watanabe, Y., & Nurse, P. (1999). Cohesin Rec8 is required for reductional chromosome segregation at meiosis. Nature, 400(6743), 461–464. https://doi.org/10.1038/22774

Watanabe, Y., Shinozaki-Yabana, S., Chikashige, Y., Hiraoka, Y., & Yamamoto, M. (1997). Phosphorylation of RNA-binding protein controls cell cycle switch from mitotic to meiotic in fission yeast. Nature, 386(6621), 187–190. https://doi.org/10.1038/386187a0

Watanabe, Y., & Yamamoto, M. (1994). S. pombe mei2+ encodes an RNA-binding protein essential for premeiotic DNA synthesis and meiosis I, which cooperates with a novel RNA species meiRNA. Cell, 78(3), 487–498. https://doi.org/10.1016/0092-8674(94)90426-X

Weber, C. M., & Henikoff, S. (2014). Histone variants: Dynamic punctuation in transcription. Genes & Development, 28(7), 672–682. https://doi.org/10.1101/gad.238873.114

Wiehle, L., & Breiling, A. (2016). Chromatin Immunoprecipitation. In C. Lanzuolo & B. Bodega (Eds.), Polycomb Group Proteins: Methods and Protocols (pp. 7–21). Springer. https://doi.org/10.1007/978-1-4939-6380-5_2

Wood, V., Gwilliam, R., Rajandream, M.-A., Lyne, M., Lyne, R., Stewart, A., Sgouros, J., Peat, N., Hayles, J., Baker, S., Basham, D., Bowman, S., Brooks, K., Brown, D., Brown, S., Chillingworth, T., Churcher, C., Collins, M., Connor, R., … Nurse, P. (2002).

The genome sequence of Schizosaccharomyces pombe. Nature, 415(6874), 871–880. https://doi.org/10.1038/nature724

Wu, H., Min, J., Lunin, V. V., Antoshenko, T., Dombrovski, L., Zeng, H., Allali-Hassani, A., Campagna-Slater, V., Vedadi, M., Arrowsmith, C. H., Plotnikov, A. N., & Schapira, M. (2010). Structural Biology of Human H3K9 Methyltransferases. PLOS ONE, 5(1), e8570. https://doi.org/10.1371/journal.pone.0008570

Xhemalce, B., Dawson, M. A., & Bannister, A. J. (2011). Histone Modifications. In Reviews in Cell Biology and Molecular Medicine. John Wiley & Sons, Ltd. https://doi.org/10.1002/3527600906.mcb.201100004

Yamagishi, Y., Sakuno, T., Shimura, M., & Watanabe, Y. (2008). Heterochromatin links to centromeric protection by recruiting shugoshin. Nature, 455(7210), 251–255. https://doi.org/10.1038/nature07217

Yamanaka, S., Mehta, S., Reyes-Turcu, F. E., Zhuang, F., Fuchs, R. T., Rong, Y., Robb, G. B., & Grewal, S. I. S. (2013). RNAi triggered by specialized machinery silences developmental genes and retrotransposons. Nature, 493(7433), 557–560. https://doi.org/10.1038/nature11716

Yamashita, A. (2019). MeiRNA, A Polyvalent Player in Fission Yeast Meiosis. Non-Coding RNA, 5(3), 45. https://doi.org/10.3390/ncrna5030045

Yamashita, A., Sakuno, T., Watanabe, Y., & Yamamoto, M. (2017a). Analysis of Schizosaccharomyces pombe Meiosis. Cold Spring Harbor Protocols, 2017(9), pdb.top079855. https://doi.org/10.1101/pdb.top079855

Yamashita, A., Sakuno, T., Watanabe, Y., & Yamamoto, M. (2017b). Synchronous Induction of Meiosis in the Fission Yeast Schizosaccharomyces pombe. Cold Spring Harbor Protocols, 2017(9), pdb.prot091777. https://doi.org/10.1101/pdb.prot091777

Yokobayashi, S., Yamamoto, M., & Watanabe, Y. (2003). Cohesins determine the attachment manner of kinetochores to spindle microtubules at meiosis I in fission yeast. Molecular and Cellular Biology, 23(11), 3965–3973.

REFERENCES

Yu, H.-G., & Dawe, R. K. (2000). Functional Redundancy in the Maize Meiotic Kinetochore. Journal of Cell Biology, 151(1), 131–142. https://doi.org/10.1083/jcb.151.1.131

Zhang, K., Mosch, K., Fischle, W., & Grewal, S. I. S. (2008). Roles of the Clr4 methyltransferase complex in nucleation, spreading and maintenance of heterochromatin. Nature Structural & Molecular Biology, 15(4), 381–388. https://doi.org/10.1038/nsmb.1406

Zhang, X.-R., Zhao, L., Suo, F., Gao, Y., Wu, Q., Qi, X., & Du, L.-L. (2022). An improved auxin-inducible degron system for fission yeast. G3 Genes|Genomes|Genetics, 12(1), jkab393. https://doi.org/10.1093/g3journal/jkab393

Zhao, Y., & Garcia, B. A. (2015). Comprehensive Catalog of Currently Documented Histone Modifications. Cold Spring Harbor Perspectives in Biology, 7(9), a025064. https://doi.org/10.1101/cshperspect.a025064

Zofall, M., & Grewal, S. I. S. (2006). Swi6/HP1 Recruits a JmjC Domain Protein to Facilitate Transcription of Heterochromatic Repeats. Molecular Cell, 22(5), 681–692. https://doi.org/10.1016/j.molcel.2006.05.010

Zofall, M., Yamanaka, S., Reyes-Turcu, F. E., Zhang, K., Rubin, C., & Grewal, S. I. S. (2012). RNA Elimination Machinery Targeting Meiotic mRNAs Promotes Facultative Heterochromatin Formation. Science, 335(6064), 96–100. https://doi.org/10.1126/science.1211651

APPENDIX

Manuscript: Cdk1-dependent phosphorylation of Clr4^{Suv39H} controls a histone H3 methylation switch that is essential for gametogenesis

APPENDIX

Cdk1-dependent phosphorylation of Clr4^{Suv39H} controls a histone H3 methylation switch that is essential for gametogenesis

Tahsin Kuzdere[1,2], Valentin Benno Flury[1,2], Thomas Schalch[3], Vytautas Iesmantavicius[1], Daniel Hess[1], Marc Bühler[1,2*]

Affiliations:

[1] Friedrich Miescher Institute for Biomedical Research, Maulbeerstrasse 66, 4058 Basel, Switzerland

[2] University of Basel, Petersplatz 10, 4003 Basel, Switzerland

[3] Department of Molecular and Cell Biology, Lancaster Road, LE1 7RH Leicester, United Kingdom

Corresponding Author:

[*]Marc Bühler email: marc.buehler@fmi.ch

Methylation of histone H3 at lysine 9 (H3K9) is a hallmark of heterochromatin that plays crucial roles in chromatin-dependent gene silencing and maintenance of genome stability by repressing repetitive DNA elements and recruiting downstream factors essential for faithful chromosome segregation[1–3]. Fundamental principles of these processes have been elucidated in the fission yeast *Schizosaccharomyces pombe (S. pombe)*, in which Clr4, the homologue of mammalian SUV39H, is the sole H3K9 methyltransferase. Although H3K9 methylation has been intensely studied in mitotic cells[4,5], its role during sexual differentiation remains unclear. Furthermore, it has recently become clear that di- and tri-methylation of H3K9 (H3K9me2 and H3K9me3, respectively) can define functionally distinct chromatin states[6]. Whether distinct H3 methylation states are relevant for gametogenesis is not known. Here, we map H3K9 methylation genome-wide during meiosis and show that constitutive heterochromatin temporarily loses H3K9me2 and becomes H3K9me3 when cells commit to meiosis. Cells lacking the ability to tri-methylate H3K9 exhibit severe meiotic chromosome segregation defects, which does not occur in mitotic cells. Artificially increasing the affinity of the fission yeast heterochromatin protein 1 (HP1) homologue Swi6 towards H3K9me2 rescues chromosome segregation in the absence of H3K9me3. Thus, the H3K9me2 to H3K9me3 switch during early meiosis serves to retain Swi6 at centromeres, which is necessary for cohesin recruitment and kinetochore assembly[7,8]. Finally, we show that the H3K9 methylation switch is regulated by differential phosphorylation of Clr4 by the cyclin-dependent kinase (CDK) Cdk1. Our results reveal how a highly conserved master regulator of the cell cycle regulates the specificity of a H3K9 methyltransferase and thereby controls the ratio of H3K9me2 to H3K9me3 to

prevent formation of facultative heterochromatin and to ensure faithful meiotic chromosome segregation. High degree of conservation of the proteins involved in our study and CDK-dependent phosphorylation of mammalian SUV39H1 suggest broad conservation of the mechanisms described here.

S. pombe grows and divides mitotically in nutrient-rich conditions. Upon nitrogen starvation and availability of a mating partner, meiosis is initiated where a premeiotic S-phase is followed by the first and second meiotic division, producing four haploid gametes[9]. It is well established that the heterochromatic state of centromeres and telomeres is important during meiosis[10–13]. However, the spatial and temporal distribution of the H3K9me2 and H3K9me3 marks that govern these sites, and their functional relevance have not been elucidated.

To profile the heterochromatic landscape during meiosis we performed chromatin immunoprecipitation followed by high throughput sequencing (ChIP-seq) at hourly intervals in diploid *S. pombe* cells undergoing synchronous meiosis[14] (Fig. 1a, Extended Data Fig. 1a, b). When comparing the genome-wide distribution of H3K9me2 and H3K9me3 marks between mitotic and early meiotic *clr4*$^{+}$*/clr4*$^{+}$ cells, we did not observe any facultative heterochromatin sites (Fig. 1b, Extended Data Fig. 2a). However, we noticed a loss of H3K9me2 at the centromeres, telomeres, and subtelomeres at 1h into meiosis. The decrease of H3K9me2 was accompanied by an increased H3K9me3 signal at these sites (Fig. 1b). These genome-wide changes in H3K9 methylation were detectable with and without the use of exogenous spike-In chromatin (Extended Data Fig. 2c). We observed elevated H3K9me3 levels at all constitutive heterochromatin regions during early meiosis (0h-1h), which started to decrease after 2h, as H3K9me3 was replaced by H3K9me2 (Fig. 1c, Extended Data

Fig. 2b). Intrigued by the anticorrelation of H3K9me2 and H3K9me3 marks at the onset of meiosis, we performed ChIP-qPCR experiments to validate H3K9me2 to H3K9me3 ratios at centromeres. Following entry into meiosis (1h), H3K9me2 levels declined drastically and H3K9me3 levels rose at the pericentromeric repeats. As meiosis progressed, the H3K9me2 signal was restored gradually reaching mitotic enrichment levels after 6-8h, which was mirrored by a decline in H3K9me3 (Fig. 1d). In conclusion, though we found no evidence for the *de novo* formation of facultative heterochromatin during meiosis, we discovered an unanticipated H3K9 methylation switch that occurs at the onset of gametogenesis.

To gain insights into the underlying mechanism and physiological relevance of the observed H3K9 methylation switch, we created diploid cells carrying a homozygous active-site mutation in Clr4 (Clr4^{F449Y}), which allows generation of H3K9me2 but blocks H3K9me3[6]. As expected, H3K9me3 was absent in diploid *clr4^{F449Y}/clr4^{F449Y}* cells (Extended Data Fig. 3a). In contrast to wild-type cells, H3K9me2 levels remained high and were unaffected in *clr4^{F449Y}/clr4^{F449Y}* cells when entering meiosis (Fig. 2a, b). This experiment confirms that the downregulation of H3K9me2 during early meiosis is not an artifact caused by the synchronization protocol but rather important for the meiotic program.

Chromosomes do not segregate properly in both mitotic and meiotic *clr4$^{\Delta}$* cells, which are devoid of pericentromeric heterochromatin[8,15,16]. When monitoring mitotically growing *clr4^{F449Y}* cells, we observed no reduction in the growth rate and there was no increased sensitivity to the microtubule-destabilizing drug thiabendazole (TBZ) (Extended Data Fig. 3b, c). We also did not observe any aberrant chromosome segregation patterns, which are hallmarks of impaired chromosome segregation[17] (Fig. 2c). Thus, H3K9me3 at the pericentromeric repeats is dispensable for

segregating chromosomes during mitosis. In contrast, *clr4*^{F449Y}/*clr4*^{F449Y} cells phenocopied *clr4*$^{\Delta}$/*clr4*$^{\Delta}$ cells during the first meiotic division, exhibiting elevated levels of missegregated chromosome and increased equational segregation of sister chromatids (Fig. 2d, f). These results underscore a critical role of H3K9me3 during meiotic chromosome segregation.

Methylated H3K9 serves as a binding site for proteins with a chromodomain (CD), whose binding affinity is positively correlated with the methylation state of the histone tail (me<me2<me3)[18]. Swi6 is such a protein and is known to regulate chromosome segregation by recruiting cohesin, promoting kinetochore assembly, and preventing inaccurate microtubule attachment[7,8]. To assess Swi6 binding to centromeres in wild-type and *clr4* mutant cells during meiosis I, we performed live cell fluorescence microscopy with cells expressing Swi6-yeGFP and a centromere marker, Mis6-mCherry. Consistent with earlier studies, the majority of Swi6 colocalized with centromeres during meiosis I in *clr4*$^{+}$/*clr4*$^{+}$ cells. Further, DNA was pulled to the opposite poles of the cell with a subset of telomere-bound Swi6 foci trailing behind[15]. In *clr4*$^{\Delta}$/*clr4*$^{\Delta}$ cells, no distinct Swi6-yeGFP localization, but a rather diffuse nuclear staining was observed. Similarly, the majority of Swi6-yeGFP signal was evenly distributed in the nucleus of H3K9me3-deficient *clr4*^{F449Y}/*clr4*^{F449Y} cells, with only a small fraction colocalizing with centromeres (Fig. 3a). This observation indicates that highest binding affinity of Swi6 towards H3 is necessary for proper subnuclear localization in meiocytes, for which H3K9 needs to be tri-methylated.

Previous studies have shown that binding of Swi6 to di-methylated histone H3-tail peptides is roughly 3-fold lower compared to tri-methylated peptides (10.28 μM and 3.34 μM, respectively)[19]. This raises the possibility that the H3K9 methylation switch at the onset of meiosis functions to maximize Swi6 binding to pericentromeric

chromatin. To test whether increased affinity of Swi6 towards H3K9me2 would rescue the meiotic segregation defects of a *clr4*^{F449Y} strain, we mutated key residues in the CD of Swi6 (E80V, V82E, S116E, D120N, and S122F) thus making it more similar to the high affinity CD of the fission yeast CD-containing protein 1 (Chp1; 0.55 μM for H3K9me2)[19]. Substituting Swi6 with Swi6$^{Chp1\text{-}like\text{-}CD}$ in the *clr4*^{F449Y}/*clr4*^{F449Y} background restored Swi6 enrichments at the pericentromeric repeats (Fig. 3b). Furthermore, we no longer observed missegregated chromosomes in *clr4*^{F449Y}/*clr4*^{F449Y} cells upon expression of Swi6$^{Chp1\text{-}like\text{-}CD}$ (Fig. 3c, d). These data strongly suggest that the *in vivo* affinity of Swi6 towards H3K9me2 is not strong enough to localize sufficient levels of Swi6 to the centromeres during the first meiotic division. Therefore, *S. pombe* has evolved a mechanism that converts all H3K9me2 to H3K9me3 at the onset of meiosis to strengthen Swi6 binding at pericentromeric regions for faithful assembly of kinetochores.

This poses the question why Swi6 did not simply evolve to have a higher affinity towards H3K9me2 rather than requiring a change from H3K9me2 to H3K9me3 in early meiosis. Therefore, we investigated what consequences a higher binding affinity of Swi6 would have in mitotically growing cells by performing ChIP-seq experiments in various Swi6 and Clr4 mutant backgrounds. Consistent with the live cell imaging results, little Swi6 was bound at the centromeric repeats in *clr4*^{F449Y} cells (Fig. 3e). Because telomeric H3K9me2 cannot be stably maintained by Clr4^{F449Y}, Swi6 was no longer enriched at telomeres (Extended Data Fig. 4a)[6]. However, centromeric Swi6$^{Chp1\text{-}like\text{-}CD}$ binding was restored (Fig. 3e). In *clr4*$^{+}$ cells, Swi6$^{Chp1\text{-}like\text{-}CD}$ was strongly enriched at the pericentromeric repeats (Extended Data Fig. 4b). Moreover, Swi6$^{Chp1\text{-}like\text{-}CD}$ was ectopically binding at many sites distributed over the genome which was accompanied by the formation of ectopic H3K9me2 islands at those sites (Fig. 3e, f).

These results show that increasing Swi6's affinity towards methylated H3K9 beyond physiological levels can cause the formation of facultative heterochromatin in mitotic cells. Therefore, it is desirable to have a low affinity Swi6 protein, as this would firstly prevent unwanted formation of facultative heterochromatin in regions with potential nucleation sites, and secondly provide the organism a means to recruit effector proteins conditionally through modulation of the H3K9 methylation state in a fast and reversible manner.

Clr4 histone methyltransferase activity is intrinsically inhibited in mitotic cells by an autoregulatory loop (ARL) that connects the SET and post-SET domains[20]. Our results imply that such inhibition is reversed at the onset of meiosis, likely via deposition or removal of a post-translational modification (PTM), which are well known to regulate protein activities in a fast and reversible manner[21]. Phosphoproteomic screens in *S. pombe* revealed multiple phosphorylation sites on Clr4. Yet, biological relevance has remained enigmatic[22–24]. To examine whether the phosphorylation state of Clr4 changes when cells enter meiosis, we analyzed the migration of 3xFLAG-tagged Clr4 (3xFLAG-Clr4) protein extracted from mitotic and meiotic cells on PhosTag gels. This revealed that Clr4 was dephosphorylated during early meiosis (0h-1h), and became gradually phosphorylated after 2h into the meiotic program (Fig. 4a, Extended Data Fig. 5a), correlating well with the timing of the H3K9 methylation switch (Fig. 1d). To determine the differentially phosphorylated Clr4 residues, we subjected mitotic and meiotic 3xFLAG-Clr4 protein to mass-spectrometry. Intriguingly, this revealed two differentially phosphorylated serine residues, S458 and S462, which are located in the ARL of Clr4 (Fig. 4b). Substituting the first serine of the ARL with a non-phosphorylatable alanine residue (Clr4^{S458A}) was sufficient to abrogate slow migration of mitotic Clr4 on PhosTag gels, mimicking migration of meiotic Clr4. Mutating S462

in addition to S458 had no noticeable additive effect (Fig. 4c). Thus, S458 is a key residue of Clr4 that is differentially phosphorylated during meiosis.

These results support a model in which constitutive phosphorylation of Clr4 dampens H3K9me3 activity during mitosis. At the onset of meiosis, Clr4 phosphorylation at S458 ceases, enabling full transition from H3K9me2 to H3K9me3. To identify the kinase responsible for $Clr4^{S458}$ phosphorylation, we performed a candidate screen making use of a phospho-specific antibody that we raised against $Clr4^{S458}$ (α-pS458) (Extended Data Fig. 5b). We selected candidate kinases based on meiotic phenotypes, minimal consensus sequence preference (S/T-P), and mitotic versus meiotic expression or activity. Of those candidates that were non-essential and could be knocked-out, none was accountable for Clr4 phosphorylation (Extended Data Fig. 6a). One candidate that we could not delete is the cyclin-dependent kinase Cdk1 (also known as Cdc2). Instead, we used an ATP analogue-sensitive *cdk1* allele (*cdk1-as*) that allows conditional inhibition of Cdk1 activity[25]. Upon inhibition of Cdk1-as, $Clr4^{S458}$ phosphorylation rapidly decreased and was undetectable 3h post-inhibition, whereas Clr4 phosphorylation levels remained unaffected in $cdk1^{+}$ cells (Fig. 4d, Extended Data Fig. 6b). Thus, phosphorylation of Clr4 at S458 critically depends on Cdk1. We made use of an *in vitro* kinase assay to test if Clr4 is a direct target of Cdk1. Indeed, human CDK1/Cyclin B phosphorylated recombinant Clr4 specifically at S458 with high efficiencies (Fig. 4e). To ultimately test if Cdk1 inhibition would trigger the conversion of H3K9me2 to H3K9me3, we performed ChIP experiments in mitotically growing $cdk1^{+}$ and *cdk1-as* cells in the absence or presence of the ATP analogue 1-NM-PP1. This revealed reduced H3K9me2, but increased H3K9me3 levels in *cdk1-as* cells specifically (Fig. 4f), mimicking the H3K9 methylation switch naturally occurring at the onset of gametogenesis.

In summary, we discovered that the ARL of Clr4 is phosphorylated in a Cdk1-dependent manner, which functions to hold up full transition from H3K9me2 to H3K9me3 during mitosis. Upon entry into meiosis, unphosphorylated Clr4 is required to achieve maximal H3K9me3 levels, which is a prerequisite for strong Swi6 binding and subsequent faithful chromosome segregation during meiosis I. Thus, in addition to its classical function in suppressing transcription, H3K9me3 is crucial for the generation of haploid gametes. Consistent with our observation that the meiotic H3K9 methylation switch correlates with the phosphorylation status of Clr4, inhibition of Cdk1 activity is essential for initiation of sexual differentiation and early meiosis. Notably, nitrogen starvation induces a G_1 arrest, which is maintained by the Cdk1 inhibitor Rum1[26]. Prior to premeiotic S-phase, Rum1 is degraded, upon which Cdk1 gets reactivated[27]. This provides a likely mechanism underlying the pre-meiotic H3K9 methylation switch occurring at the very same time.

Interestingly, Cdk1-dependent phosphorylation of the proline-directed serine within the SET and the post-SET domains of Clr4 appears to be conserved in the mammalian system. That is, SUV39H1^{S391}, analogous to Clr4^{S458}, is phosphorylated by CDK2[28]. Whether SUV39H1 phosphoregulation similarly affects methyltransferase specificity and is also controlling faithful division of chromosomes during meiosis in humans remains to be investigated. If so, this could have key implications for understanding genetic disorders associated with aberrant chromosome segregation resulting in aneuploidy, such as Down syndrome or certain forms of cancer[29].

APPENDIX

REFERENCES

1. Lachner, M. & Jenuwein, T. The many faces of histone lysine methylation. *Curr Opin Cell Biol* 14, 286–298 (2002).

2. Martin, C. & Zhang, Y. The diverse functions of histone lysine methylation. *Nat Rev Mol Cell Bio* 6, 838–849 (2005).

3. Bloom, K. S. Centromeric Heterochromatin: The Primordial Segregation Machine. *Annu Rev Genet* 48, 1–28 (2014).

4. Allshire, R. C. & Ekwall, K. Epigenetic Regulation of Chromatin States in Schizosaccharomyces pombe. *Csh Perspect Biol* 7, a018770 (2015).

5. Grewal, S. I. S. & Jia, S. Heterochromatin revisited. *Nat Rev Genet* 8, 35–46 (2007).

6. Jih, G. *et al.* Unique roles for histone H3K9me states in RNAi and heritable silencing of transcription. *Nature* 547, 463–467 (2017).

7. Bernard, P. *et al.* Requirement of Heterochromatin for Cohesion at Centromeres. *Science* 294, 2539–2542 (2001).

8. Yamagishi, Y., Sakuno, T., Shimura, M. & Watanabe, Y. Heterochromatin links to centromeric protection by recruiting shugoshin. *Nature* 455, 251–255 (2008).

9. Yamashita, A., Sakuno, T., Watanabe, Y. & Yamamoto, M. Analysis of Schizosaccharomyces pombe Meiosis. *Cold Spring Harb Protoc* 2017, pdb.top079855 (2017).

10. Chikashige, Y. *et al.* Telomere-led premeiotic chromosome movement in fission yeast. *Science* 264, 270–273 (1994).

11. Ellermeier, C. *et al.* RNAi and heterochromatin repress centromeric meiotic recombination. *Proc National Acad Sci* 107, 8701–8705 (2010).

12. Watanabe, Y. & Nurse, P. Cohesin Rec8 is required for reductional chromosome segregation at meiosis. *Nature* 400, 461–464 (1999).

13. Hall, I. M., Noma, K. & Grewal, S. I. S. RNA interference machinery regulates chromosome dynamics during mitosis and meiosis in fission yeast. *Proc National Acad Sci* 100, 193–198 (2003).

14. Cipak, L., Polakova, S., Hyppa, R. W., Smith, G. R. & Gregan, J. Synchronized fission yeast meiosis using an ATP analog–sensitive Pat1 protein kinase. *Nat Protoc* 9, 223–231 (2014).

15. Klutstein, M., Fennell, A., Fernández-Álvarez, A. & Cooper, J. P. The telomere bouquet regulates meiotic centromere assembly. *Nat Cell Biol* 17, 458–469 (2015).

16. Ekwall, K. *et al.* Mutations in the fission yeast silencing factors clr4+ and rik1+ disrupt the localisation of the chromo domain protein Swi6p and impair centromere function. *J Cell Sci.* 2637–2648 (1996).

17. Pidoux, A. L., Uzawa, S., Perry, P. E., Cande, W. Z. & Allshire, R. C. Live analysis of lagging chromosomes during anaphase and their effect on spindle elongation rate in fission yeast. *Journal of Cell Science* 4177–4191 (2000).

18. Eissenberg, J. C. Structural biology of the chromodomain: Form and function. *Gene* 496, 69–78 (2012).

19. Schalch, T. *et al.* High-Affinity Binding of Chp1 Chromodomain to K9 Methylated Histone H3 Is Required to Establish Centromeric Heterochromatin. *Mol Cell* 34, 36–46 (2009).

20. Iglesias, N. *et al.* Automethylation-induced conformational switch in Clr4 (Suv39h) maintains epigenetic stability. *Nature* 560, 504–508 (2018).

21. Olsen, J. V. *et al.* Global, In Vivo, and Site-Specific Phosphorylation Dynamics in Signaling Networks. *Cell* 127, 635–648 (2006).

22. Carpy, A. *et al.* Absolute Proteome and Phosphoproteome Dynamics during the Cell Cycle of Schizosaccharomyces pombe (Fission Yeast)*. *Mol Cell Proteomics* 13, 1925–1936 (2014).

23. Kettenbach, A. N. *et al.* Quantitative Phosphoproteomics Reveals Pathways for Coordination of Cell Growth and Division by the Conserved Fission Yeast Kinase Pom1*. *Mol Cell Proteomics* 14, 1275–1287 (2015).

24. Swaffer, M. P., Jones, A. W., Flynn, H. R., Snijders, A. P. & Nurse, P. Quantitative Phosphoproteomics Reveals the Signaling Dynamics of Cell-Cycle Kinases in the Fission Yeast Schizosaccharomyces pombe. *Cell Reports* 24, 503–514 (2018).

25. Dischinger, S., Krapp, A., Xie, L., Paulson, J. R. & Simanis, V. Chemical genetic analysis of the regulatory role of Cdc2p in the S. pombe septation initiation network. *J Cell Sci* 121, 843–853 (2008).

26. Stern, B. & Nurse, P. Cyclin B Proteolysis and the Cyclin-dependent Kinase Inhibitor rum1p Are Required for Pheromone-induced G1 Arrest in Fission Yeast. *Mol Biol Cell* 9, 1309–1321 (1998).

27. Daga, R. R., Bolaños, P. & Moreno, S. Regulated mRNA Stability of the Cdk Inhibitor Rum1 Links Nutrient Status to Cell Cycle Progression. *Curr Biol* 13, 2015–2024 (2003).

28. Park, S. H., Yu, S. E., Chai, Y. G. & Jang, Y. K. CDK2-dependent phosphorylation of Suv39H1 is involved in control of heterochromatin replication during cell cycle progression. *Nucleic Acids Res* 42, 6196–6207 (2014).

29. Gordon, D. J., Resio, B. & Pellman, D. Causes and consequences of aneuploidy in cancer. *Nat Rev Genet* 13, 189–203 (2012).

30. Bähler, J. *et al.* Heterologous modules for efficient and versatile PCR-based gene targeting in Schizosaccharomyces pombe. *Yeast* 14, 943–951 (1998).

31. Ekwall, K. & Thon, G. Setting up Schizosaccharomyces pombe Crosses/Matings. *Cold Spring Harb Protoc* 2017, pdb.prot091694 (2017).

32. Stunnenberg, R. *et al.* H3K9 methylation extends across natural boundaries of heterochromatin in the absence of an HP1 protein. *Embo J* 34, 2789–2803 (2015).

33. Gaidatzis, D., Lerch, A., Hahne, F. & Stadler, M. B. QuasR: quantification and annotation of short reads in R. *Bioinformatics* 31, 1130–1132 (2015).

34. Hagan, I. M. Immunofluorescence Microscopy of Schizosaccharomyces pombe Using Chemical Fixation. *Cold Spring Harb Protoc* 2016, pdb.prot091017 (2016).

35. MacLean, B. *et al.* Skyline: an open source document editor for creating and analyzing targeted proteomics experiments. *Bioinformatics* 26, 966–968 (2010).

36. Krapp, A. *et al.* Analysis of the S. pombe Meiotic Proteome Reveals a Switch from Anabolic to Catabolic Processes and Extensive Post-transcriptional Regulation. *Cell Reports* 26, 1044-1058.e5 (2019).

37. Mata, J., Lyne, R., Burns, G. & Bähler, J. The transcriptional program of meiosis and sporulation in fission yeast. *Nat Genet* 32, 143–147 (2002).

APPENDIX

Supplementary Information is linked to the online version of the paper at www.nature.com/nature.

Code availability

All custom codes used to analyze data and generate figures are available upon reasonable request.

Data availability

Genome-wide data sets are deposited at GEO under the accession number GSE182250.

Acknowledgements

We thank Fabio Mohn for discussion, advise, data deposition, and feedback on the manuscript. We thank Yukiko Shimada and Nathalie Laschet for technical support and Max Louski for his contribution generating strains. We would like to thank the FMI Functional Genomics facility for assistance in library construction and next generation sequencing and Jan Seebacher for discussions. We are grateful to Laurent Gelman and Steven Bourke for assistance during imaging and we thank Juraj Gregan and Viesturs Simanis for sharing strains. Also, we thank Viesturs Simanis for commenting on the manuscript. This work has received funding from the European Research Council (ERC) under the European Union's Horizon 2020 research and innovation programme (grant agreement no. 681213 - REpiReg) and the Novartis Research Foundation.

Author Contributions

T.K., V.F., and M.B. conceived ideas and designed experiments. T.K. generated strains, performed experiments, and analyzed data. T.S. performed *in vitro* experiments and V.I. and D.H. acquired and analyzed mass spectrometry data. T.K. and M.B. prepared figures and wrote the manuscript. All authors discussed results and commented on the manuscript. M.B. supervised the study and secured funding.

Author Information

Reprints and permissions information is available at www.nature.com/reprints. The authors declare competing financial interests: FMI receives significant financial contributions from the Novartis Research Foundation. Published research reagents from the FMI are shared with the academic community under a Material Transfer Agreement (MTA) having terms and conditions corresponding to those of the UBMTA (Uniform Biological Material Transfer Agreement). Correspondence and requests for materials should be addressed to marc.buehler@fmi.ch.

APPENDIX

FIGURE LEGENDS

Figure 1. H3K9me2 transitions to H3K9me3 at the onset of meiosis.

a, Exemplary images of ethanol-fixed and DAPI-stained *pat1-as2/pat1-as2 mat-Pc* cells synchronized for meiotic progression. 0h corresponds to cells after 7h of pre-meiotic nitrogen starvation and marks the start of 1-NM-PP1 addition. The timing of pre-meiotic S-phase (S), meiosis I (MI), and meiosis II (MII) are indicated above the images.

b, Genome browser snapshot of H3K9me2 (black), H3K9me3 (blue), and total H3 (brown) ChIP-seq reads in asynchronous mitotic and early meiotic (1h) cells mapped to chromosome I. Reads were normalized to library size and are shown as reads per million; tel1L = left telomere 1, cen1 = centromere 1, tel1R = right telomere 1.

c, H3K9me2 (top) and H3K9me3 (bottom) ChIP-seq enrichments (scaled) at constitutive heterochromatin regions during meiotic progression. Multi-mapping reads were normalized to library size and total H3 ChIP-seq enrichments. Two independent biological replicates were sequenced and the average enrichment is displayed.

d, ChIP-qPCR experiments to assess H3K9me2 (top) and H3K9me3 (bottom) levels at pericentromeric repeats (*cendh*) during mitosis and meiosis. ChIP enrichments were normalized to total H3 levels and *adh1*$^{+}$ and are shown relative to mitotic cells; Error bars, s.d.; n = 3 independent biological replicates; P values between two time points were calculated using two-tailed student's t-test, P_{Anova} was calculated using ANOVA.

Figure 2. H3K9me3 is dispensable for mitotic but not meiotic chromosome segregation.

a, b, ChIP-qPCR experiments to assess (**a**) H3K9me2 and (**b**) H3K9me3 levels at pericentromeric repeats (*cendg*) in *clr4*$^{+}$/*clr4*$^{+}$ (black) and *clr4*^{F449Y}/*clr4*^{F449Y} (blue) cells during mitosis and early meiosis. ChIP enrichments were normalized to total H3 levels and *adh1*$^{+}$ and are shown relative to mitotic cells; Error bars, s.d.; *n* = 3 independent biological replicates.

c, d, Comparison of requirement for H3K9 methylation for (**c**) mitotic and (**d**) meiotic chromosome segregation. Exemplary IF microscopy images of the indicated fission yeast strains are shown. DNA and tubulin was stained with DAPI and anti-TAT-1, respectively. Missegregated chromosomes are indicated with a yellow arrow; Scale bar = 5 μM. Quantification of chromosome segregation phenotypes are shown below the microscopy images. *P* values were calculated using Fisher's exact test. Number of total cells counted is indicated in each bar.

e, Schematic illustration showing the distribution of sister chromatids (green and black dots, respectively) during meiosis I and meiosis II. In wild-type cells, sister chromatids first co-segregate (also called reductional segregation) during meiosis I and then undergo equational segregation during meiosis II. Therefore, sister chromatids end up in adjacent ascospores. If co-segregation during meiosis I is impaired, sister chromatids undergo equational segregation during both meiotic divisions, resulting in non-adjacent distribution of sister chromatids in the resulting ascospore.

f, Comparison of requirement for H3K9me3 for co-segregation of centromere I (CenI) during meiosis I. Exemplary live cell microscopy images of the indicated fission yeast strains during meiosis I and meiosis II are shown. Heterozygous CenI-GFP was used to follow the segregation pattern during meiosis; Scale bar = 5 μM. Quantification of CenI-GFP segregation during meiosis I are shown below the microscopy images. *P*

values were calculated using Fisher's exact test. Number of total cells counted is indicated in each bar.

Figure 3. Restoration of Swi6 binding to pericentromeric repeats rescues the meiotic chromosome segregation phenotype in H3K9me3-depleted cells.

a, Comparison of Swi6 localization depending on H3K9 methylation during meiosis I. Exemplary live cell microscopy images of the indicated fission yeast strains are shown. Swi6 and the centromere marker Mis6 were visualized by tagging with yeGFP and mCherry, respectively; Scale bar = 5 µM.

b, ChIP-qPCR experiment to assess Swi6 levels at the pericentromeric repeats (*cendg*) in the indicated fission yeast strains. ChIP enrichments were normalized to *adh1*$^{+}$ and are shown relative to *swi6*$^{\Delta}$ cells; Error bars, s.d.; *n* = 4 independent biological replicates. *P* values were calculated using two-tailed student's *t*-test.

c, Comparison of meiotic chromosome segregation in cells lacking H3K9me3 depending on Swi6's affinity towards H3K9me2. Exemplary IF microscopy images of the indicated fission yeast strains are shown. DNA and tubulin was stained with DAPI and anti-TAT-1, respectively. Missegregated chromosome is indicated with a yellow arrow; Scale bar = 5 µM.

d, Quantification of meiotic chromosome segregation phenotypes. *P* values were calculated using Fisher's exact test. Number of total cells counted is indicated in each bar.

e, Genome browser snapshot of Swi6, H3K9me2, and H3K9me3 ChIP-seq reads in the indicated strains mapped to chromosome I. Reads were normalized to library size and are shown as reads per million; tel1L = left telomere 1, cen1 = centromere 1, tel1R = right telomere 1.

f, Quantification of H3K9me2 (black) and H3K9me3 (blue) enrichments at the top 100 ectopic Swi6$^{Chp1\text{-}like\text{-}CD}$ peaks in *swi6*$^{+}$ and *swi6*$^{Chp1\text{-}like\text{-}CD}$ cells. Input normalized ChIP enrichments are shown in log2 scale.

g, Quantification of gene expression levels in *swi6*$^{+}$ and *swi6*$^{Chp1\text{-}like\text{-}CD}$ cells at either the top 100 ectopic Swi6$^{Chp1\text{-}like\text{-}CD}$ peaks (black) or random non-peak genes (blue). Reads were normalized to gene length and to million mapped reads (RPKM) and are shown in log2 scale.

Figure 4. Clr4^{S458} is differentially phosphorylated in a Cdk1-dependent manner in mitosis versus early meiosis.

a, Western blot of whole-cell lysates (WCL) using a PhosTag gel for anti-FLAG (top) and a Bis-Tris gel for anti-Act1 detection (bottom), respectively. WCL were prepared from mitotic and meiotic *3xFLAG-clr4*$^{+}$*/3xFLAG-clr4*$^{+}$ cultures at the indicated time points.

b, Comparing the relative abundance of the differentially phosphorylated Clr4 peptide (DF**S**PVQ**S**QK) in mitosis and early meiosis by IP-MS.

c, Western blot of FLAG IPs using a PhosTag gel to asses phosphorylation levels of Clr4 in the indicated homothallic strains.

d, Western blot of FLAG IPs in *3xFLAG-clr4*$^{+}$ *cdc2-as* cells, treated with 2 µM 1-NM-PP1 for the indicated amount of time. The blot was first probed with the phospho-specific anti-pS458 antibody, stripped, and reprobed with an anti-FLAG antibody.

e, *In vitro* kinase assay of recombinant Clr4 and Clr4^{S58A} in presence and absence of human CDK1/Cyclin B. Phosphorylation events were analyzed by IP-MS.

f, ChIP-qPCR experiments to assess H3K9me2 (left) and H3K9me3 (right)

levels at pericentromeric repeats (*cendg*) in *cdk1*$^{+}$ and *cdk1-as* cells treated with and without 3 μM 1-NM-PP1. ChIP enrichments were normalized to total H3 levels and *adh1*$^{+}$ and are shown relative to untreated cells; Error bars, s.d.; *n* = 3 independent biological replicates; *P* values were calculated using two-tailed student's *t*-test.

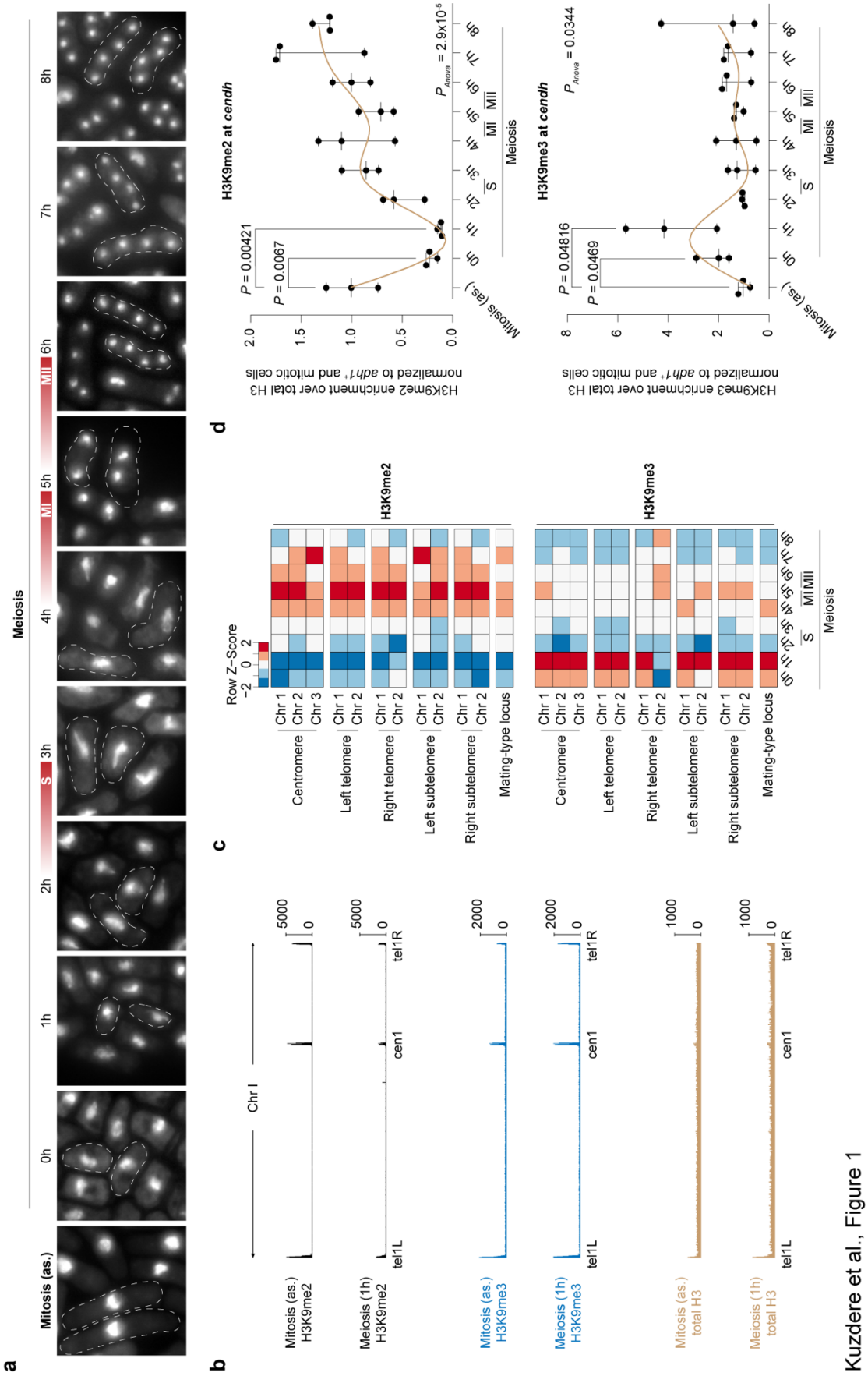

Kuzdere et al., Figure 1

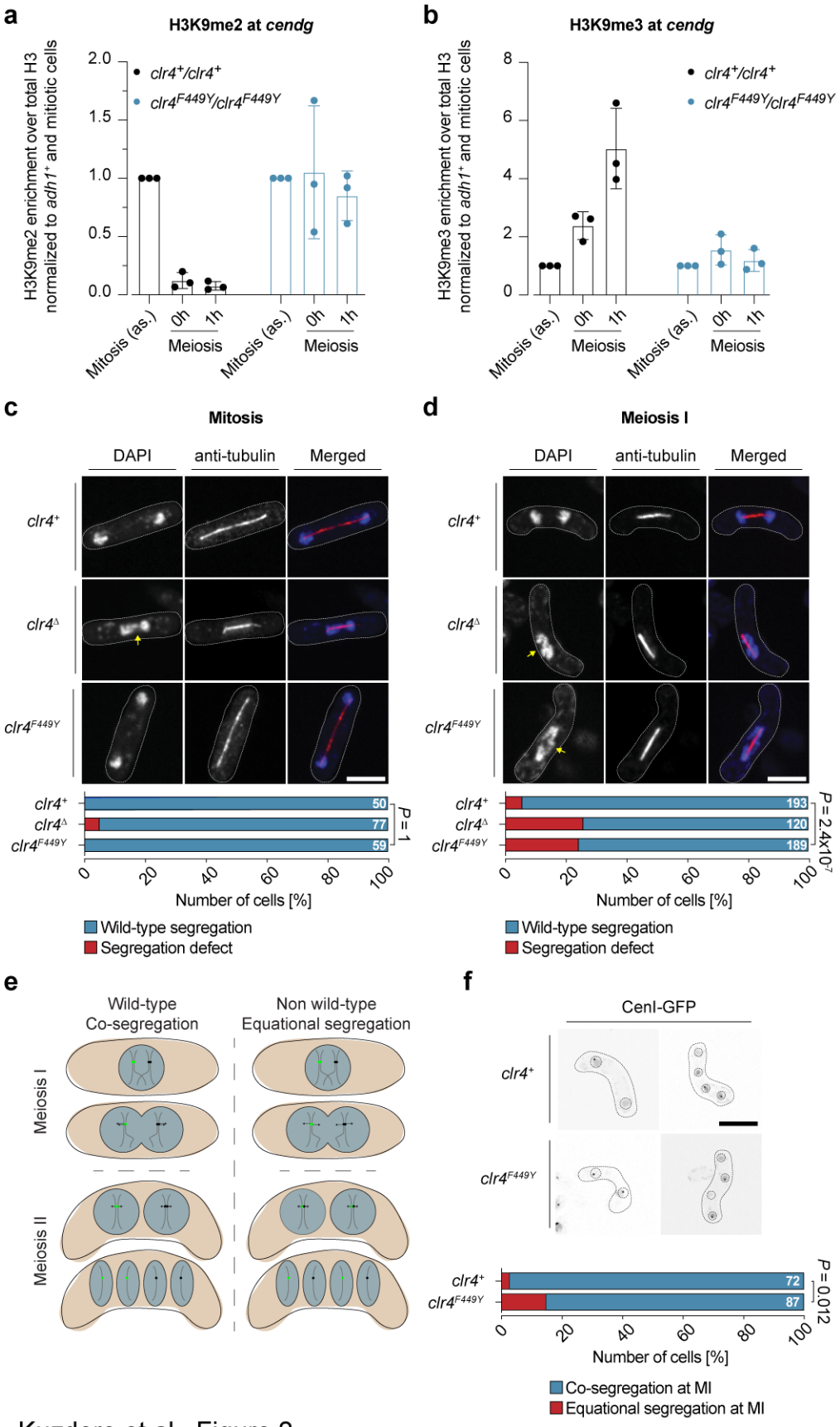

Kuzdere et al., Figure 2

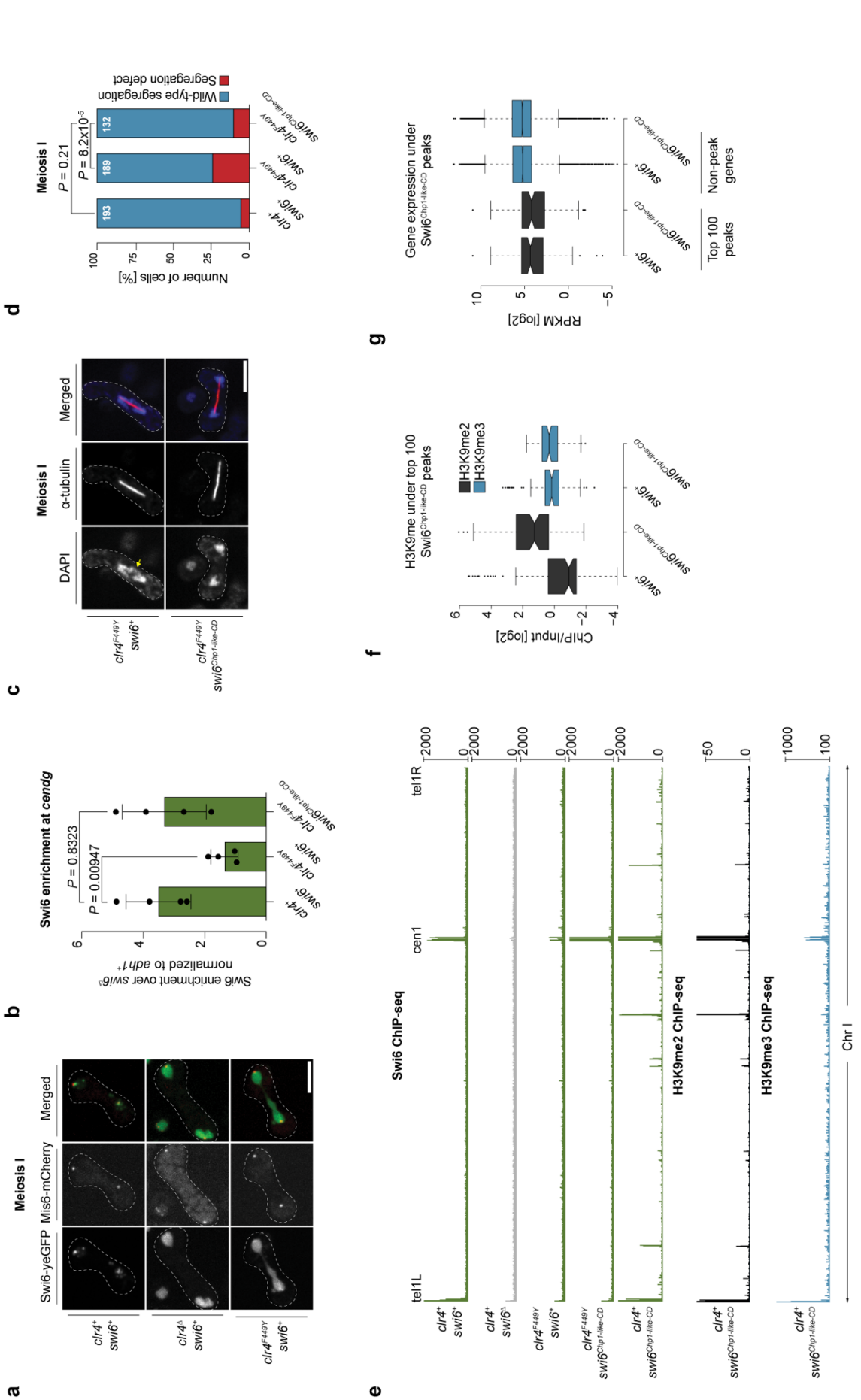

Kuzdere et al., Figure 3

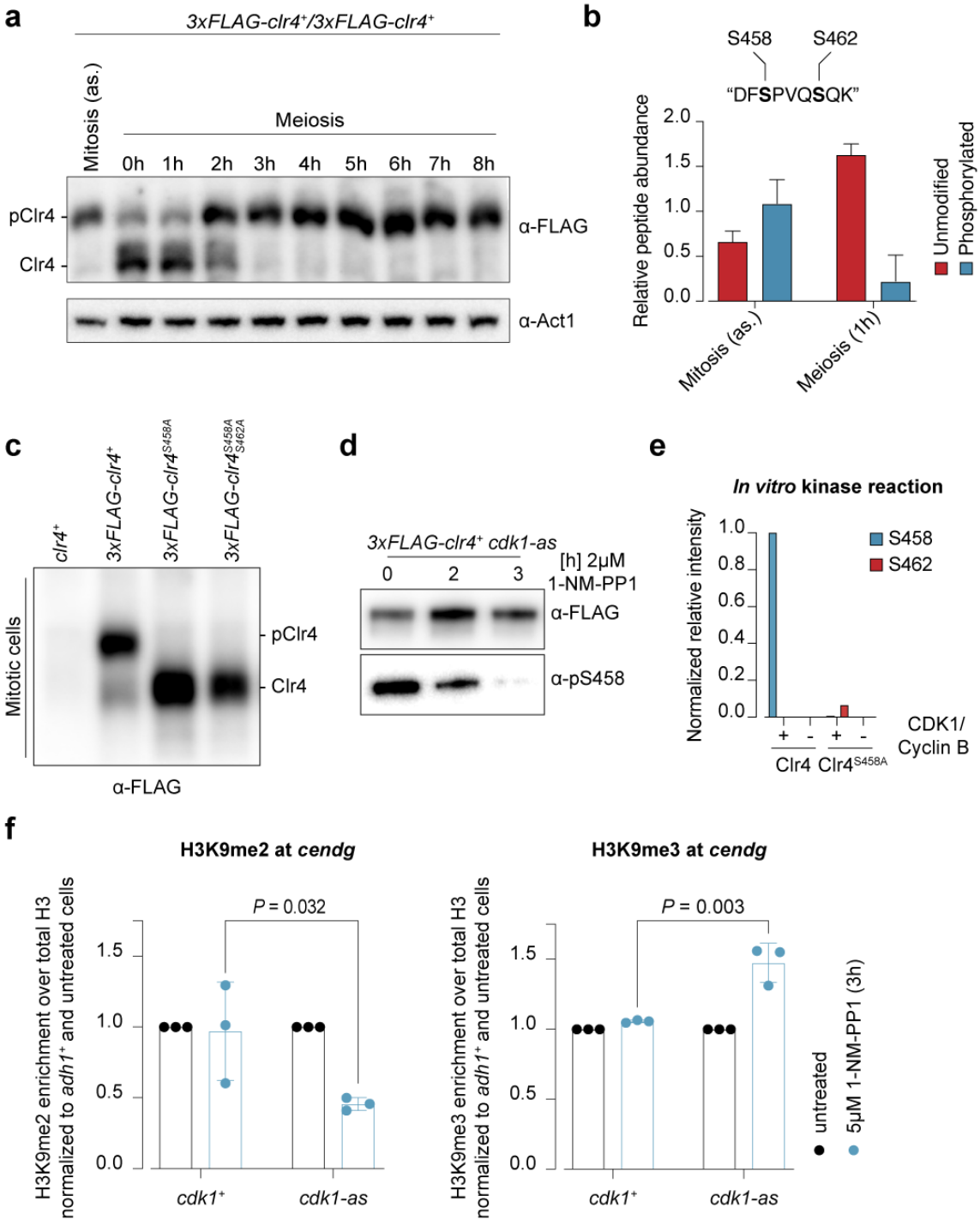

Kuzdere et al., Figure 4

APPENDIX

METHODS

Strains and plasmids. The diploid *h⁻/h⁻ pat1-as2/pat1-as2* strains were grown at 25 °C in YE4S-ade. Cells carrying the *cdc2-as* mutation were grown at 25 °C in YES. All other fission yeast strains were grown at 30 °C in YES. All strains were constructed following the prevailing fission yeast protocol[30] or by standard mating and sporulation. The diploid *h⁻/h⁻ pat1-as2/pat1-as2* strains were created by protoplast fusion[31]. Strains and plasmids generated in this study are shown in Supplementary Tables 1 and 2.

Synchronization of fission yeast meiosis. Fission yeast meiosis was synchronized as previously described[14]. Briefly, diploid *h⁻/h⁻ pat1-as2/pat1-as2 S. pombe* cells were grown to OD_{595} of 0.55 at 25 °C in YE4S-ade. Cells were harvested (2000 g, 2 min, 25 °C), washed twice with sterile water, and resuspended in EMM2 - NH_4Cl medium. Premeiotic nitrogen starvation was carried out for 7 h at 25 °C (referred to as “0 h”). Afterwards, cells were harvested (2000 g, 2 min, 25 °C), resuspended in EMM2 + NH_4Cl, and 25 µM 1-NM-PP1 (Toronto Research Chemicals) was added. The cell culture was grown at 25 °C until the desired time points were reached.

Flow cytometry analysis of DNA content. 1 ml of cell culture (OD_{595} of 0.55 – 1.2) was pelleted (4000 g, 2 min, 4 °C) and resuspended in 1 ml 70% ice-cold ethanol. Fixed cells were kept at 4 °C if cells from multiple time points were collected. 500 µl fixed cells were centrifuged (3000 g, 5 min, 25 °C) and washed twice with 1 ml 50 mM sodium citrate. Cell pellets were resuspended by vortexing. After the last washing step, pellets were treated with 500 µl 50 mM sodium citrate + 0.1 mg/ml RNase A for at least 1.5 h at 37 °C. Subsequently, 500 µl 50 mM sodium citrate + 2 µM Sytox Green (Thermo Fisher Scientific) were added and samples were mixed by vortexing. To

break apart cell aggregates, samples were sonicated for 5 s on a 550 Sonic Dismembrator (Thermo Fisher Scientific) before being transferred to 5 ml FACS tubes (Becton Dickinson). Flow cytometry measurements were performed on a BD LSRII SORP Analyzer (Becton Dickinson) using a 488 nm excitation laser (flow rate = low; mode = linear). Per sample 20000 cells were counted and the data was post-processed and visualized with FlowJo.

Chromatin Immunoprecipitation. For H3K9me2, H3K9me3, and total H3 ChIP 50 ml of fission yeast culture were either grown to mid-log phase (or synchronized as described before) and crosslinked with 1% formaldehyde (15 min, 25 °C). For Swi6 ChIP cells were incubated for 2 h at 18 °C, resuspended in 5 ml PBS (3000 rpm, 3 min, 18 °C), double-crosslinked with 1.5 mM EGS (30 min, 25 °C) and 1% formaldehyde (30 min, 25 °C). The crosslinking reaction was quenched by the addition of 130 mM glycine (5 min, 25 °C). Cells were washed twice (3000 rpm, 4 min, 4 °C) with 15 ml ice-cold PBS and transferred to a 2 ml screw cap tube with 500 µl ice-cold PBS. Cells were spun down (3000 rpm, 3 min, 4°C), flash-frozen in liquid nitrogen, and stored at -80 °C until use. For the ChIP, cell pellets were thawed on ice and resuspended in 400 µl ice-cold complete lysis buffer (50 mM HEPES/KOH pH 7.5, 140 mM NaCl, 1 mM EDTA, 1% Triton X-100, 0.1% sodium deoxycholate (fresh), 1x HALT protease inhibitor cocktail (Thermo Fisher Scientific)). Silica beads (0.5 mm) were added up to the meniscus of the cell suspension and cells were lysed at 4 °C using a FastPrep-24 bead beating grinder (MP biomedicals) (3x 60s at 6.5 m/s). To prevent overheating during bead beating, the reaction tubes were cooled down for 2 min on ice between each round. The reaction tubes were punctured with a 25 G needle and the crude lysate was collected by centrifugation (1000 rpm, 1 min, 4 °C). The lysates

were adjusted to 1.5 ml with complete lysis buffer in 15 ml Bioruptor Pico tubes (Diagenode) and sonicated for 2 rounds at 4 °C (12 cycles, 30 s on/30 s off) using the Bioruptor Pico system (Diagenode). Samples were cooled down on ice for 5 min between each round. Afterwards, lysates were cleared twice by centrifugation (13000 rpm, 4 °C) for 5 min and 15 min, respectively. In the meantime, 2.5 µg of anti-H3K9me2 (MABI0307), anti-H3K9me3 (MABI0308), anti-histone H3 (ab1791), or anti-Swi6[32] antibody was pre-coupled to either 30 µl anti-mouse IgG or anti-rabbit IgG dynabeads (Thermo Fisher Scientific) for 30 min at 25 °C. The cleared lysates were normalized by total protein concentration and the conjugated dynabeads were added (2 h, 4 °C). If needed, 50 µl of lysate was saved as an input control. The dynabeads were separated using a magnetic rack and washed three times with 1 ml ice-cold lysis buffer, once with 1 ml ice-cold wash buffer I (10 mM Tris-HCl pH 8.0, 250 mM LiCl, 0.5% NP-40, 0.5% sodium deoxycholate (fresh), 1 mM EDTA), and once with 1ml ice-cold 1x TE. The ChIPs were eluted first in 100 µl 1% TES (1% SDS, 1x TE) (10 min, 65 °C) and a second time in 150 µl 0.67% TES (0.67% SDS, 1x TE) (5 min, 65 °C). The eluates were combined (V_t = 250 µl) and decrosslinked overnight at 65 °C. Samples were treated with 40 µg RNase A (1 h, 37 °C) and 60 µg Proteinase K (1 h, 65 °C). DNA was precipitated by addition of 150 mM NaCl and 1 volume isopropanol (15 min, 25 °C), cleaned-up using 30 µl AMPure XP beads, and eluted in 20 µl elution buffer (10 mM Tris-HCl pH 8.0, 1 mM EDTA).

Quantitative real-time PCR. ChIP DNA was diluted 1:20 and real-time PCR was performed using the SsoAdvanced SYBR Green supermix (Bio-Rad) and a CFX96 Real-Time System (Bio-Rad). Primer sequences of oligos used for qPCR are given in Supplementary Table 3.

ChIP-sequencing. ChIP sequencing libraries were generated using the NEBNext Ultra II DNA Library Prep Kit (New England Biolabs) and sequenced with an Illumina HiSeq2500 (50bp single-end). Raw data was demultiplexed, converted to fastq format using bcl2fastq2 (v1.17), and mapped using STAR (Genome_build: Spombe.ASM294v2.24). For bigwig track generation by bedtools (v2.26.0) and bedGraphToBigWig (from UCSC binary utilities), non-aligned reads were discarded and read coverage was normalized to 1 million genome mapping reads (RPM). All ChIP-sequencing experiments were done at least twice.

Total RNA isolation and sequencing. Total RNA was extracted using the MasterPure Yeast RNA Purification kit (Lucigen). Libraries were prepared with the TruSeq Stranded Total RNA kit (Illumina) according to the manufacturer's instructions and sequenced with an Illumina HiSeq2500 (50bp single-end). Reads were processed, normalized, and analyzed using QuasR with two mismatches allowed[33].

Immunofluorescence microscopy. IF experiments were performed as described previously[34] with minor modifications. In brief, to analyze mitotic chromosome segregation 10 ml yeast culture were grown to mid-log phase and fixed with 3% formaldehyde and 0.25% glutaraldehyde (1 h, 25 °C). To investigate chromosome segregation during meiosis I, 10 ml of exponentially growing homothallic cells were harvested (3000 rpm, 3 min, 25°C) and plated on a SPAS plate overnight. The next day cells were scraped off, resuspended in 10 ml sterile water, and fixed as described before. Cells were permeabilized with 0.75 mg/ml lysing enzyme from *Trichoderma harzianum* (Sigma) and 0.375 mg/ml Zymolyase (Zymo Research) for 45 min at 25 °C. 1:10 diluted TAT1 anti-tubulin tissue culture supernatant (00020911) was used as

the primary antibody and 1:500 diluted Alexa Fluor 568-conjugated anti-mouse antibody (Thermo Fisher Scientific) was used as the secondary antibody. Cells were mounted on lectin-coated (Sigma) microscopy slides using SlowFade Gold Antifade Mountant with DAPI (Thermo Fischer Scientific). Images were acquired on an inverted AxioObserver7 microscope (Zeiss), equipped with a Yokogawa CSU W1-T2 spinning disk and a PlanApo 100x/1.40 oil objective, using the software Visiview. Z-stacks of cells exhibiting mitotic and meiotic spindles, respectively, were acquired and chromosome segregation was scored by presence and absence of missegregated DAPI signal. Maximum intensity projections were created using FIJI.

Live cell imaging. 1 ml of exponentially growing homothallic *swi6-yeGFP mis6-mCherry* cells were harvested (3000 rpm, 3 min, 25°C) and plated on a SPAS plate overnight. The next day cells were scraped off, resuspended in 500 µl EMM2 + NH_4Cl, and mounted on lectin-coated (Sigma) microscopy slides. Images were acquired on an inverted AxioObserver7 microscope (Zeiss), equipped with a Yokogawa CSU W1-T2 spinning disk and a PlanApo 100x/1.40 oil objective, using the software Visiview. Z-stacks of meiocytes with two Mis6-mCherry foci at each end of the cell (meiosis I) were acquired. Maximum intensity projections were created using FIJI.

Generation of phospho-specific α-pS458 antibody. The “Phospho-Specific Antibody Services” of GenScript was used to generate the rabbit polyclonal anti-pS458 antibody. “CTFDYAGAKDF(pS458)PVQ” was used as the antigen peptide.

Immunoprecipitation. Unless stated otherwise, all steps were carried out on ice (or at 4 °C) and with ice-cold buffers. 100 ml of fission yeast culture were grown to mid-

log phase (or synchronized as described before) and pelleted (2500 rpm, 4 min). Synchronized cultures were harvested in the presence of 1 mM PMSF. Pellets were washed twice with 5 ml TBS (50 mM Tris-HCl pH 7.5, 150 mM NaCl), resuspended in 500 µl TBS, harvested (6000 rpm, 30 s), and flash-frozen in liquid nitrogen. Cell pellets were stored at -80 °C until use. For the IP, pellets were thawed on ice and resuspended in 400 µl lysis buffer (20 mM HEPES/KOH pH 7.5, 500 mM NaCl, 5 mM $MgCl_2$, 1 mM EDTA, 10 % glycerol, 0.25 % Triton X-100, 0.5 mM DTT (fresh), 1x HALT protease and phosphatase Inhibitor cocktail (Thermo Fisher Scientific)). Silica beads (0.5 mm) were added up to the meniscus of the cell suspension and cells were lysed using a FastPrep-24 bead beating grinder (MP biomedicals) (3x 20s at 6.5 m/s). To prevent overheating during bead beating, the reaction tubes were cooled down for 2 min on ice between each round. The reaction tubes were punctured with a 25 G needle and the crude lysate was collected by centrifugation (1000 rpm, 1 min). The lysates were cleared twice by centrifugation (13000 rpm, 10 min) and protein concentration of the supernatant was estimated using a Bradford assay (Bio-Rad). Samples were normalized to 2-3 mg total protein in 800 µl complete lysis buffer. 2.5 µg anti-FLAG M2 antibody (Sigma) were pre-coupled to 30 µl anti-mouse IgG dynabeads (Thermo Fischer Scientific) for 30 min at 25 °C and incubated for 2h with the cell lysates. The dynabeads were separated using a magnetic rack and washed twice with 500 µl complete lysis buffer and twice with 500 µl wash buffer (20 mM HEPES/KOH pH 7.5, 150 mM NaCl, 5 mM $MgCl_2$, 10 % glycerol, 0.25 % Triton X-100). Depending on the downstream application, beads were treated differently from this point onwards.

Western blot. IP-dynabeads were boiled in 25 µl 1x sample buffer (62.5 mM Tris-HCl pH 6.8, 10% glycerol, 2% SDS, 5% β-mercaptoethanol, 0.005% bromophenol blue)

for 5 min at 95 °C. 12 µl of the supernatant were loaded either on a Bolt 4-12% Bis-Tris gel (Thermo Fisher Scientific) or a SuperSep PhosTag gel (Wako). Gels were transferred using the Trans-Blot Turbo Transfer System (Bio-Rad). All steps were carried out according to the manufacturer's instructions.

Phosphatase assay. IP-dynabeads were transferred to a fresh reaction tube with 500 µl B100-nd buffer (10 mM Tris-HCl pH 7.5, 2 mM $MgCl_2$, 100 mM NaCl) and washed twice on a magnetic rack. The phosphatase assay was carried out using Lambda Protein Phosphatase (λ-PP) (New England Biolabs) according to the manufacturer's instructions. The reactions were performed in the presence and absence of λ-PP and 1x HALT phosphatase inhibitor cocktail (Thermo Fisher Scientific).

Mass spectrometry. IP-dynabeads were transferred to a fresh reaction tube with 500 µl B100-nd buffer (10 mM Tris-HCl pH 7.5, 2 mM $MgCl_2$, 100 mM NaCl) and washed twice on a magnetic rack. Beads were digested for 2 h at 25°C with 0.2 µg Lys-C in 5 µl HTC buffer (20 mM HEPES/KOH pH 8.5, 5 mM TCEP, 10 mM CAA) containing 8 M urea. Subsequently, 17 µl HEPES/KOH pH 8.5 and 0.2 µg trypsin were added and the digestion reaction was incubated overnight at 37 °C. Peptides generated by trypsin digestion were acidified with 0.8% TFA (final) and analyzed by LC–MS/MS on an EASY-nLC 1000 (Thermo Scientific) with a two-column set-up. The peptides were applied onto a peptide µPAC™ trapping column in 0.1% formic acid, 2% acetonitrile in H_2O at a constant flow rate of 5 µl/min. Using a flow rate of 500 nl/min, peptides were separated at RT with a linear gradient of 3%–6% buffer B in buffer A in 4 min followed by an linear increase from 6 to 22% in 55 min, 22%–40% in 4 min, 40%–80% in 1 min, and the column was finally washed for 10 min at 80% buffer B in buffer A

(buffer A: 0.1% formic acid; buffer B: 0.1% formic acid in acetonitrile) on a 50 cm µPAC™ column (PharmaFluidics) mounted on an EASY-Spray™ source (Thermo Scientific) connected to an Orbitrap Fusion LUMOS (Thermo Scientific). The survey scan was performed using a 120,000 resolution in the Orbitrap. The PRM analysis was optimized using synthetic heavy peptides. The Clr4 peptides were targeted based on their retention times and fragmented using HCD followed by an orbitrap detection using a 120,000 resolution. The acquired PRM data were processed using Skyline 4[35]. The transition selection was systematically verified and adjusted when necessary to ensure that no co-eluting contaminant distorted.

Whole-cell lysate extraction. Whole-cell lysates (WCL) for 3xFLAG-Clr4 detection were extracted as described previously[36]. For histone H3 and H3K9me3 detection WCL were prepared using trichloroacetic acid (TCA).

Statistics. For statistical analysis of ChIP-qPCR data a two-tailed Student's *t*-test was used. Significance of chromosome segregation defects was determined with a Fisher's exact test. In both cases $P < 0.05$ was used as the significance level. No statistical methods were used to predetermine sample size.

Supplementary Table 1: Fission yeast strains used in this study.

Name	Genoytpe	Obtained from
Spb2819	*h-/h- ade6-M210/ade6-M216 pat1::NatR/pat1::NatR pat1-as(L95A)::HygR/pat1-as(L95A)::HygR cen2(D107)::KanR-ura4+-lacO his7+::lacI-GFP lys1::MatPc-Bleo*	Juraj Gregan, University of Vienna, Austria*
Spb4136	*h-/h- ade6-M210/ade6-M216 pat1::NatR/pat1::NatR pat1-as(L95A)::HygR/pat1-as(L95A)::HygR lys1::MatPc-Bleo*	
Spb4137	*h-/h- ade6-M210/ade6-M216 pat1::NatR/pat1::NatR pat1-as(L95A)::HygR/pat1-as(L95A)::HygR clr4::clr4F449Y/clr4::clr4F449Y lys1::MatPc-Bleo*	
Spb594	*h90 ade6-M216 leu1-32 ura4-DS/E*	Nakayama, RIKEN Center for Developmental Biology, Japan
Spb595	*h90 ade6-M216 leu1-32 ura4-DS/E clr4Δ::ura4+*	Nakayama, RIKEN Center for Developmental Biology, Japan
Spb3475	*h90 ade6-M216 leu1-32 ura4-DS/E clr4::clr4F449Y*	
Spb4168	*h90 ade6-M216 leu1-32 ura4-DS/E swi6-yeGFP::HygR mis6-mCherry::KanR*	
Spb4182	*h90 ade6-M216 leu1-32 ura4-DS/E clr4Δ::ura4+ swi6-yeGFP::HygR mis6-mCherry::KanR*	
Spb4183	*h90 ade6-M216 leu1-32 ura4-DS/E clr4::clr4F449Y swi6-yeGFP::HygR mis6-mCherry::KanR*	
Spb721	*h90 ade6-M210 leu1-32 ura4-DS/E mat3M::GFP-NatR swi6Δ::ura3+*	
Spb1073	*h90 ade6-M210 leu1-32 ura4-DS/E mat3M::GFP-NatR swi6::swi6E80V-V82E-S116E-D120N-S122F*	
Spb4712	*h90 ade6-M210 leu1-32 ura4-DS/E mat3M::GFP-NatR swi6::swi6E80V-V82E-S116E-D120N-S122F clr4::clr4F449Y*	
Spb4713	*h-/h- ade6-M210/ade6-M216 pat1::NatR/pat1::NatR pat1-as(L95A)::HygR/pat1-as(L95A)::HygR clr4::3xFLAG-clr4-clr4ter-KanR/clr4::3xFLAG-clr4-clr4ter-KanR lys1::MatPc-Bleo*	
Spb4563	*h90 ade6-M216 leu1-32 ura4-DS/E clr4::3xFLAG-clr4-clr4ter-KanR*	
Spb4564	*h90 ade6-M216 leu1-32 ura4-DS/E clr4::3xFLAG-clr4S458A-clr4ter-KanR*	
Spb4566	*h90 ade6-M216 leu1-32 ura4-DS/E clr4::3xFLAG-clr4S458A-S462A-clr4ter-KanR*	
Spb4621	*h+ cdc2-as ura4-D18 clr4::3xFLAG-clr4-clr4ter-KanR*	Viesturs Simanis, EPFL, Switzerland
Spb4575	*h90 ade6-M216 leu1-32 ura4-DS/E clr4::3xFLAG-clr4-clr4ter-KanR spk1::NatR*	
Spb4576	*h90 ade6-M216 leu1-32 ura4-DS/E clr4::3xFLAG-clr4-clr4ter-KanR gsk3::NatR*	
Spb4577	*h90 ade6-M216 leu1-32 ura4-DS/E clr4::3xFLAG-clr4-clr4ter-KanR tor1::NatR*	
Spb4578	*h90 ade6-M216 leu1-32 ura4-DS/E clr4::3xFLAG-clr4-clr4ter-KanR pef1::NatR*	
Spb4579	*h90 ade6-M216 leu1-32 ura4-DS/E clr4::3xFLAG-clr4-clr4ter-KanR bub1::NatR*	
Spb71	*h- ade6-M210 leu1-32 ura4-D18 his3-D1*	
Spb4153	*h- ade6-M210 leu1-32 ura4-D18 his3-D1 clr4::clr4F449Y*	
Spb4232	*h+ ad6-M210 leu1-32 ura4-D18 his7+::lacI-GFP lys1+::lacOp*	Taro Nakamura, Osaka University, Japan
Spb4777	h+ ad6-M210 leu1-32 ura4-D18 his7+::lacI-GFP lys1+::lacOp clr4::clr4F449Y	
Spb64	*h90 968*	Charles Hoffman, Boston College, USA
Spb65	*h- 972*	Charles Hoffman, Boston College, USA
Spb66	*h+ 975*	Charles Hoffman, Boston College, USA

* Cipak et al., 2014, Nature protocols

Supplementary Table 2: List of plasmids used in this study.

Name	Insert
pMB0725	pGEX - swi6E80V-V82E-S116E-D120N-S122F
pMB0463	pFA6a - link-yEGFP-HygR
pMB0167	pFA6a - mCherry-KanR
pMB2190	pJET1.2 - 3xFLAG-clr4-clr4ter-KanR
pMB2191	pJET1.2 - 3xFLAG-clr4S458A-clr4ter-KanR
pMB2192	pJET1.2 - 3xFLAG-clr4S458A-S462A-clr4ter-KanR

Extended Data Figure Legends

Extended Data Figure 1. Validation of synchronization efficiency of meiotic fission yeast cultures.

a, Flow cytometry analysis to compare DNA content of asynchronous mitotic fission yeast cells and cells during synchronized meiotic progression. DNA was stained with Sytox Green and 20000 cells were counted for each time point.

b, mRNA expression levels of meiotic genes during synchronized meiotic progression. Two genes per meiotic expression cluster (nitrogen-induced, early, middle, and late) were selected[37]. mRNA reads were normalized to library size and are shown in log2 scale.

Extended Data Figure 2. Genome-wide H3K9me2 and H3K9me3 profiles during fission yeast meiosis.

a, Genome browser snapshot of H3K9me2 (black), H3K9me3 (blue), and total H3 (brown) ChIP-seq reads in asynchronous mitotic and early meiotic (1h) cells mapped to chromosome II (left) and chromosome III (right), respectively. Reads were normalized to library size and are shown as reads per million; tel2L = left telomere 2, cen2 = centromere 2, tel2R = right telomere 2, cen3 = centromere 3.

b, H3K9me2 (top) and H3K9me3 (bottom) ChIP-seq enrichments (scaled) at constitutive heterochromatin regions during meiotic progression. Uniquely mapping reads were normalized to library size and total H3 ChIP-seq enrichments. Two independent biological replicates were sequenced and the average enrichment is displayed.

c, H3K9me2 and H3K9me3 ChIP-seq enrichments (scaled) at constitutive heterochromatin regions in mitotic and meiotic (1h) cells. Uniquely mapping reads were normalized to mESC spike-In chromatin instead to library size.

Extended Data Figure 3. H3K9me3 is dispensable for chromosome segregation and normal growth rates in mitosis.

a, Western blot of whole-cell lysates (WCL) from the indicated *clr4* strains, probed with anti-histone H3 and anti-H3K9me3 antibodies, respectively.

b, c, Comparison of requirement for H3K9 methylation for mitotic growth (**b**) in liquid culture and (**c**) on solid media with and without TBZ.

Extended Data Figure 4. The effects of Clr4 and Swi6 mutations on telomeric heterochromatin and centromeric Swi6 binding, respectively.

a, ChIP-qPCR experiments to assess H3K9me2 and H3K9me3 levels at the telomeres (*TAS1/2*) in $clr4^{+}$ (black) and $clr4^{F449Y}$ (blue) cells. ChIP enrichments were normalized to $act1^{+}$ and are shown relative to $clr4^{\Delta}$ cells; Error bars, s.d.; *n* = 3 independent biological replicates.

b, ChIP-qPCR experiment to assess Swi6 levels at the centromeric repeats (*cendg*) in $swi6^{+}$ and $swi6^{Chp1\text{-}like\text{-}CD}$ cells. ChIP enrichments were normalized to $adh1^{+}$ and are shown relative to $swi6^{\Delta}$ cells; Error bars, s.d.; *n* = 4 independent biological replicates.

Extended Data Figure 5. Clr4 is differentially phosphorylated during mitosis and early meiosis.

a, Western blot of FLAG IPs using a PhosTag gel to asses phosphorylation levels of Clr4 during mitosis and early meiosis in $3xFLAG\text{-}clr4^{+}$/$3xFLAG\text{-}clr4^{+}$ cells.

b, Phosphatase assay of 3xFLAG-Clr4^{+} and 3xFLAG-Clr4^{S458A} in presence and absence of λ-protein phosphatase (PP) and PP inhibitor. Treated IPs were analyzed by western blotting and detected with anti-FLAG and anti-pS458, respectively.

Extended Data Figure 6. Candidate screen to identify the kinase responsible for Clr4 phosphorylation.

a, Western blot of FLAG IPs using a PhosTag gel to asses phosphorylation levels of Clr4 in 3xFLAG-*clr4*$^{+}$, 3xFLAG-*clr4*^{S458A}, and the indicated kinase knock-out strains.

b, Western blot of FLAG IPs using a PhosTag gel. *3xFLAG-clr4*$^{+}$ *cdc2*$^{+}$ cells were treated with 5 μM 1-NM-PP1 for the indicated amount of time.

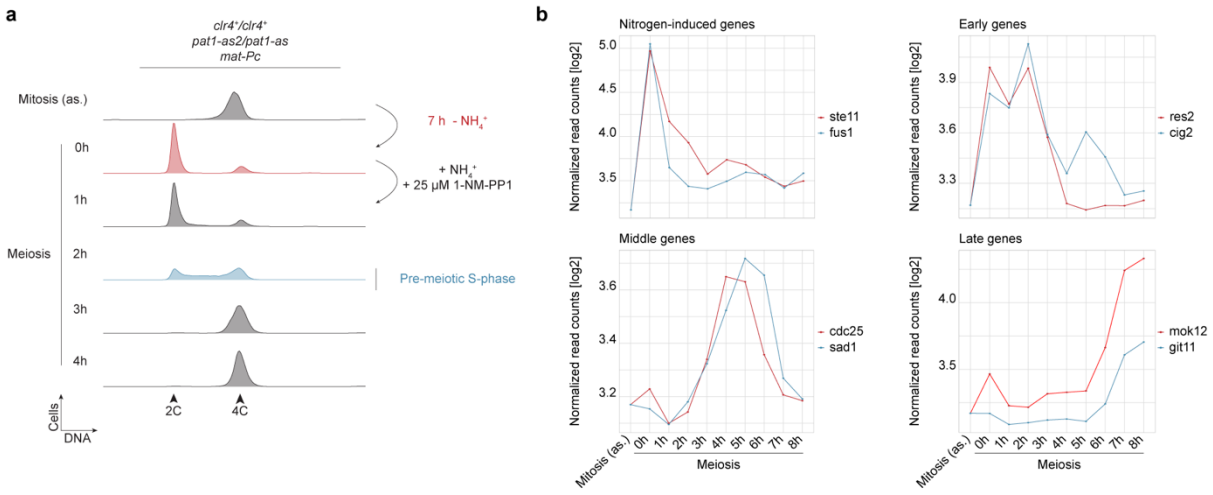

Kuzdere et al., Extended Data Figure 1

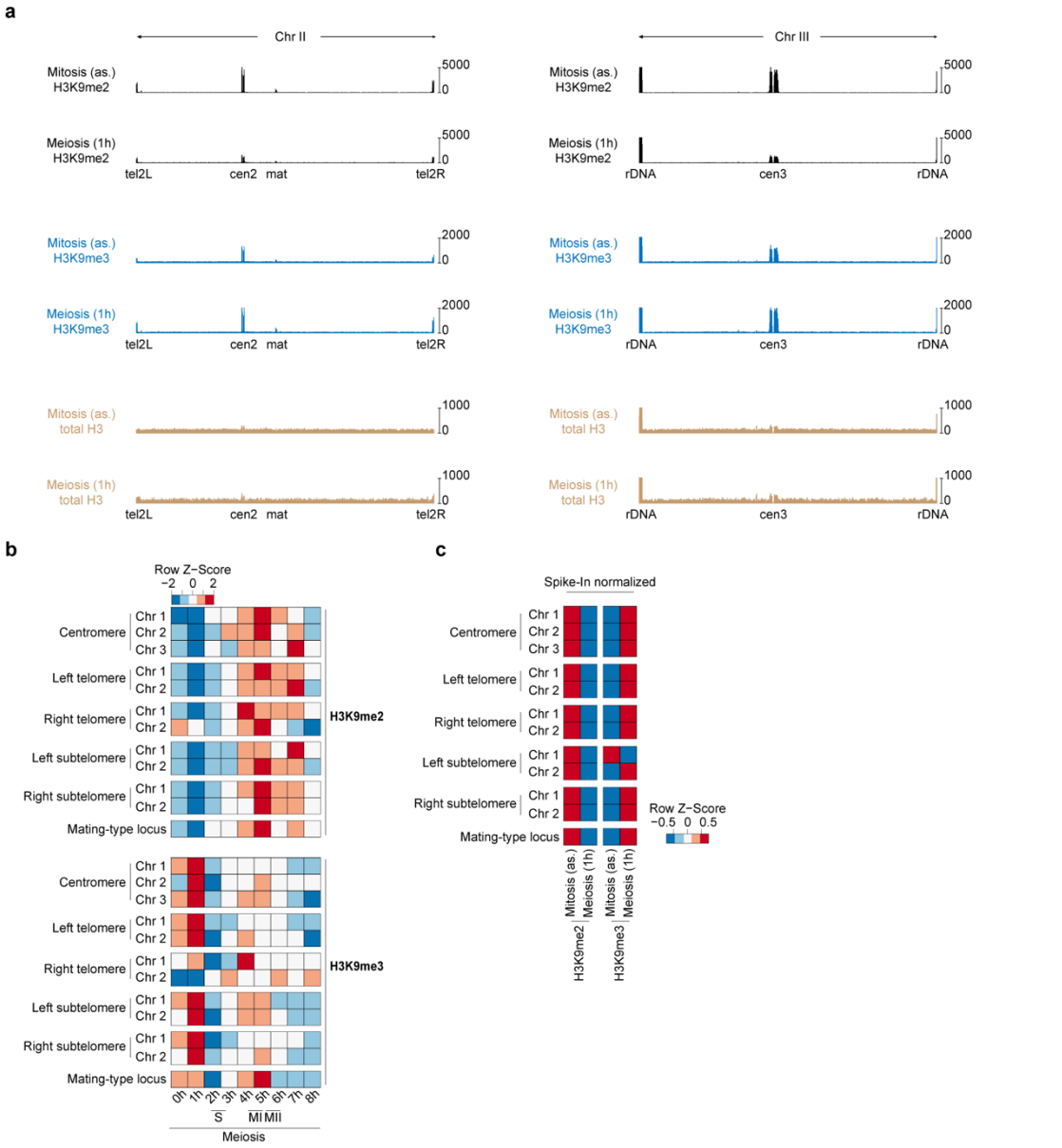

Kuzdere et al., Extended Data Figure 2

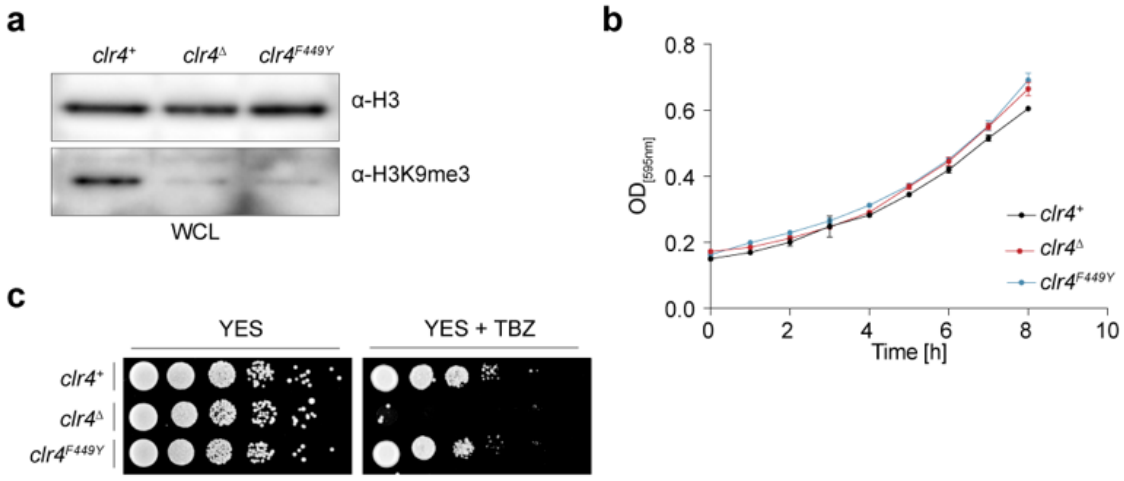

Kuzdere et al., Extended Data Figure 3

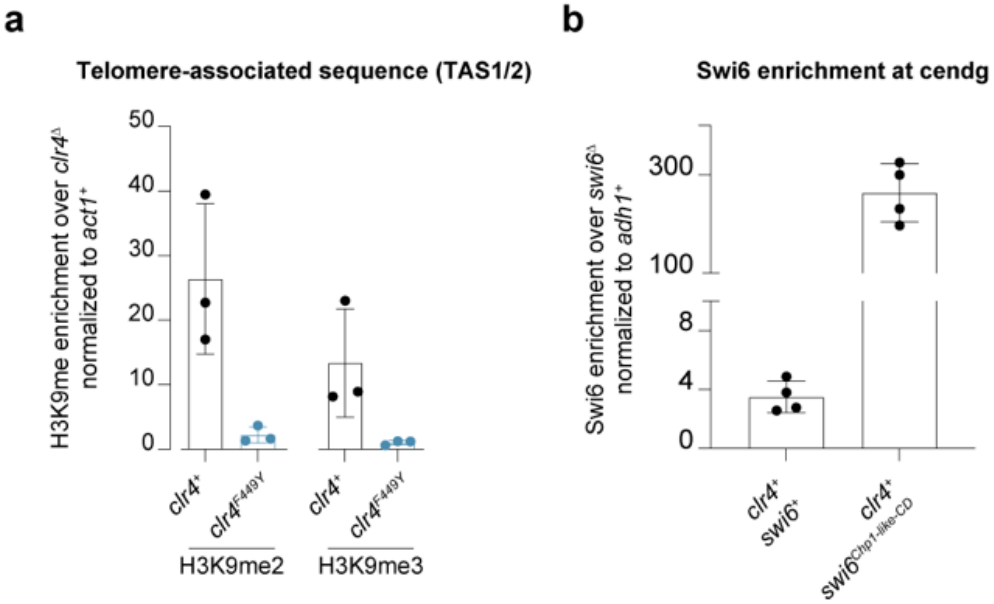

Kuzdere et al., Extended Data Figure 4

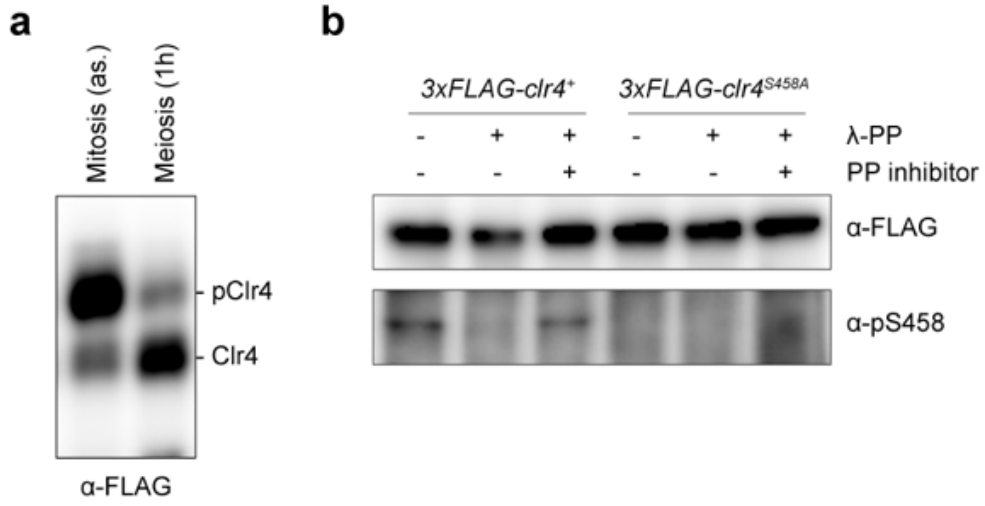

Kuzdere et al., Extended Data Figure 5

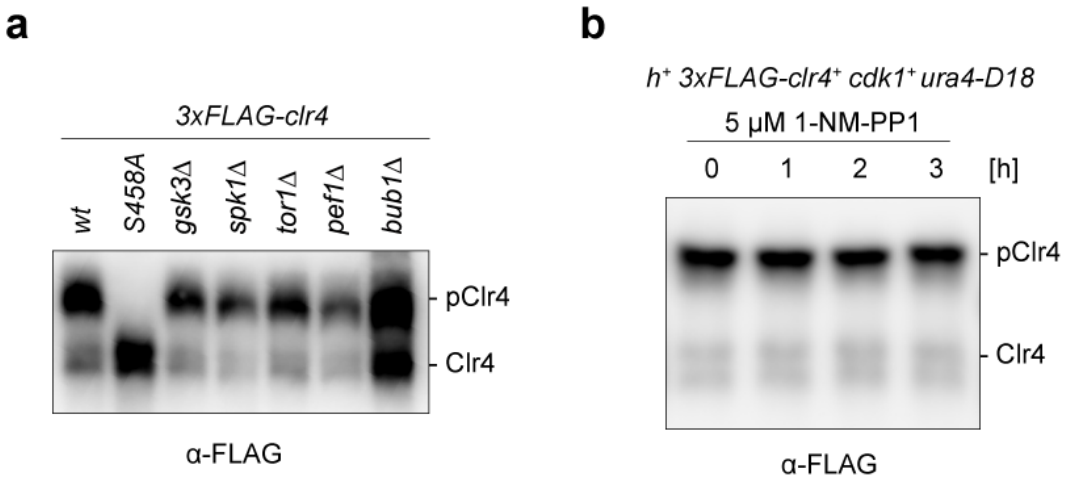

Kuzdere et al., Extended Data Figure 6